Advanced CSP Teaching Materials

Chapter 5
Parabolic Trough Technology

Authors
Matthias Günther[1]
Michael Joemann[1]
Simon Csambor[1]

Reviewers
Amenallah Guizani[2]
Dirk Krüger[3]
Tobisas Hirsch[4]

[1] Institute for Electrical Engineering, Rational Energy Conversion, University of Kassel, Wilhelmshöher Allee 73, 34121 Kassel
[2] Centre des Recherches et Technologies de L'Energie , BP 95 Hamam lif 2050, Tunisia
[3] German Aerospace Center (DLR) -Solar Research, Linder Höhe 51147 Cologne, Germany
[4] German Aerospace Center (DLR)-Solar Research, Pfaffenwaldring 38-40, 70569 Stuttgart, Germany

Table of Contents

Summary 6
1 Introduction 7
2 History of parabolic trough power plant technology 9
3 Power plant components 13
3.1 Parabolic trough collector 14
3.1.1 Collector geometry 14
3.1.2 Mirror material 22
3.1.3 Bearing structure 27
3.1.4 Sun Tracking System 40
3.2 Receiver 44
3.2.1 Receiver components 45
3.2.2 Receiver efficiency 51
3.3 Heat transfer fluid 55
3.3.1 Heat transfer fluid in indirect steam generation power plants 55
3.3.2 Direct steam generation 58
3.4 Solar field 64
3.4.1 Solar field orientation 64
3.4.2 Solar field structure 65
3.4.3 Solar field size 68
4 Power plant integration 71
4.1 Solar field size, storage, solar multiple 71
4.2 Base load, intermediate load and peak load plant configuration 73
4.3 Hybridisation 75
5 Efficiency of parabolic trough power plants 80
5.1 Solar-to-electric efficiency 80
5.2 Solar field efficiency 81
5.3 Power block losses 87
5.4 Parasitic energy uses 88
Reference List 89
Annex 94
1 Proof that a parabola has a focal point 94
2 Proof that parabolas with the same rim angle are geometrically similar 96
3 Derivation of the relation between rim angle, focal length and aperture width 98
4 Derivation of the parabolic trough surface area 98
Questions 100

Answers 102
Exercises 103
Solutions 106

Nomenclature

Symbol	Meaning	Unit
Latin letters		
a	aperture width	m
A	surface area	m²
$A_{rec,act}$	active receiver surface area	m²
$A_{ap,c}$	collector aperture area	m²
$A_{ap,r}$	receiver aperture area	m²
A_{ap}	aperture area	m²
A_{total}	total receiver surface area	m²
b	insulation thickness	m
C	concentration ratio	-
C_G	geometrical concentration ratio	-
d	receiver diameter	m
f	focal length of parabolic trough	m
$G_{b,ap}$	direct irradiance on the collector aperture	W/m²
G_{im}	irradiance in the Sun image	W/m²
G_{rec}	irradiance on receiver	W/m²
h	heat transfer coefficient	
IAM	incidence angle modifier	-
l	collector length	m
P_{el}	rated electrical power	W
P_{in}	total energy input	W
P_{use}	useable energy output	W
$\dot{Q}_{abs,glass}$	power that is absorbed by the receiver glass tube	W
$\dot{Q}_{cond}$	conductive heat transfer	W
$\dot{Q}_{conv}$	convective heat transfer	W
$\dot{Q}_{conv,abs}$	convective heat loss of the absorber tube	W
$\dot{Q}_{conv,glass}$	convective heat loss of the receiver glass tube	W
$\dot{Q}_{loss,opt}$	optical receiver loss	W
$\dot{Q}_{loss,therm}$	thermal receiver loss	W/m
$\dot{Q}_{rad}$	heat transfer through radiation	W
$\dot{Q}_{rad,abs}$	power loss due to radiant emittance of the absorber	W
$\dot{Q}_{rad,glass}$	power loss due to radiant emittance of the receiver glass tube	W
$\dot{Q}_{refl,abs}$	power loss due to reflection on the absorber	W
$\dot{Q}_{refl,glass}$	power loss due to reflection on the receiver glass tube	W
$\dot{Q}_{use}$	useable energy flow	W
r_r	distance between absorber tube and mirror rim	m
s	tracking angle	°, rad
S	parabola length (trough cross-section)	m
SM	solar multiple	-
T_{amb}	ambient temperature	°C, K
T_H	high temperature level in a thermodynamic cycle	°C, K
T_{HTE}	surface temperature of heat transfer element	°C, K
T_L	low temperature level in a thermodynamic cycle	°C, K
T	temperature	°C, K

Greek letters

α	absorptance	-
α_D	sun beam angle	', rad
α_T	weighted average absorptance for black-body radiation at temperature T	-
α_λ	spectral absorptance	-
γ	azimuth angle	°
γ_s	solar azimuth angle	°
δ	dispersion angle	', rad
ε_T	weighted average emissivity for black-body radiation at the temperature T	-
ε_λ	emissivity (in specific spectral range)	-
η	efficiency	-
η_{PB}	power block efficiency	-
$\eta_{SF,opt}(\theta)$	optical solar field efficiency at incidence angle θ	-
η_{SF}	solar field efficiency	-
$\eta_{tm,max}$	maximum thermal-to-mechanical conversion efficiency	-
θ	incidence angle	°
θ_z	solar zenith angle	°
λ	wavelength	M
λ	thermal conductivity	W/(mK)
ξ_{CL}	collector length use factor	-
ξ_{IC}	intercept variance factor	-
ξ_{OP}	optical parameter variance factor	-
ρ	reflectivity	-
σ	Stefan-Boltzmann constant	W/(m²K^4)
τ	transmittance	-
ψ	rim angle	°
ω	hour angle	°

Acronyms

ASE	Archimede Solar Energy
BOP	Balance of plant
CSP	Concentrating Solar Power
DISS	Direct Solar Steam
DLR	German Aerospace Center
DNI	Direct Normal Irradiation
DSG	Direct steam generation
HCE	Heat Collection Element
HTE	Heat Transfer Element
HTF	Heat Transfer Fluid
IAM	Incidence Angle Modifier
NREL	National Renewable Energy Laboratory
PCM	Phase Change Material
PSA	Plataforma Solar de Almería
SCA	Solar Collector Assembly
SEGS	Solar Energy Generating System
SM	Solar Multiple

Summary

In this section we will get to know the currently most frequent form of large scale CSP plants: parabolic trough power plants. We will learn about their history and their current status. We will understand their structure and how their components work. Important design parameters will be explained. At the end, the efficiency of the generation of electricity with parabolic trough power plants will be specified.

Key questions

- Which is currently the dominating CSP technology?
- What are the milestones in the history of parabolic trough power plants?
- What are the main components of a parabolic trough power plant and how do they work?
- What are central parameters in the design of a parabolic trough power plant?
- How efficient are parabolic trough power plants?

1 Introduction

Parabolic trough power plants use parabolic trough collectors to concentrate the direct solar radiation onto a tubular receiver. Large collector fields supply the thermal energy, which is used to drive a steam turbine, which, on its part, drives the electric generator.

Figure 1: Parabolic power plants in southern Spain (Andasol 1 and 2, in the back ground on the right side the prepared construction ground for Andasol 3, source: Solar Millenium)

Parabolic trough power plants constitute the biggest share of the installed concentrating solar power technology. Distinguishing between parabolic trough power plants, Fresnel power plants, solar tower power plants and dish/Stirling systems, the parabolic trough power plants provide over 90% of the capacity of concentrating solar power plant technology that is in operation or in construction in September 2010. Among the planned additional capacity (at the same date) more than 50% are constituted by parabolic trough power plants. The following figure shows the absolute numbers and the shares of the four technology types among the plants in operation, in construction, in the planning stage, and, finally, the sum of all of them.[5]

[5] Photon, Sept. 2010 (German journal for solar technology)

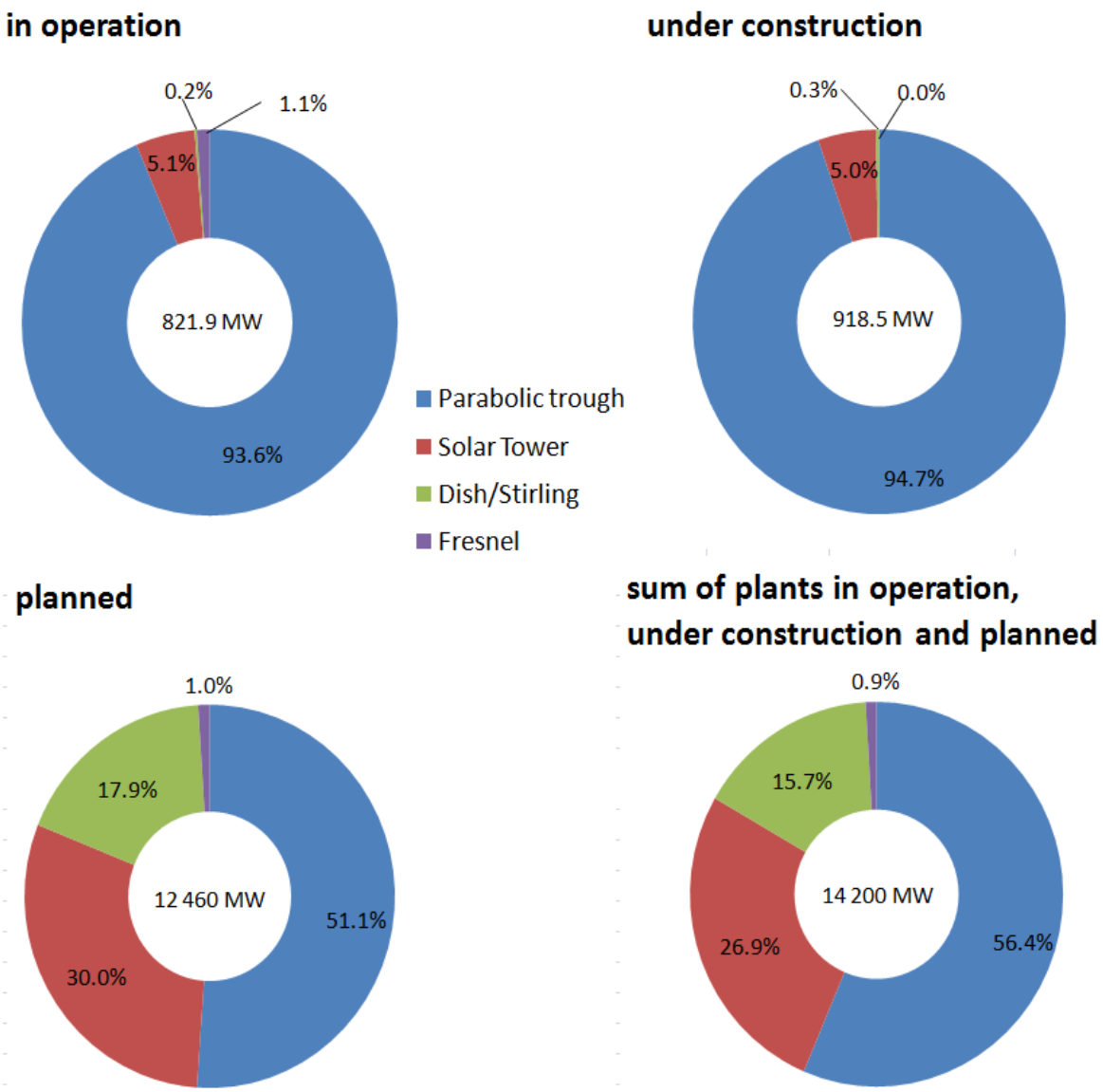

Figure 2: Percentage of different solar thermal power technologies

2 History of parabolic trough power plant technology

John Ericsson constructed in 1880 the first known parabolic trough collector. He used it to power a hot air engine. In 1907, the Germans Wilhelm Meier and Adolf Remshardt obtained the first patent of parabolic trough technology. The purpose was the generation of steam.[6]
In 1913, the English F. Shuman and the American C.V. Boys constructed a 45 kW pumping plant for irrigation in Meadi, Egypt, which used the energy supplied by trough collectors. The pumps were driven by steam motors, which received the steam from the parabolic troughs. The constructors used parabolic trough collectors with a length of 62m and an aperture width of 4m. The total aperture area was 1,200 m².[7] The system was able to pump 27,000 litres of water per minute.[8]
Despite the success of the plant, it was shut down in 1915 due to the onset of World War I and also due to lower fuel prices, which made more rentable the application of combustion technologies.

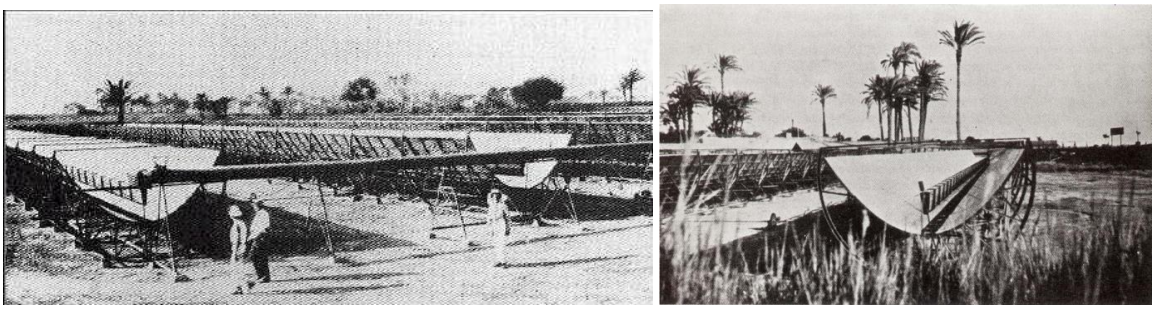

Figure 3: Parabolic trough collector application in Egypt built in 1913 (source: Ragheb 2011)

The interest in the parabolic trough technology did not rise again until 1977, when the US Department of Energy as well as the German Federal Ministry of Research and Technology began to fund the development of several process heat machines and water pump systems with parabolic trough collectors. Higher fossil fuel prices encouraged the governments to take new measures.
Results of these measures were, for instance, the following:

- Between 1977 and 1982, the company Acurex installed parabolic trough demonstration systems with a total aperture area of almost 10,000 m² in the USA for process heat applications.
- The first modern line-focusing solar power plant was a 150 kWe facility that was built in 1979 in Coolidge/Arizona.[9]
- Nine member states of the International Energy Agency participated in the project of building demonstration facilities with a rated power of 500 kW at the Plataforma Solar de Almeria, which was put into operation in 1981.
- The first private financed process heat machine with 5580 m² parabolic trough collectors was successfully put into operation in 1983 in Arizona for thermal heating of electrolyte tanks in a copper processing company.[10] These trough systems developed for industrial process heat application were capable of generating temperatures higher than 260°C.

In 1983, Southern California Edison (SCE) signed an agreement with Luz International Limited to purchase power from the first two commercial solar thermal power plants that should be constructed in the Mojave Dessert in California. These power plants, called Solar Electric Generating System

[6] See Geyer et al. 2002.
[7] See Nava et al. 1996.
[8] See Ragheb 2011.
[9] See Winter et al. 1991, p. 216.
[10] See Geyer et al. 2002.

(SEGS) I and II, started operation in the years 1985 and 1986. Later, Luz signed a number of standard offer contracts with SCE that led to the development of the SEGS III to SEGS IX plants. Initially, the plant size was limited to 30 MW. It was later raised to 80 MW. In total, nine plants with a total capacity of 354 MW were built.[11]

Figure 4: SEGS III–SEGS VII solar plants in California (source: Sandia National Laboratory)

[11] See Price et al. 2002.

Table 1: Characteristics of SEGS plants I – IX (Price et al. 2002)

SEGS Plant	First year of operation	Net output [MWe]	Solar field outlet temperature [°C]	Solar field area [m^2]	Turbine efficiency [%]	Annual output [GWh_e]	Dispatchability provided by
I	1985	13.8	307	82 960	31.5/ n.a.	30	3 hours – thermal storage
II	1986	30	316	190,338	29.4/ 37.3	80	Gas fired superheater
III/IV	1987	30	349	230,300	30.6/ 37.4	93	Gas-fired boiler
V	1988	30	349	250,500	30.6/ 37.4	93	Gas-fired boiler
VI	1989	30	390	188,000	37.5/ 39.5	91	Gas-fired boiler
VII	1989	30	390	194,280	37.5/ 39.5	93	Gas-fired boiler
VIII	1990	80	390	464,340	37.6/ 37.6	253	Gas-fired heat transfer fluid heater
IX	1991	80	390	483,960	37.6/ 37.6	256	Gas-fired heat transfer fluid heater

Until today these plants still continue in operation. The constructional and operational experience with these plants pushed the parabolic trough technology a considerable step forward and provided the basics for further technologic developments and project planning.

A further expansion of the installed capacity of parabolic trough power plants did not take place until 2007, when Nevada Solar One with a capacity of 64MW_e was opened in Nevada.
The first commercial parabolic trough power plant in Europe, Andasol I, is generating electricity since December 2008 at a high plane near the Sierra Nevada mountains in the Spanish Province of Granada. In the middle of 2009 Andasol II, which has the same capacity, was completed and connected to the grid. It is located directly besides Andasol I. The same holds for Andasol III, which is under construction since September 2009.[12] Each of the three plants has a capacity of 50 MW_e. The Andasol power plants were the first CSP power plants with large thermal storage systems. The solar multiple is 2; heat can be stored for 7.5 full load hours. In summer, the power plants can be operated nearly 24 hours a day.

Current political support, which is reflected in the application of financial support schemes (like feed-in-tariffs or renewable energy quotas), makes many new parabolic trough power plant projects possible. Most of these projects are located in the USA or in Spain, but there are also several projects under construction or in planning phase in India, China, Egypt, Algeria, Morocco, Australia and other countries.

Additionally to electricity generation, parabolic troughs can also be used to provide process heat for industrial processes. Process heat is required at different temperature levels. The major part of the required process heat (e.g. in the chemical, food or textile industry) is needed in the medium temperature range between 80 to 250°C. Low temperature process heat (< 100°C) can be provided

[12] See http://www.solarmillennium.de/index,lang2.html

with non concentrating solar thermal collectors. Temperatures between 150 and 250°C, on the contrary, require concentrating solar thermal collectors. There are several parabolic trough collectors under development for the medium temperature range. Usually these collectors are smaller than the parabolic trough collectors for electric power generation.

An example is an application in the pharmaceutical industry in Cairo. It has the following characteristics:

Installed capacity:	1330 kW
Collector area:	1900 m²
Number of collectors:	36
Heat transfer medium:	steam
Operating temperature:	173°C
Operating pressure:	8 bars

Figure 5: Process steam at a pharmaceutical company in Egypt (source: Weiss 2005)

3 Power plant components

The energy flow in a parabolic trough power plant has the following structure: Direct solar radiation is concentrated and converted into thermal energy. The thermal energy is converted into pressure energy of vapour, which is converted into kinetic energy. The kinetic energy is finally transformed into electrical energy, the final product of the power plant.
These energy conversion steps are realized in the respective power plant components: The parabolic trough collector and the tracking system are essential for the concentration process. The receiver converts the radiation energy into thermal energy. Heat transfer medium and thermal storage are carriers of the thermal energy. The steam generator has the function to convert the thermal energy into pressure energy of a gaseous medium. This is done by the evaporation of water. The cooling system has the aim to complete the liquid/gaseous-cycle converting the steam back to water. The steam turbine converts the pressure energy in the steam into rotational energy. The electric generator, finally, converts the rotational energy into electric energy, which can be supplied to the electric grid. The following figure shows the mentioned main components of the plant and relates them to their respective place in the energy conversion chain.

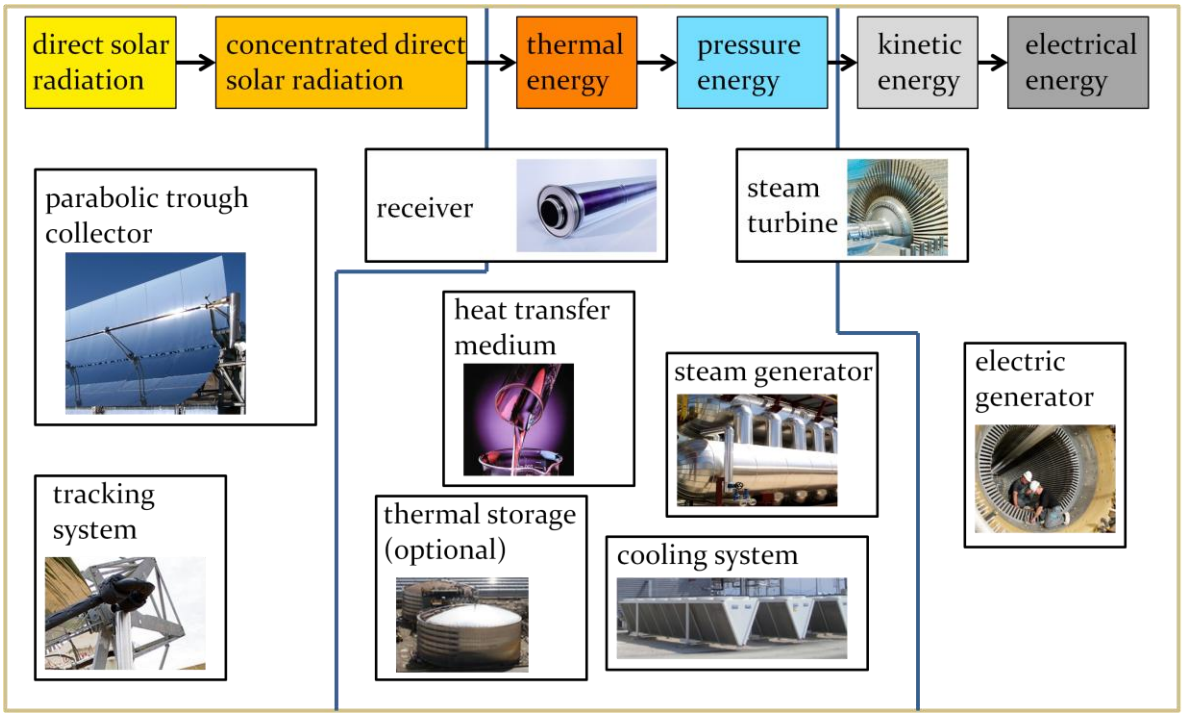

Figure 6: Energy conversion chain in a parabolic trough power plant and corresponding plant components

In this chapter, we will discuss the plant components that are specific for CSP plants. The conventional power plant components were explained in the preceding chapter.

3.1 Parabolic trough collector

3.1.1 Collector geometry

The collector, the parabolic trough, is a trough the cross-section of which has the shape of a part of a parabola. More exactly, it is a symmetrical section of a parabola around its vertex.

Radiation concentration at a parabolic trough

Parabolic troughs have a focal line, which consists of the focal points of the parabolic cross-sections. Radiation that enters in a plane parallel to the optical plane[13] is reflected in such a way that it passes through the focal line.

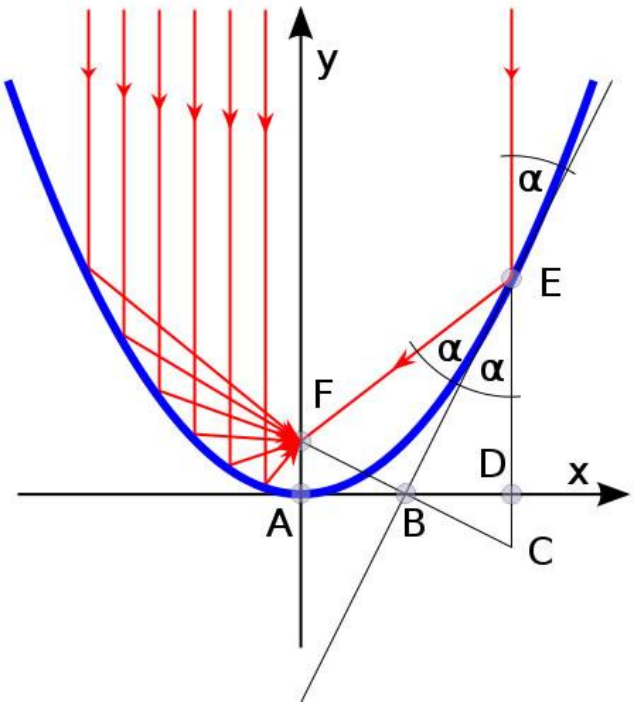

Figure 7: Path of parallel rays at a parabolic mirror

A proof of the existence of a focal point is presented in the annex. An appropriate analytic representation of a parabola is

$$y = \frac{1}{4f}x^2, \qquad (1)$$

where f is the focal length, i.e. the distance between the vertex of the parabola and the focal point.

[13] With "optical plane" we mean the plane that contains the optical axes of the parabolic cross-sections of the trough.

Parameters for the geometrical description of a parabolic trough

In order to describe a parabolic trough geometrically, the parabola has to be determined, the section of the parabola that is covered by the mirrors, and the length of the trough.
The following four parameters are commonly used to characterize the form and size of a parabolic trough: **trough length**, **focal length**, **aperture width**, i.e. the distance between one rim and the other, and **rim angle**, i.e. the angle between the optical axis and the line between the focal point and the mirror rim:

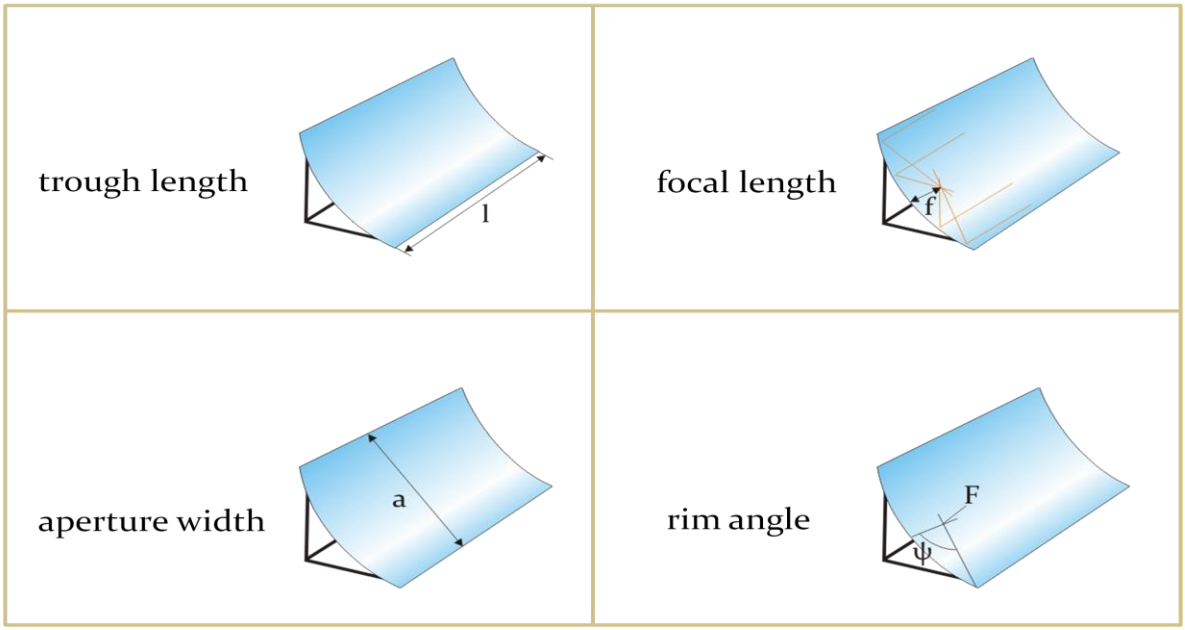

Figure 8: Geometrical parabolic trough parameters

The **length of the trough** is an unproblematic measure and does not need any explanation.

The **focal length**, i.e. the distance between the focal point and the vertex of a parabola, is a parameter that determines the parabola completely (in the mentioned mathematical expression of a parabola, $y = \frac{1}{4f}x^2$, the focal length f is the only parameter).

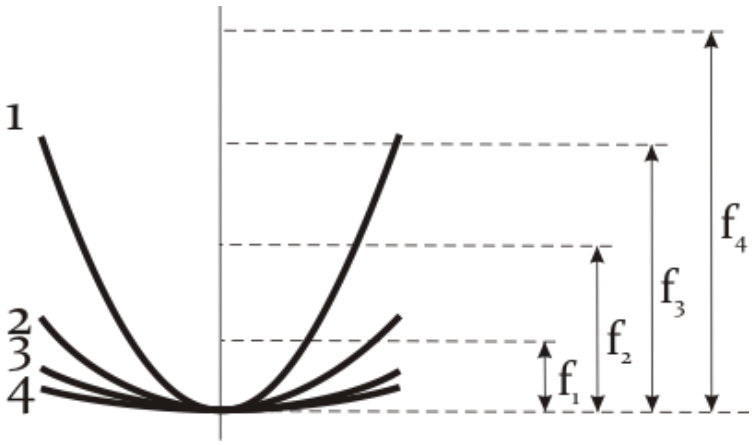

Figure 9: Focal length as shape parameter

The **rim angle,** i.e. the angle between the optical axis and the line between the focal point and the mirror rim, has the interesting characteristics that it alone determines the shape of the cross-section of a parabolic trough. That means that the cross-sections of parabolic troughs with the same rim angle are geometrically similar. The cross-sections of one parabolic trough with a given rim angle can be made congruent to the cross-section of another parabolic trough with the same rim angle by a uniform scaling (enlarging or shrinking). If only the shape of a collector cross-section is of interest, but not the absolute size, then it is sufficient to indicate the rim angle. A proof that the cross-sections of parabolic troughs with the same rim angle are geometrically similar is presented in the annex.

Two of the three parameters **rim angle**, **aperture width** and **focal length** are sufficient to determine the cross-section of a parabolic trough completely, i.e. shape and size. This also means that two of them are sufficient to calculate the third one. ψ can be expressed as a function of the ratio of the aperture width to the focal length:

$$\tan\psi = \frac{\frac{a}{f}}{2-\frac{1}{8}\left(\frac{a}{f}\right)^2}. \qquad (2)$$

or, alternatively, the ratio of the aperture width to the focal length can be expressed as a function of the rim angle:

$$\frac{a}{f} = -\frac{4}{\tan\psi} + \sqrt{\frac{16}{\tan^2\psi} + 16} \qquad (3)$$

The following diagram represents the a-f ratio in dependence on the rim angle.

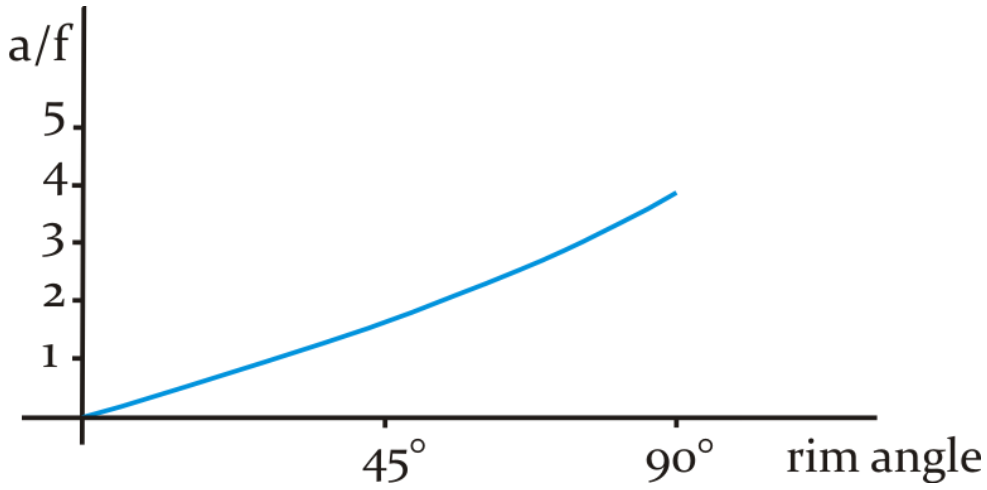

Figure 10: Relation between the rim angle and the a/f-value

Geometrical parameters of real parabolic troughs

We will have a look now at the values that take these parameters at real parabolic troughs.
First, we see that the **rim angle** should neither be too small nor too large. The rim angle is related to the distance between the different parts of the mirrors and the focal line. Taking a fixed aperture width the following figure represents this relation:

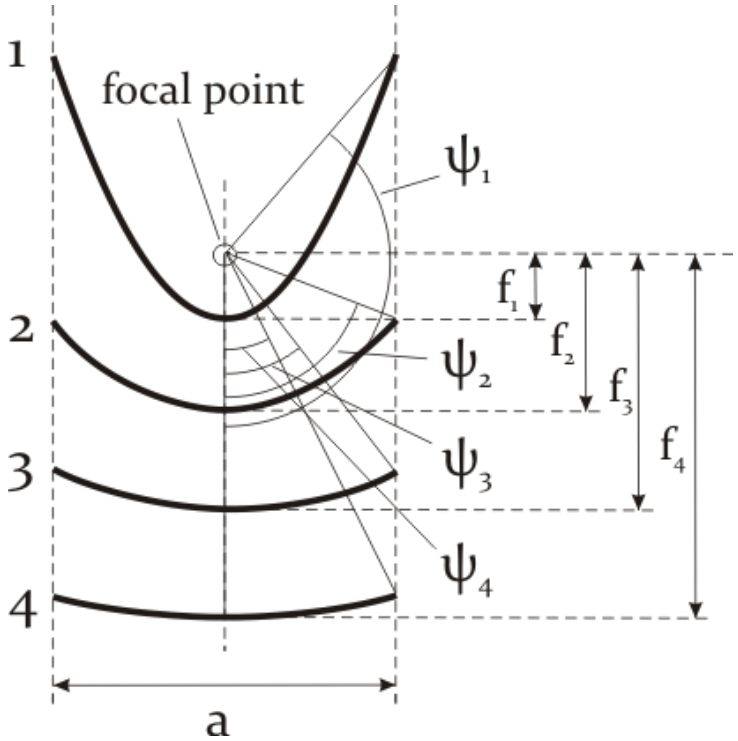

Figure 11: Relation between the focal length and the rim angle for a constant trough aperture width

The rim angle is a very important constructive trait of collectors. For instance, it has an effect on the concentration ratio and on the total irradiance per meter absorber tube [W/m]. Qualitatively, we can understand in the following way that there must be some ideal rim angle range and that is should neither be too small nor too large:

- We consider, first, perfect mirrors, disregarding possible slope errors.[14]
  If the rim angle is very small, then the mirror is very narrow and it is obvious that a broader mirror (with a larger rim angle) would enhance the power projected onto the absorber tube.[15]
  If the rim angle is very big, then the way of the reflected radiation from the outer parts of the mirror is very long and the beam spread is very big, reducing, hence, the concentration ratio. A mirror with a smaller rim angle and the same aperture width would permit a higher concentration ratio.

[14] In the chapter "Solar Radiation" we demonstrated that at a rim angle of 45° the highest concentration ratio is reached. This result, however, is valid only for plane receivers. At tubular receivers the situation is different. The optimal rim angle is bigger because the problem of the Sun image widening due to high incidence angles on the focal plane at high rim angles does not exist in the same way.

[15] Alternatively, the mirror could be allocated nearer to the absorber tube (with the same aperture width and a larger rim angle) and the beam spread (which exists due to the extension of the Sun disc) could be reduced, what would increase the concentration ratio.

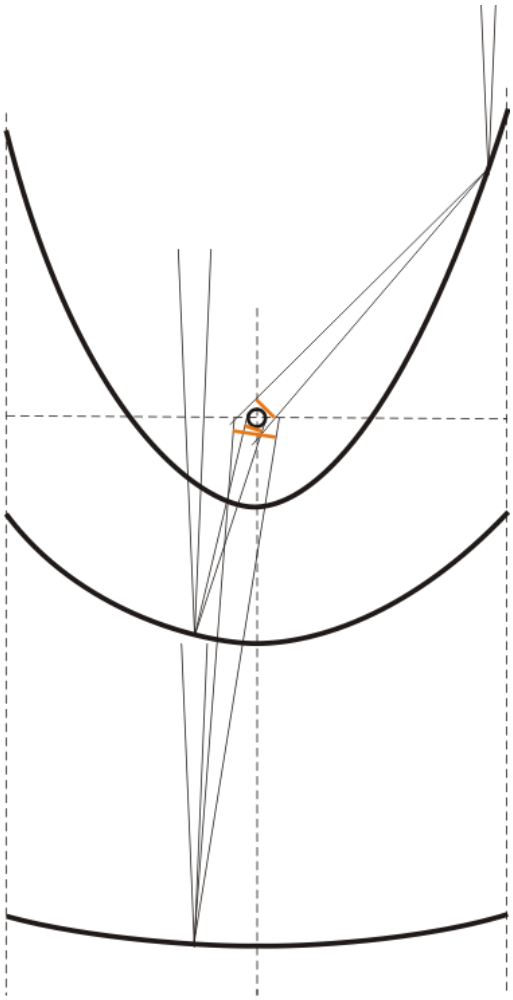

Figure 12: Dependence of the focal spot size on the rim angle (at a given trough aperture width)

- Additionally, if we consider real mirrors with a certain degree of geometrical inexactness, then it is important to maintain a low distance to the absorber also because the effect of these geometrical mirror errors. The larger the distance to the absorber, the more weight carries the radiation aberration due to mirror slope errors. Once more, at a given aperture width, very small rim angles as well as very large rim angles imply large distances between the mirror and the focal line (in the case of very large rim angles for the outer parts of the mirror) and should be avoided.

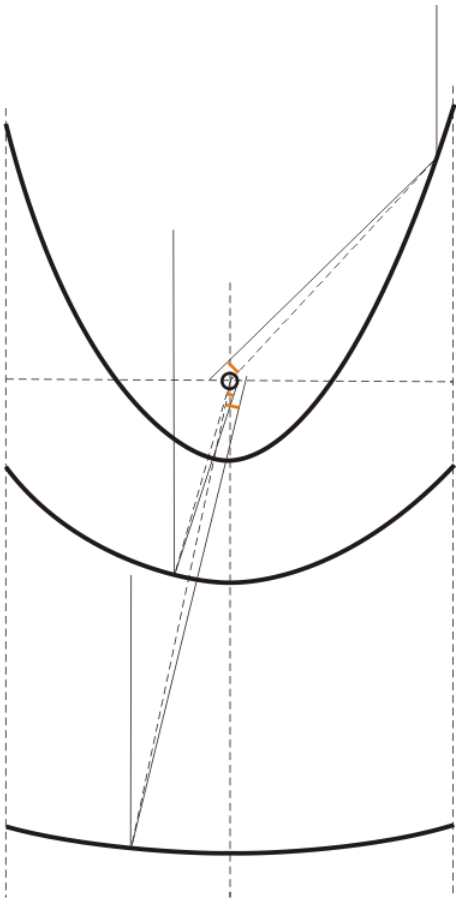

Figure 13: Effects of slope errors in dependence on the rim angle

- Last but not least there is an economical aspect that limits the reasonable rim angle: At high rim angles the outer parts have a low contribution to the energy yield in relation to the mirror area. That means a high investment is necessary, which contributes only little to the energy yield.

So, there are several criteria, which together determine the rim angle. The rim angle of real parabolic troughs is around 80°.

The **aperture width** of most actual collectors amounts to approximately 6m, the **focal length** is (correspondingly to the rim angle and aperture width values) approximately 1.75m, and the module length is between 12 and 14m. There are some collectors that have smaller (Solarlite) or larger aperture widths (Skyfuel, Heliotrough) with corresponding different focal lengths.

Mirror area and aperture area

Besides the mentioned linear measures, also surface area measures are important. There is, first, the aperture area, which is an important constructive measure. At a given DNI and a given Sun position it determines the radiation capture. The aperture area A_{ap} is calculated as the product of the aperture width a and the collector length l:

$$A_{ap} = a \cdot l \,, \qquad (4)$$

The surface area of a parabolic trough may be important to determine the material need for the trough. The area is calculated as follows:

$$A = \left(\frac{a}{2} \sqrt{1 + \frac{a^2}{16f^2}} + 2f \cdot \ln \left(\frac{a}{4f} + \sqrt{1 + \frac{a^2}{16f^2}} \right) \right) \cdot l \, . \qquad (5)$$

A derivation of this equation is presented in the annex.

Concentration ratio

The concentration ratio is one of the central parameters of the collector. It is decisive for the possible operating temperatures of the parabolic trough power plant. The concentration ratio C is defined as the ratio of the radiant flux density at the focal line, or, what is the same, at the Sun image, G_{im}, to the direct irradiance at the aperture of the collector, $G_{b,ap}$:

$$C = \frac{G_{im}}{G_{b,ap}} \qquad (6)$$

Now, the irradiance is different in different points of the Sun image. That's why we can consider, first, a punctual concentration ratio. In this case, G_{im} has to be determined at a point within the focal line in order to determine the concentration ratio in relation to that specific point. Or we can consider, second, a mean concentration ratio taking C as the ratio of the mean irradiance at the focal line to the direct normal irradiance.
Concerning the mean concentration ratio (contrary to the punctual one) there is an easy way to specify it without any measurement: The **geometrical concentration ratio** C_G is a useful approximation. It is defined as the ratio of the collector aperture area to the receiver aperture area.

$$C_G = \frac{A_{ap,c}}{A_{ap,r}} \qquad (7)$$

While it is clear what the collector aperture area is (see above), it is much less clear what has to count as the receiver aperture. In many cases, the projected area of the absorber tube is chosen. In this case the receiver aperture area is a rectangle with the area $d \cdot l$, where d is the absorber tube diameter.

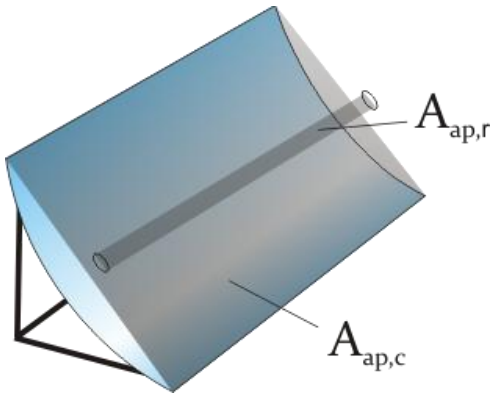

Figure 14: Collector aperture area and receiver aperture area

The concentration ratio is, then:

$$C_G = \frac{a \cdot l}{d \cdot l} = \frac{a}{d} \qquad (8)$$

In the chapter "Solar Radiation" it was demonstrated that the maximal mean concentration ratio in linear focussing collectors, taking the Sun image area in the focal plane for $A_{ap,r}$, is 107.5. The maximal geometrical concentration ratio in real systems, accepting the projected absorber tube area as $A_{ap,r}$, is 82.

Another possibility is to take the irradiated absorber surface area as the receiver aperture area. In real parabolic troughs this would mean that the whole absorber tube surface area $\pi \cdot d \cdot l$ is the receiver aperture area[16]:

$$C_G = \frac{a \cdot l}{\pi \cdot d \cdot l} = \frac{a}{\pi \cdot d}\,. \qquad (9)$$

This definition would lead to a lower geometrical concentration ratio. However, the concentration ratio according to the projected areas is more commonly used.

[16] We take into consideration that the absorber tube is not only irradiated by the reflected radiation but also by the radiation that reaches the tube directly so that the whole absorber tube surface is irradiated.

3.1.2 Mirror material

The main requirements for appropriate mirror materials are their reflective properties. The reflectivity must be high. The reflectivity of a surface is a number that indicates the fraction of the incident radiation that is reflected by the surface. In general, the reflectivity is different for different wavelengths so that it has to be specified for a given wavelength or a given wavelength range, for instance for the visible light range. In the case of solar applications, the solar spectrum is of interest. Generally, a "solar weighted reflectivity" is indicated that takes into consideration that there are different energy contents at different wavelengths in the solar spectrum. The solar weighted reflectivity indicates, hence, the fraction of solar energy that is reflected on a mirror.
Furthermore, reflection can be distinguished in specular reflection and diffuse reflection. Specular reflection means that the light that comes from a single incoming direction is reflected into a single outgoing direction. Specular reflection is mirror-like reflection. According to the law of reflection the direction of the incoming light and the direction of the outgoing light have the same angle with respect to the mirror surface normal. At diffuse reflection, on the contrary, the incoming light is reflected in a broad range of directions. In CSP applications, only specular reflectivity is of interest, because the reflected radiation must have a defined direction. The decisive quality criterion for efficient mirrors is, hence, the "solar weighted specular reflectivity".[17]

Silver coated glass mirrors

The most common parabolic mirrors today consist of silver coated glass mirrors. Indeed, all realized commercial parabolic trough power plants use them. There are experiences with these mirrors since the first parabolic trough power plants were built in the 1980s. The mirrors have proven to be durable: Even after more than ten years of operation they hardly showed any decrease in specular reflectivity.

Figure 15: Mounting of a parabolic trough with silver coated glass mirror facets (source: CSP Services)

[17] See Sargent & Lundy 2003, p. 328.

The glass for the mirror facets is normally manufactured with the float glass method where the molten glass flows continuously on a bath of liquid tin. This method guarantees a very high evenness of the manufactured glass. Low-iron glass is used to increase the light transmission in the solar spectrum. After the glass is cut to the right size and got grinded, it is formed to the parabolic form in an oven. One possibility is to form the glass on a mould using its own weight. Another possibility is to press it to achieve the desired parabolic form.
High geometric mirror accuracies could be reached. The company Flabeg indicates a reduction of slope errors to 0.132°. This value indicates the average slope deviation from the design form. Correspondingly high intercept factors could be reached. Applications in the Eurotrough registered an intercept factor of 99.9% for an absorber tube with a diameter of 70 mm (the common absorber tube diameter of most commercially available receivers) and 95.5% for an absorber tube with a diameter of 40 mm. The intercept factor is defined as the percentage of the radiation reflected by the collector that reaches the absorber.[18]
The mirrors have a multilayered structure. The first layer below the glass is the reflective layer, i.e. the silver coating. The following diagram shows the high reflectivity of silver in the solar spectrum range.

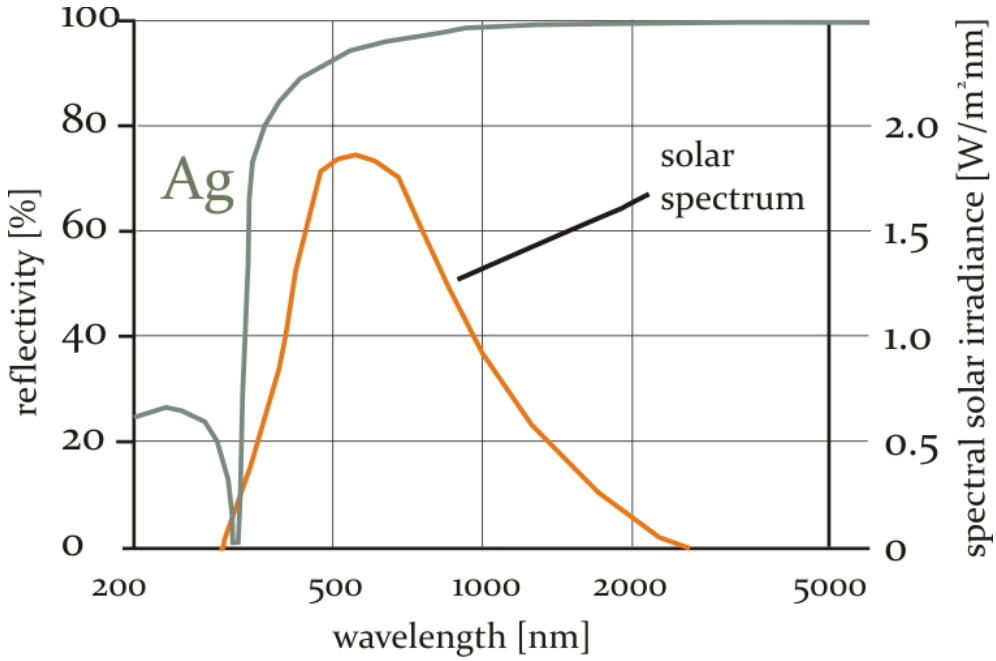

Figure 16: Reflectivity of silver

A protective copper layer is applied next to the silver layer, on which three epoxy varnishes are added: a prime coat, intermediate and protective top coat. In most solar mirrors that were applied until now the first and second coat contain a certain percentage of lead, but protection layers without copper and lead are in development. The thickness of the complete mirror amounts to 4 to 5 mm. In the following figure the multilayered structure is shown.

[18] For information about silver coated glass mirrors see www.flabeg.de and Mohr et al. 1999, p. 8.

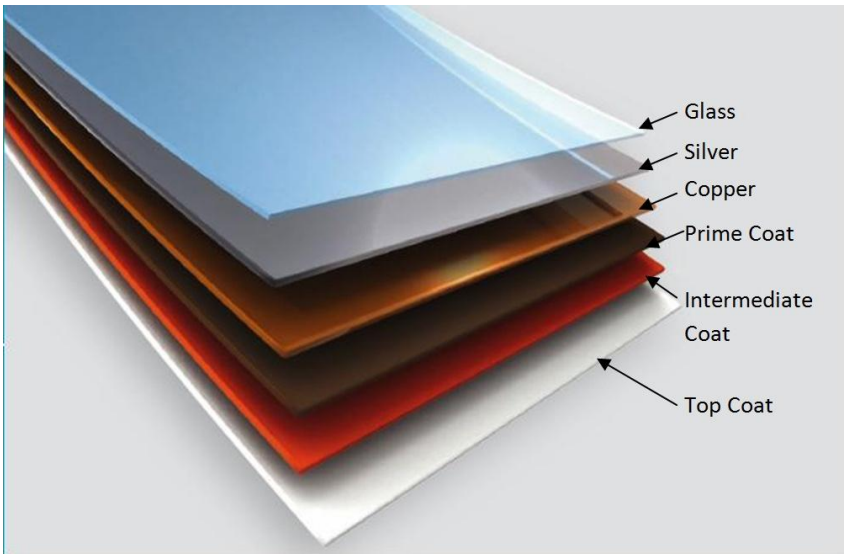

Figure 17: Flabeg multilayered mirror (source: Flabeg)

The average solar weighted direct reflectivity of the Flabeg mirrors is indicated to be 93.5%.[19]
Most parabolic mirrors that consist of silver coated glass mirrors are not constructed in one piece, but they are composed of mirror facets. The Eurotrough with an aperture width of 5.77 m and a module length of 12 m long contains 28 mirror facets per module, four facets distributed over the width and seven facets distributed over the length. The size and also the shape of the outer and inner mirror facets differ due to different sections of the parabola they cover. The area of the inner facets is 2.79 m^2 and of the outer ones 2.67 m^2. The reflective area of one module amounts to 76.44 m^2. Ceramic pads with a nut are glued on the backside of the mirror facet for the mounting on the metallic bearing structure. While this system uses rigid mirrors (the most common technique for parabolic troughs), flexible thin glass facets are used in an alternative system chosen by Solarlite GmbH. These flexible facets are glued on a parabolic mould of glass fiber-reinforced plastic, which is the main trough body.

Alternative mirror materials

The mirrors account for a considerable part of the solar field investment for a parabolic trough power plant. There are ongoing efforts to find alternative materials that could lower the solar field costs.[20] We will present two alternative mirror materials that have been proposed: silver coated polymer films and front side aluminium mirrors. However, until now (March 2011) they have not yet been applied in commercial parabolic trough power plants.

- In the 1990s, NREL developed a silver coated polymer film as reflector material for solar applications. Its commercial name is now ReflecTech. It is a rollable reflective film that can be applied to any smooth non porous material. It is made out of multiple polymer layers with a reflective silver layer. Mirrors with ReflecTech have been tested since 2002 in the SEGS plants in California. Until now they did not show any decrease of reflectivity.
  It is claimed that ReflecTech offers a considerable economic advantage compared to glass mirrors. The mirror manufacturing process and the assembling process of the collector could be accelerated. Flexible facets could be put in a guide rail with a parabolic form. An advantage

[19] See Flabeg 2010.
[20] See Kennedy et al. 2005 and Kennedy 2008.

is that the mirrors are not susceptible to breakage. The company Skyfuel, which commercializes the ReflecTech technology, indicates the reflectivity to be 94%.[21]

Figure 18: ReflecTech film (source: Skyfuel)

- Alanod offers a front surface aluminized mirror, which consists of an aluminium reflective layer, an anodized layer beneath and above as well as further protective coatings.[22]

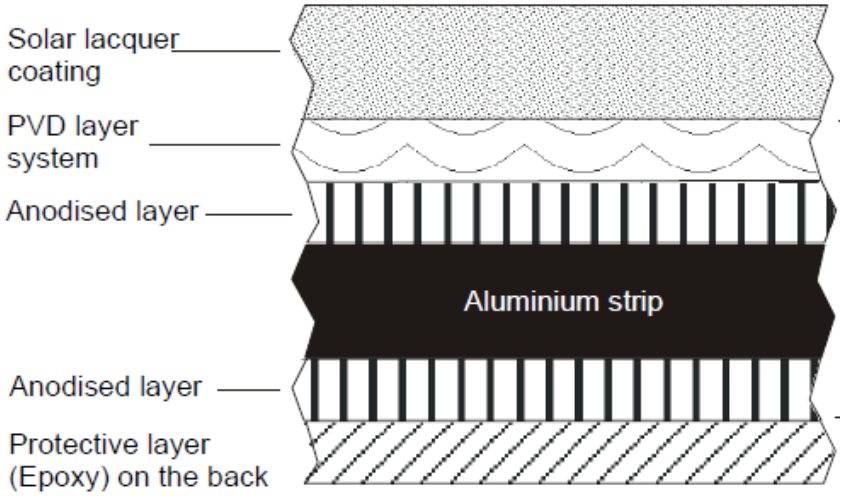

Figure 19: Alanod's aluminum mirror (source: Alanod)

Because of the lower solar spectrum reflectivity of aluminium in comparison to silver (see the following diagram), the reflectivity of the Alanod mirrors is slightly lower than the reflectivity of the other presented mirror types. A value of 90% is indicated.

[21] See www.skyfuel.com.
[22] See http://alanod-solar.com/opencms/opencms/Reflexion/Produkte.html.

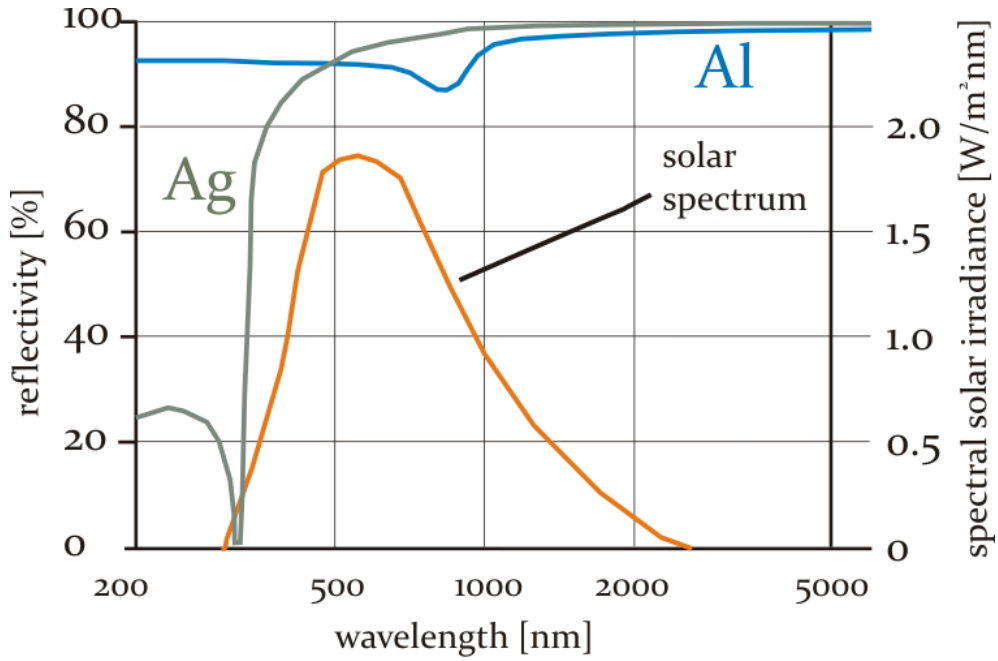

Figure 20: Reflectivity of aluminium compared to silver and related to the solar spectrum

3.1.3 Bearing structure

The bearing structure of a parabolic trough has the function to carry the mirrors in the right position, to give stability to the troughs and to allow an exact Sun tracking.
In order to comply with these functions, the structures have to fulfil some construction requirements. In particular, the stiffness requirements are very high, because any deviation from the ideal parabolic collector shape causes losses in the optical efficiency of the system. It is important that the parabolic troughs are neither deformed by their own weight nor by wind loads. The aperture area represents a large area that is exposed to the wind so that the resulting wind loads are considerable. The collector has to be constructed in such a way that it withstands these loads with only very small geometrical deviations.
Additionally, a high stiffness allows longer troughs so that the number of pylons and tracking units can be reduced, which reduces costs. The modules of the Heliotrough, which will be presented below, for instance, are 19m long and the assemblies that are moved by one drive unit are 191m long. A high stability is also important for the construction of troughs with a larger aperture width. For a long time, the standard aperture width was 5.76m or 5.77m. The new Skyfuel trough and the Heliotrough have a larger aperture width: Skyfuel 6m and the Heliotrough 6.77m.
The stiffness must be combined with lightweight constructions, which allow the usage of weaker foundations and tracking mechanisms. A light construction is also less prone to deformations due to the own weight. Additionally, light structures reduce the energy demand for the collector tracking. Anyway, the parasitic energy consumption of a parabolic trough power plant is quite high in comparison to other power plants; and one of the two most important consumers is the tracking system (the other is the heat transfer fluid pumping).
It is obvious that an appropriate bearing structure should involve low material and manufacturing costs. It has to be taken into consideration that the solar field is the most expensive part of a parabolic trough power plant. In the case of the Andasol power plants in Spain the solar field covers 30% of the total costs.[23] That means that a cost reduction of the solar field has an important effect on the total power plant costs.

Generally, the bearing structure of a collector consists of a main body, which in most cases is a space frame or tube structure made out of steel or aluminium. Only in the case of the mentioned Solarlite collector, the central body is made out of non-metallic materials. Further elements of the bearing structure are:

- Mirror support points on the space frame structure or on special cantilever arms,
- Receiver support, also called heat collection element (HCE) support,
- Structure for the mounting to the pylons
- Pylons, among them drive pylons, and foundations.

These elements are found, for example, in the Eurotrough collector. The following two figures show a photo of the main collector body and a schematic representation of the collector components.

[23] See IEA 2010, p. 27.

Figure 21: Space frame structure of a Eurotrough collector module (source: Lüpfert, DLR)

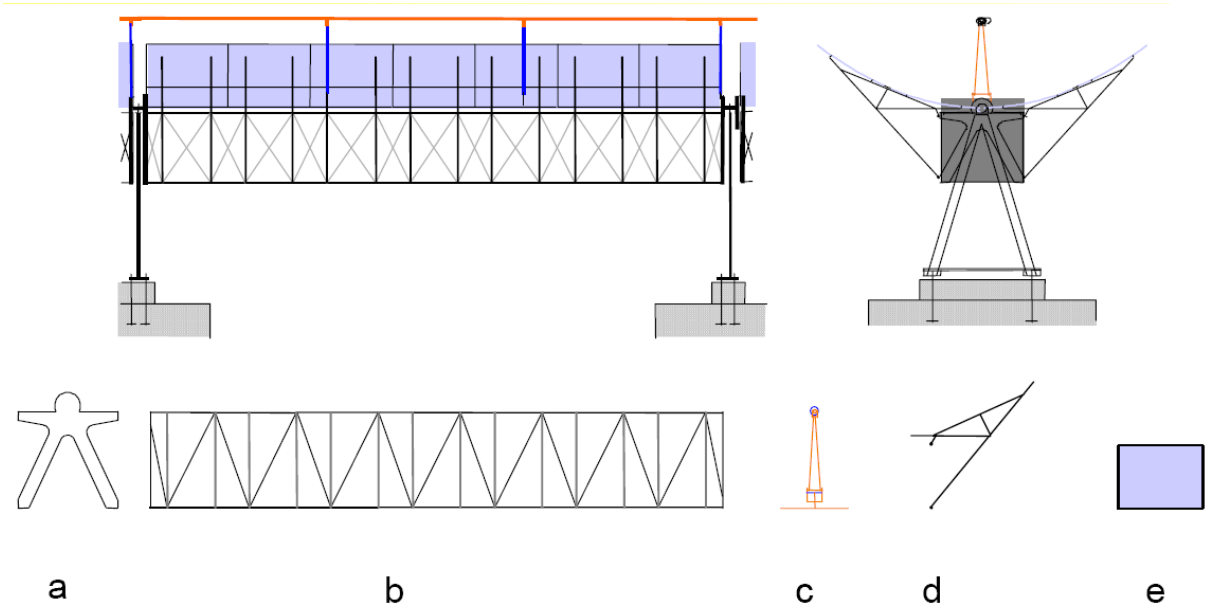

Figure 22: Eurotrough module structural elements: (a) front and rear endplates for mounting to the pylons, (b) space frame structure, (c) receiver supports, (d) cantilever arm, (e) mirror facet (source: Lüpfert, DLR).

The construction of the collector modules is done on the plant site. The module elements are brought to the plant site, where they are assembled in a production hall. Many companies use assembly jigs, around which the modules are composed. After that, the modules are taken to the solar field and introduced into it.

Figure 23: Assembly of the Eurotrough module with the help of an assembly jig (source: Lüpfert, DLR)

Figure 24: Mounting of the Eurotrough collector to the pylon (source: Solar Millenium)

The collector modules are combined to collector assemblies. A collector assembly is a serial of modules that is moved by one tracking drive unit, which is located in the centre of the collector assembly.

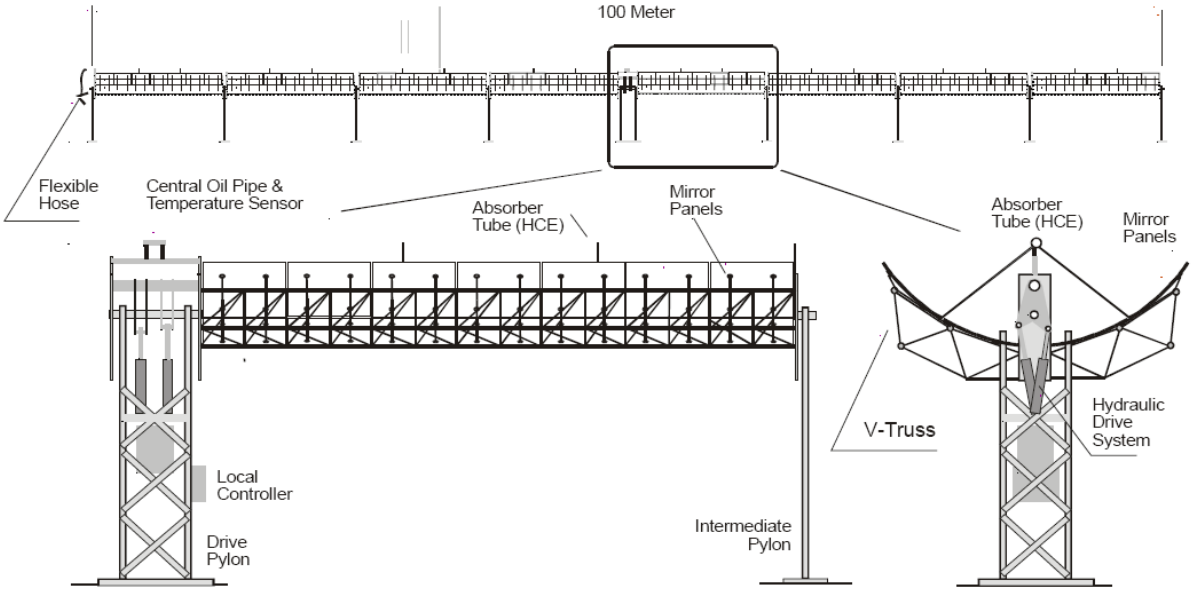

Figure 25: Solar collector (LS-3) assembly (source: Geyer, DLR)

In the following, the bearing structure designs of the collectors of different producers are presented. We use this section also to present the different producers of parabolic trough collectors.

Luz Industries: LS-1, LS-2, LS-3

One of the first companies that developed parabolic trough collectors was the American-Israeli company Luz Industries Ltd. The first collector type was the LS-1, which was applied in SEGS I and II. LS-2 was also installed in SEGS I and II as well as in SEGS III – VII. The collector LS-3 was used in SEGS VII – IX. While the Ls-2 collector was realised with a torque tube and several cantilever arms, the LS-3 collector was based on a broad space frame structure, which was claimed by Luz to be more resistant to bending and torsion.

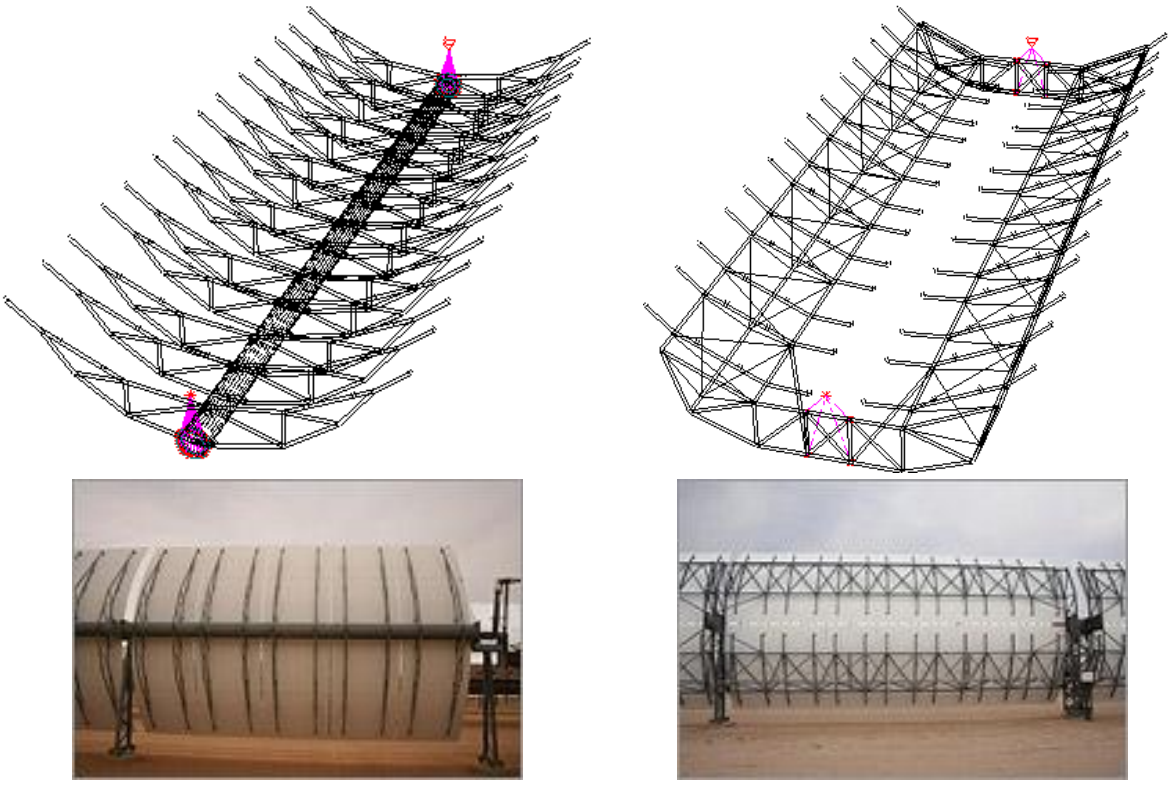

Figure 26: LS-2 and LS-3 collector design of Luz Industries Lt. (sources: Geyer, DLR, NREL)

A LS-3 collector assembly, which is moved by one tracking drive in the middle, consists of eight modules with a length of 12 meters each and has a total length of 100 m.

Eurotrough Consortium: Eurotrough 100 & Eurotrough 150

Based on the knowledge and experience that was made with the Luz collectors, a European consortium of several companies as well as R&D Institutions developed the Eurotrough I (ET-100) between 1998 and 2002, and after that the Eurotrough II (ET-150). Participating parties in the development were Inabensa, Pilkington, SBP, Fichtner, Flabeg, Iberdrola, Solel, Ciemat, Cres and DLR. The main difference between the types I and II is the length of the collector assemblies. The Eurotrough II, which is designed for a collector assembly length of 150 m, allows material savings in comparison to the Eurotrough I, which is designed for a collector assembly length of 100m, because less tracking drive units are needed in the solar field.

The Eurotrough uses a space truss with a cross-sectional area of 1.5 x 1.4 m to achieve a rigid support structure. This central body, also called torque box, is made up of four ladder beams, each of which is tension-locked to girts. The cross-section is reinforced using diagonal struts and end frames. 14 cantilevered arms are located at hollow sections on each side of the box side ladder beams, providing the support points for the 28 mirror facets. The Eurotrough module is manufactured on-site on an assembly jig. In case of the ET 150, six modules are connected at each side of a drive pylon, i.e. the collector assemblies contain 12 modules.[24]

[24] See Schiel 2007.

Figure 27: Eurotrough collector, test facility at the PSA (source: Lüpfert, DLR)

From 2003 on, the Eurotrough collector design was tested in the SEGS V plant under commercial use conditions and showed a thermal efficiency improvement by 10% compared to the Luz collectors. It is now distributed by the Flagsol GmbH under the product name SKAL-ET. The collector design was selected for the Andasol plants in Spain as well as for the Kuraymat project in Egypt.

ENEA

ENEA, the Italian National Agency for New Technologies, Energy and Sustainable Economic Development, together with industrial partners, designed the first collector that uses molten salt as heat transfer fluid. It has been used in a 5 MW demonstration power plant in Sicily since July 2010. The collector has a torque tube (instead of a space frame structure) with parabola-shaped cantilever arms as mirror supports. The collector assemblies are 100 m long, while one module has a length of 12.5 m. The aperture width is 5.76 m.[25]

[25] See Kearney 2007.

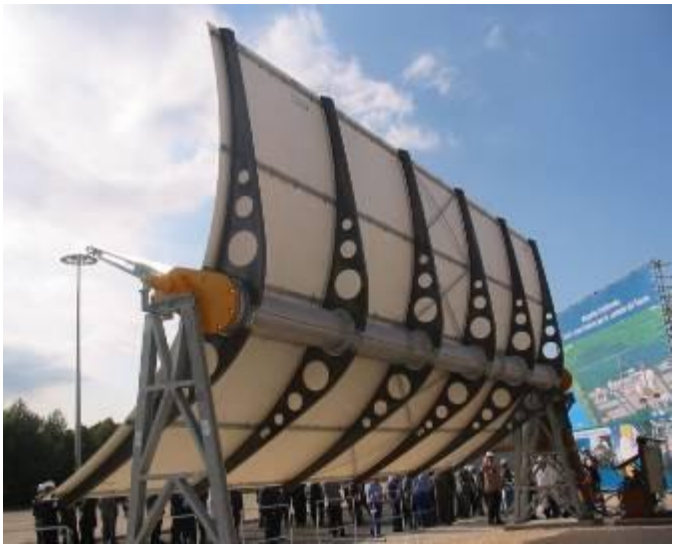

Figure 28: Enea's parabolic trough (source: Geyer, DLR)

Solargenix Energy: SGX-1 and SGX-2

Solargenix Energy (formerly Duke Solar Energy) and NREL developed the SGX collector under a funding program of the U.S. Department of Energy. The collector is made from extruded aluminium. Its bearing structure consists of a space frame that uses technology that was developed for the construction of buildings and bridges. The design has the advantage of being very light and to require very few fasteners.[26] The aperture width measures also 5.77 m. The modules have a length of 12m. The collector assemblies can have a length from 100 to 150 m. The SGX-1 was successfully installed in the Saguaro plant in Arizona (1 MW). The newer collector SGX-2 was first deployed in 2006 in the Nevada Solar One power plant (64MW).[27]

Figure 29: Solargenix collector (source: Kearney, NREL, gossamersf.com)

SENER: Senertrough

The Spanish company Sener developed a collector that also uses a torque tube (like the ENEA and LS-2 collectors). The mirrors are connected to the cylindrical tube via cantilever arms. These mirror support structures are manufactured with sheet stamping technologies that are applied typically in the automotive industry. It is claimed that this allows the reduction of manufacturing costs.

[26] http://www.nrel.gov/csp/troughnet/solar_field.html
[27] http://www.solarpaces.org/Tasks/Task1/nevada_solar_one.htm

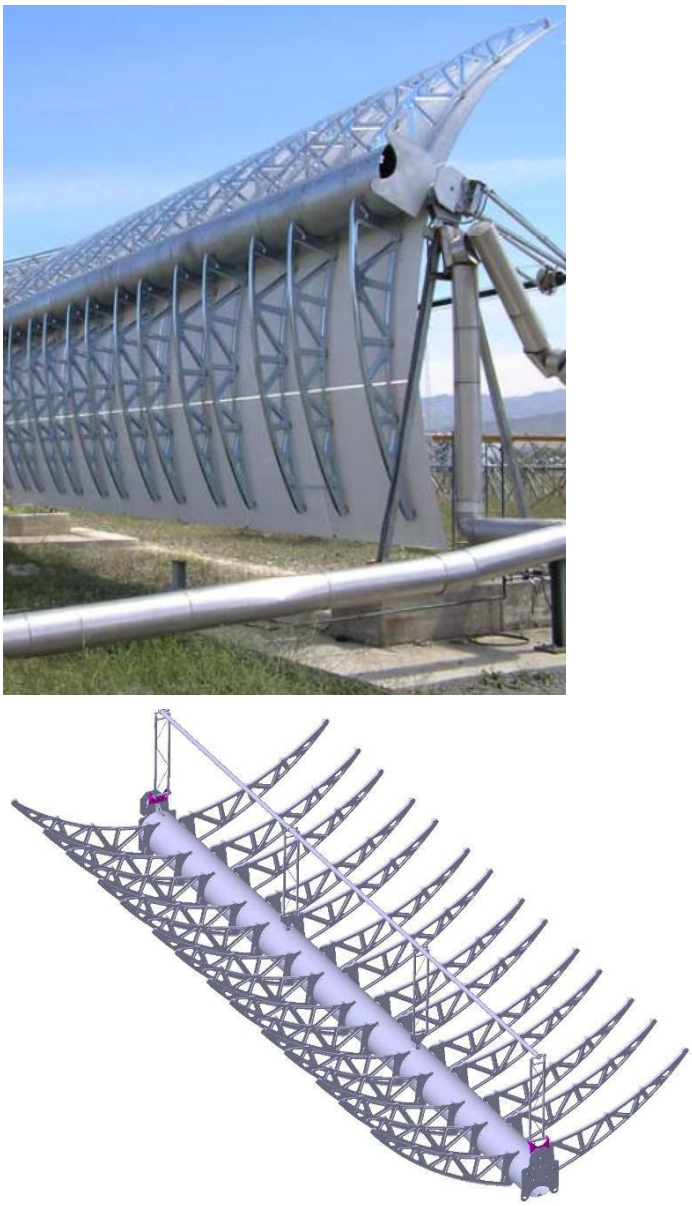

Figure 30: Torque tube of the Senertrough (source: Kearney 2007, Castañeda et al. 2006)

Figure 31: A stamped cantilver arm of the Senertrough (Source: Castañeda, SENER)

One Senertrough module is 12 m long and has an aperture width of 5.76 m. A collector assembly consists of 12 modules and is approximately 150 m long.[28] Two prototype modules were mounted and tested at the Plataforma Solar de Almería in October 2005 and in February 2006. Also in Andasol 1, a loop was installed. The first two plants that use the Senertrough are Extresol I & II in the Spanish region of Extremadura. It is also used in the power plants Valle I & II near Cádiz. Sener is currently developing a new, larger collector.

Flagsol GmbH & Partners: Heliotrough

Flagsol GmbH, together with with Schlaich, Bergermann & Partner (SBP), the Fraunhofer Institute for Material Flow and Logistics (IML) and DLR are developing the Heliotrough collector. The Heliotrough uses a torque tube as central stabilizing element. One module has a length of 19.1 m. A collector assembly consists of 10 modules and is 191 m long. The Heliotrough collector is one of the first designs with a bigger aperture width compared to the former collectors. While most previous collectors had an aperture width of 5.76 m, the Heliotrough aperture width is 6.77 m. This goes along with larger absorber tube diameters (90 mm instead of 70 mm).
A special characteristic of the Heliotrough is that the collector does not have mirror gaps at the pylons. The mirror surface covers continuously the bearing structure. This allows a higher land use efficiency. Counterweights are used to locate the centre of gravity of the collector within the tracking axis. The collector has been tested since 2009 under real operation conditions within a demonstration loop in one of the SEGS plants.

[28] See Castañeda et al. 2006.

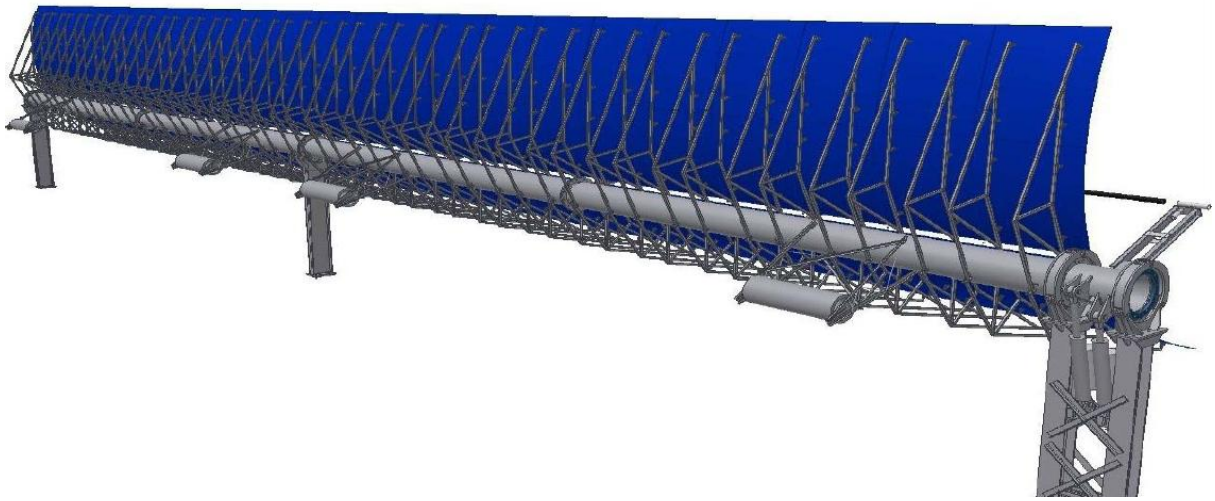

Figure 32: Model of the Heliotrough collector (source: Flagsol)

Figure 33: Installation of a Heliotrough collector element in one of the SEGS plants (source: Flagsol)

Skyfuel: Skytrough

The collector of the American company Skyfuel uses a space frame structure which is made out of extruded aluminium struts. Similar to the Solargenix Collector SGX-2, Skyfuel does not apply a central body like a torque tube or a torque box, but a big strutted space frame. With an aperture width of 6 m, it is a little broader than most other collectors. In 2010, Skytrough collectors were delivered to the Sunray Energy Inc. for the operation in the SEGS II plant.[29]

[29] See www.skyfuel.com.

Figure 34: The Skytrough collector (source: Skyfuel)

Siemens (Solel) Collector

The collector design of Siemens is taken over from Solel and is based on the LS-3 concept, but uses a torque tube instead of the v-truss of LS-3. In 2009, Siemens provided the collectors for the Lebrija solar power plant (50 MW) in southern Spain.

Figure 35: Siemens/ Solel Collector installation in Lebrija, Spain (source: Siemens)

Solarlite GmbH: SL 4600

The Solarlite GmbH developed the SL4600 parabolic trough collector, which has an alternative structure in comparison to the other collectors. Its central body is made of fibre glass and resin enclosing foam. A space frame structure at the back side takes the torsion forces. The aperture width is 4.60 m and the module length is 12 m. Silvered thin glass mirrors are used. In 2011, a 5 MW_e power plant was erected in Kanchanaburi, Thailand. It is the first parabolic trough power plant with direct steam generation.

Figure 36: The Solarlite SL 4600 collector (source: Solarlite)

An overview of some types of parabolic trough collectors and their technical data is given in the following figure.

Collector	LS-2	LS-3	Euro trough	ENEA	SGX-2	Sener trough	Helio trough	Sky trough	Solel / Siemens LS 6	Solarlite SL 4600
Bearing structure	Torque Tube	V-truss frame-work	Torque box	Torque tube	Aluminium space frame	Torque tube, stamped cantilever arms	Torque tube	Alumi-nium space frame	Torque tube	Fibre class and resin body, reinforced with space frame structure
Year	1985	1989	2002	2004	~2005	2005	2009	2010		2010
Aperture [m]	5	5.7	5.76	5.76	5.77	5.76	6.77	6	5.77	4.60
SCA length [m]	47	99	100-150	100	100-150	150	191	115	99	
Module length [m]		12	12	12.5	12	12	19.1	14		12
Rim angle [°]	80	80	80	~77		80	89.5	82.5		
Focal length [m]	1.49	1.71	1.71	1.8		1.70	1710	1.71		
Geometric concentration ratio	71	82	82	75-80	82	~80	76	75		
References	SEGS	SEGS	SEGS V, Andasol 1, 2, 3/Spain, Kuraymat/Egypt	Archimede power plant/Italy	Saguaro, Nevada Solar One	Extresol 1, 2/Spain	Test loop SEGS	Test loop SEGS	Lebrija/Spain	Kanchanaburi/ Thailand
Absorber tube diameter [m]	0.07	0.07	0.07		0.07	0.07	0.09	0.08		

Table 2: Important parabolic trough collectors

3.1.4 Sun Tracking System

Like any collector of a CSP system, parabolic troughs have to track the Sun in order to reach a continuous concentration of the direct solar radiation. As line concentrating collectors, parabolic troughs have a one-axis tracking system (while point concentrating systems need two-axis tracking).[30] The following figure gives a general idea of the tracking of a parabolic trough. The rotational axis is normally at the vertex line of the parabolic trough or in a parallel position slightly below it.

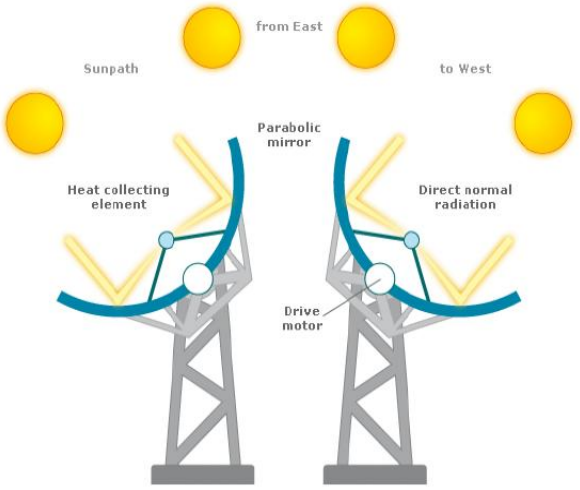

Figure 37: Single axis tracking of parabolic troughs (source: Abengoa Solar)

Theoretically, the parabolic troughs in the solar field of a CSP plant can have any horizontal orientation. Sun tracking is always possible. However, there is a preferred orientation, which is the north-south alignment with the respective east-west tracking. East-west alignment with the respective north-south tracking was applied only for experimental purposes. The reasons for the preference of the north-south alignment will be explained in the section "Solar field".
We want to specify now the tracking angles in the north-south alignment and in the east-west alignment:

- The orientation for north-south alignment can be described by the zenith angle s, which is the angle between the optical plane and the line to the zenith, and the azimuth angle γ, which indicates the orientation of the mirror aperture in relation to the horizon, where south=0° and west=90°. γ can have only two values: $\gamma = -90°$ if $\gamma_s < 0°$ and $\gamma = 90°$ if $\gamma_s > 0°$, where γ_s is the solar azimuth angle. This means that the mirror aperture is oriented to the east in the morning and to the west in the afternoon. The tracking angle is then the angle s, which is calculated as follows:

$$\tan s = \tan\theta_z |\cos(\gamma - \gamma_s)| \qquad (10)$$

  where θ_z is the solar zenith angle.

[30] Two-axis tracking for parabolic troughs was also tested in the beginning of the technology, but it did not achieve acceptance.

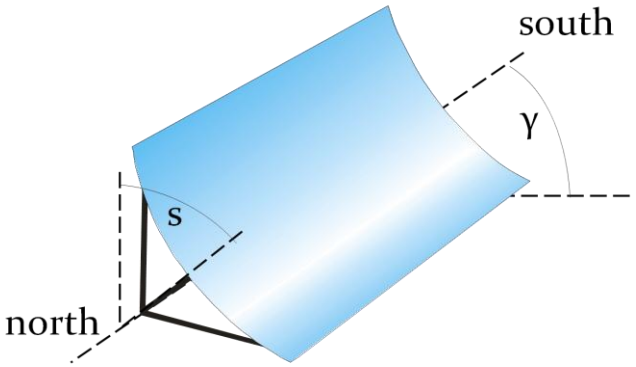

Figure 38: Tracking angles at parabolic trough systems with north-south alignment

- In the case of the east-west alignment, the tracking angle s is determined as follows:

$$\tan s = \tan\theta_z |\cos\ \gamma_s| \qquad (11)$$

For γ, the following determination holds: $\gamma = 0°$ if $|\gamma_s| < 90°$ and $\gamma = 180°$ if $|\gamma_s| > 90°$, which means that the mirror aperture is oriented to the south if the Sun is south of the east-west line and to the north if the Sun is north of the east-west line (what happens on the northern hemisphere between spring equinox and autumn equinox in the early morning, before 6:00 solar time, and in the late evening, after 18:00 solar time).

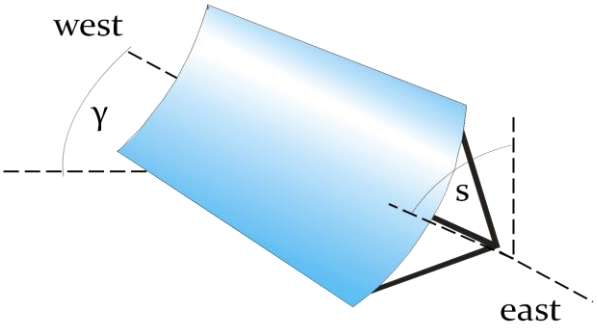

Figure 39: Tracking angles at parabolic trough systems with north-south alignment

The collector movement is realized by a drive unit that moves a collector assembly (a row of connected collector modules). Collector assemblies can be very long. The Eurotrough collector reaches 150 m and the new Heliotrough collector even 191 m. The drive units must be sufficiently strong to be able to move such large collector assemblies and to maintain them in the right position also under wind conditions. Mechanically, the drive unit can be realized as a motor-gearbox unit, like in the LS-2 system, or as an electro-hydraulic system as in the Eurotrough or the LS-3 collector. In the case of the latter, the drive unit consists of two cylinders, which are controlled by two valves, determining the direction of rotation.[31]
The design tracking accuracy in the SEGS plants is guaranteed until a wind speed of 9 m/s. Power plant operation is possible until a wind speed of 16-20 m/s, but at the expense of a reduced tracking accuracy.

[31] Dependent on the location of the collector in the solar field, the cylinders differ in size. The collectors at the border of the solar field need a stronger hydraulic drive, and consequently bigger cylinders, because they have to withstand higher wind loads than the collectors in the centre of the solar field.

The control of the collector tracking needs information about the Sun position. This information can be provided in two ways:

- The Sun position can be calculated with an exact mathematical algorithm. This is implemented, for instance, in the Eurotrough. The collector axis position is compared to the calculated Sun position and a possible difference is closed by the drive unit.[32]
- The Sun position can be measured by sensors that give a signal to the local controller which operates the electrical motors or hydraulic cylinders. This system is applied in the SEGS plants. The sun sensor can consist of convex lenses which guide the sun beams onto two photocells. By measuring the differential current between the two photocells, aberrations of the collector orientation in relation to the Sun position are detected. The resolution is about 0.05°. Such a system needs an additional simple rough Sun tracking algorithm for cloudy conditions and for start-up and shut-down. The photocell system reaches an accuracy of ± 0.1°.[33]

A central controller registers environmental conditions like the wind speed. If there are hazardous operating conditions then all collectors are moved to a safety position, which is nearly the vertical position, with a slight inclination of the mirrors to the bottom. During the night, the collectors are also in the safety position.

Figure 40: Hydraulic actuator of Skyfuel's Skytrough (left), electrical gear drive of the LS-2 collector (source: Skyfuel)

[32] For further information about the algorithm, see for instance Blanco-Muriel et al. 2001.
[33] See Mohr et al. 1999.

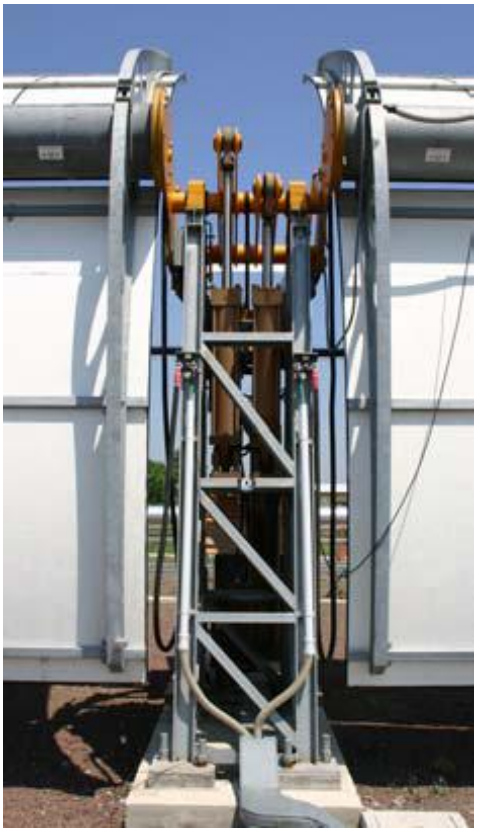

Figure 41: Hydraulic drive pylon of the Enea collector (source: NREL)

3.2 Receiver

Receivers for parabolic trough power plants have the task to convert the radiation that is projected onto them into heat and to transport the heat to the pipes, which leads it further to the power block. Important are high radiation absorption and low heat losses. A constructive challenge is the heat expansion of the receiver due to the changing temperatures between operation and non-operating state. It has also to be taken into account that the receivers in a parabolic trough power plant are moveable parts which require flexible pipe connections.
The receiver has to fulfil several geometrical and physical requirements. The reflected radiation has to hit the absorber surface, which implies geometric constraints. The radiation has to be converted as completely as possible into heat and the optical and thermal losses at the surfaces of the receiver components should be as small as possible. Special coatings and thermal insulation measures are applied to achieve this.

Parabolic trough power plant receivers are produced by the German Schott AG, the Italian Archimede Solar Energy (ASE) and the German Siemens AG, which acquired in 2009 the Israeli company Solel Solar Systems that had developed a receiver.[34] Schott and Siemens receivers use thermo oil as heat transfer fluid. Therefore the receivers are designed for an operation temperature of 400°C. Siemens receivers are also used in the first direct steam generating plants. Archimede, on the other hand, developed a receiver for molten salt as heat transfer fluid. It is designed for a maximum operation temperature of 580°C.

[34] The information about the receivers of these three suppliers that appears in the present section is taken from the fact sheets at the pages
http://www.energy.siemens.com/co/en/power-generation/renewables/solar-power/concentrated-solar-power/receiver.htm for the Siemens UVAC 2010 receiver,
http://www.archimedesolarenergy.com/receiver_tube.htm for the Archimede HEMS08 receiver, and
http://www.schottsolar.com/de/produkte/solarstromkraftwerke/schott-ptr-70-receiver for the Schott PTR 70 receiver.

Figure 42: Absorber tube integrated in a parabolic trough collector (above left), Siemens UVAC 2010 (above right), Archimede HEMS08 (below left), Schott PTR 70 (below right) (sources: DLR, www.energy.siemens.com, www.archimedessolarenergy.com, www.pressebox.de)

3.2.1 Receiver components

The receiver has to be constructed in such a way that high radiation absorption and low thermal losses are realized. Low thermal losses refer to low radiative losses as well as low convective and conductive losses. In the following we will describe how and with which components the receiver fulfils these functional requirements. We will refer to the absorber tube, the evacuated glass tube and a group of further specific constructive elements (bellows for thermal expansion, glass-to-metal joints and getter).

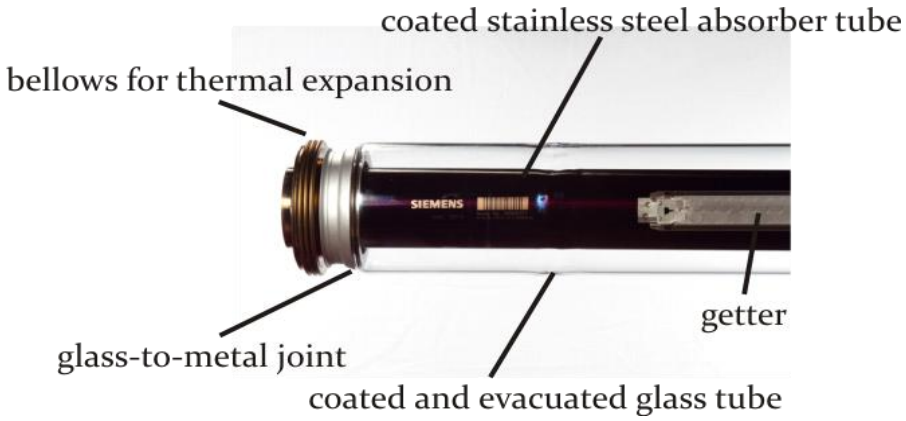

Figure 43: Structure of a parabolic trough receiver (source: Siemens)

Absorber tube

In order to reach high radiation absorption and a low radiative heat loss at the absorber tube, its absorptance must be high in the visible light range and its emissivity must be low in the infrared range. Remember that the absorptance and the emissivity of a body for a specific spectral range are always identical: $\alpha_\lambda = \varepsilon_\lambda$ (Kirchhoff's law). However, as indicated by the index λ, this is valid in relation to a given wavelength. For different spectral ranges, absorptance and emissivity can be (and normally *are*) different. In the case of the absorber tube, the absorptance must be high for one spectral range, the solar spectral range ($250\text{nm} \leq \lambda \leq 2500\text{nm}$), and the emissivity must be low for another spectral range, the infrared range ($3000\text{nm} \leq \lambda \leq 50000\text{nm}$). This is physically possible and special selective coatings have been developed to reach this. Selective coatings for the absorber tubes are made of cermet, which is a material that consists of metallic nano-particles that are embedded in a ceramic matrix. (The combination of ceramic (cer) and metallic materials (met) motivates the name "cermet".)
More exactly, the coating consists of different layers. First, there is a reflection layer made out of a metal that is highly reflective in the infrared range, for instance copper, aluminium or molybdenum. Second there is the cermet layer, which itself can be divided into different layers with higher and lower metal content. The cermet layer consists of an oxide like Al_2O_3 or SiO_2 and a metal like molybdenum. The antireflection ceramic layer consists of oxides like Al_2O_3 or SiO_2.

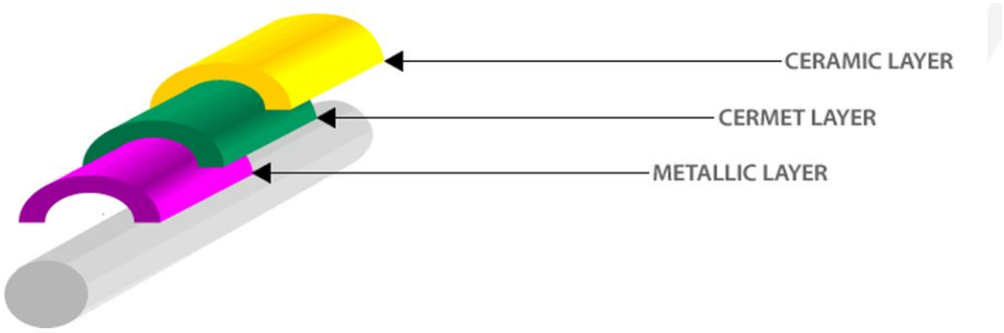

Figure44: Multi-layer coating of the absorber tube (source: Archimede)

Additional adhesion layers are introduced that guarantee the adhesion of the functional layers on the structural tube material. An additional gas diffusion barrier layer can be applied to minimize the gas diffusion through the absorber tube.[35]
An absorptance of 0.95 (Schott, Archimede) or even 0.96 (Siemens) for the solar radiation have been reached, and an emissivity of 0.1 (Schott, Archimede) or even 0.09 (Siemens) for the thermal radiation at 400°C. Archimede indicates additionally an emissivity of less than 0.15 at 580°C for the molten salt receivers, which are designed to resist higher temperatures than the therm0 oil systems of Schott and Siemens. The higher the temperatures are, the more difficult is the design of an efficient selective coating because there is a larger overlap of the thermal emission spectrum and the solar spectrum. Already at 400°C there is a non-negligible spectral overlap in the range of 1500 to 2500 nm.
The following diagram shows the absorptance and emissivity of an optimized selective coating for parabolic trough power plant receivers. More exactly, it shows the reflectivity, which has the value of 100% minus absorptance resp. emissivity. It is shown the reflectivity of a coating with the following layers: molybdenum/cermet Mo-SiO_2 (high metal volume fraction)/cermet Mo-SiO_2 (low metal volume fraction)/SiO_2. Additionally, the spectral ranges of the solar radiation (orange line) and the thermal radiation of a black body at 400°C (green line) are shown.

[35] See Kuckelkorn/Graf 2004.

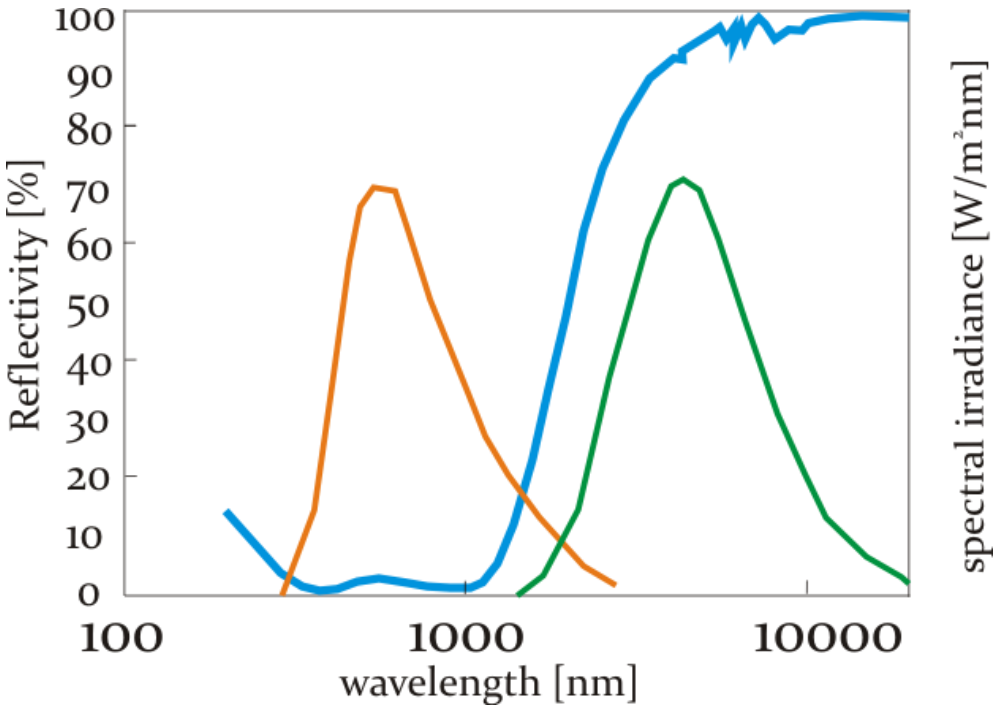

Figure45: Reflectivity for an optimized spectrally selective coating (blue line) and spectral ranges of the solar radiation (orange line) and the black-body radiation at 400 °C (green line), spectral irradiance without scale (source: Esposito et al. 2009)

The absorber tube must have a sufficient diameter to permit a *high intercept factor*. The intercept factor is the ratio of the total reflected radiation to the reflected radiation that hits the absorber surface. On the other hand, the absorber diameter should not be too big in order to maintain the thermal losses low. An absorber tube with a big diameter has a large surface area per meter and loses therefore more heat than an absorber tube with a smaller diameter.

In order to estimate the appropriate absorber tube diameter, we will take an absorber, the diameter of which is just sufficient to receive all the radiation reflected by a geometrically perfect parabolic mirror, i.e. by a parabolic mirror that does not have slope errors and that does not widen the beam radiation due to microscopic errors. The necessary absorber diameter to reach an intercept factor of 1 depends, then, on the distance of the absorber tube from the mirror and on the solar beam angle. The solar beam angle is the opening angle of the direct solar radiation. It amounts to 32' (it is not zero because of the extension of the Sun disc). Because of this beam angle the Sun image at an ideal parabolic trough is not a one-dimensional mathematical line but has a two-dimensional extension. The rays that are reflected from the mirror are reflected with a corresponding angular variance of 32'.

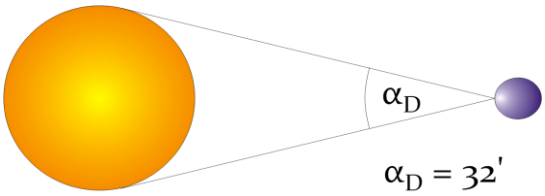

Figure 46: Sun beam angle

The distance between the mirror and the absorber is different for the different points of the mirror. The largest distance is between the mirror rim and the absorber. So we take the rim of the parabolic mirror to determine the absorber diameter.

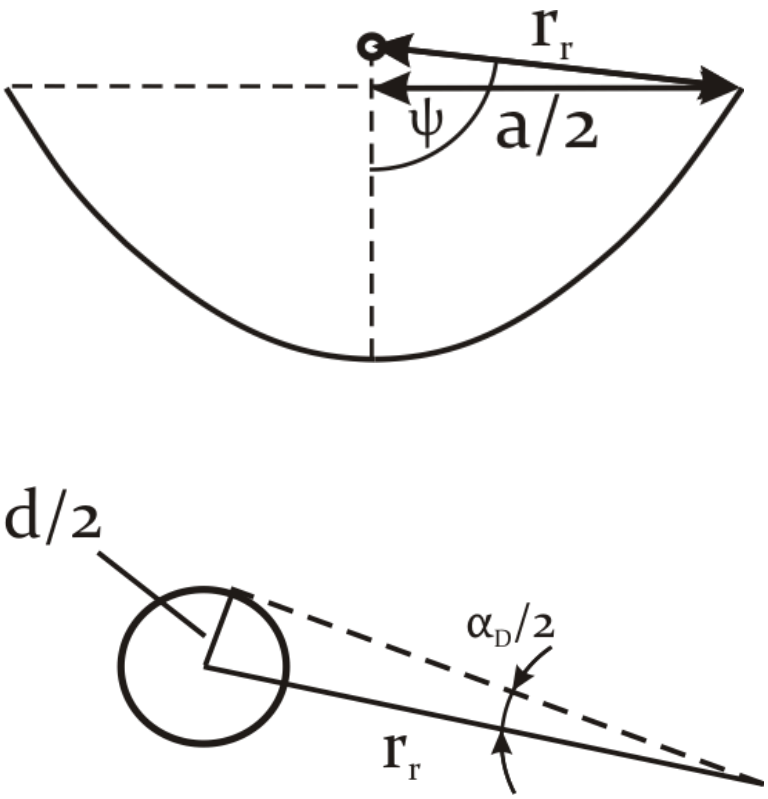

Figure 47: Geometrical parameters at the collector and the receiver

The foregoing figures illustrate the relation between the absorber tube diameter, the half solar beam angle and the distance between the absorber tube and the mirror rim:

$$d/_2 = r_r \cdot sin\frac{a_D}{2}, \tag{12}$$

where d is the absorber diameter, a_D the Sun beam angle and r_r the distance between the absorber tube and the mirror rim. The absorber diameter is, consequently:

$$d = 2r_r \cdot sin\frac{a_D}{2}. \tag{13}$$

Alternatively, the diameter can be expressed with the aperture width and the rim angle. Taking into consideration that

$$r_r = \frac{a}{2\,sin\psi}, \tag{14}$$

the result is:

$$d = \frac{a \cdot \sin\frac{a_D}{2}}{\sin\psi}. \tag{15}$$

This is valid for perfect mirrors without surface imperfections. Additionally, the calculation supposes that the direct radiation hits the collector with the incidence angle zero, because only in this case the distance from the mirror rim to the absorber tube is a/2 for the reflected light. Generally, the incidence angle is not zero and the distance for the reflected light is larger. That means that the absorber tube has

to be dimensioned a bit larger in order to maintain high intercept factors also in situations when the incidence angle is large. In order to take into account the effect of the varying incidence angle θ the value indicated in equation (15) has to be divided by $\cos\theta$. However, it is an optimization task to find the ideal absorber diameter that allows to reach a high average intercept factor without being too large and to cause too high thermal losses.

If we take into consideration mirror imperfections that widen the beam beyond the solar beam angle, the absorber diameter must be larger than indicated until now, if the absorber still shall have an intercept factor of 1. In order to quantify the mirror imperfections, an additional dispersion angle δ can be defined (see the following figure) so that the whole beam spread after the reflection on the mirror is $a_D + \delta$. The absorber diameter is now[36]:

$$d = \frac{a \cdot \sin\frac{a_D+\delta}{2}}{\sin\psi} \qquad (16)$$

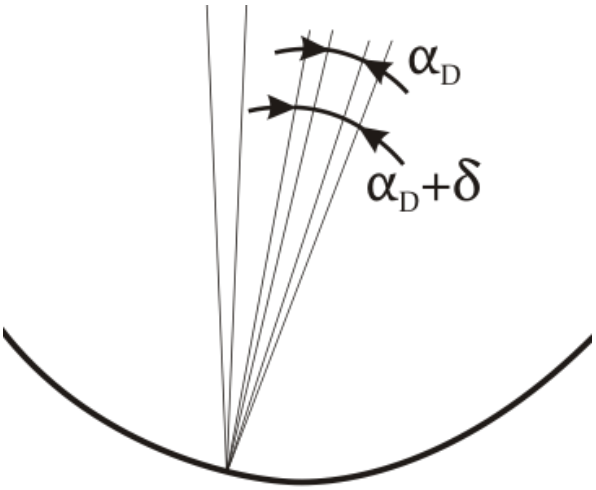

Figure 48: Sun beam angle and additional dispersion angle

Once more, this does not take into account the additional beam widening that is caused by incidence angles larger than zero.

Most of the receivers produced by the three mentioned companies have an absorber tube diameter of $d = 70\text{mm}$. The glass tube has a diameter of 125mm at the Schott and the Archimede receivers and 115mm at the Siemens receiver.

Taking into consideration that these receivers are used, for instance, in the Eurotrough collector with an aperture width of $a = 5.77\text{m}$ and a focal length of $l = 1.71\text{m}$, i.e., according to $tan\psi = \frac{\frac{a}{f}}{2-\frac{1}{8}\cdot\left(\frac{a}{f}\right)^2}$ (see "collector geometry"), with a rim angle of 80.3°, $a_D + \delta$ would be 1.37° and the dispersion angle δ would amount to 0.84° if no incidence angle effect is considered. If the incidence angle effect is taken into account, the dispersion angle would be smaller.

Recently, Schott developed receivers with a larger diameter for larger collectors. The new PTR 80 and PTR 90 have an absorber diameter of 80mm and 90mm respectively.

[36] See Duffie/Beckman 2006.

Glass tube

In order to reach a low convective (and also conductive) heat loss, the absorber tube is protected with a glass sheath around it, which hinders the air to flow around the hot absorber tube. Additionally, the glass body is evacuated so that the convective and conductive heat loss is reduced further. Schott indicates a remaining gas pressure of $\leq 10^{-3}$mbar, Archimede even of $\leq 10^{-4}$mbar.
The transmittance of the glass tubes, which are made out of borosilicate glass, is indicated to be at least 0.96 for the solar radiation. A special antireflective coating guarantees a low reflectivity of the glass sheath. Archimede indicates that this coating increases the transmittance by 0.04 (from 0.92 without coating to the mentioned 0.96 with coating).
The glass material has quite a low transmittance in the infrared range. This also contributes slightly to the insulation effect because a part of the emitted thermal radiation of the absorber tube is maintained in the system: It heats the glass, reduces thereby the convective heat loss from the absorber to the glass tube and generates additional thermal radiation back onto the absorber tube (which, however, is hardly absorbed because of the selective coating, which we will explain below).
The following diagram illustrates the transmittance of borosilicate glass. In the case of the Archimede receiver, the thickness of the receiver glass tubes is 3 mm. Remember that the solar radiation is principally in the spectral range of 250 to 2000 nm. The thermal radiation at 400°C is principally within the spectral range of 2500 to 9000 nm.

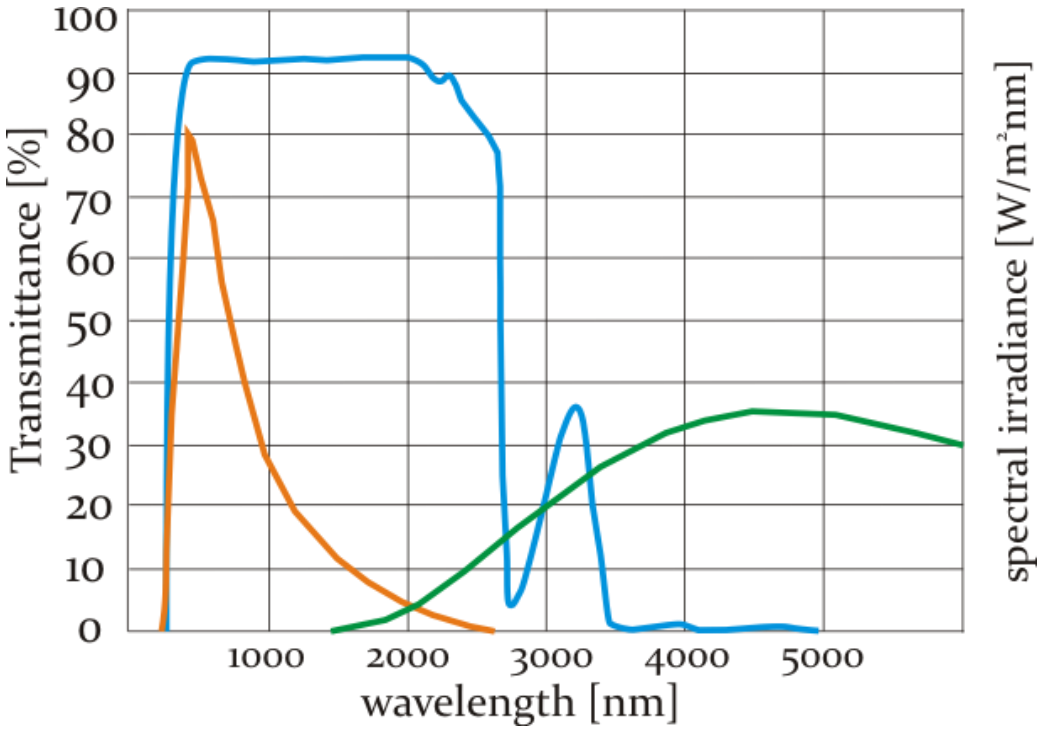

Figure 49: Transmittance of borosilicate glass without antireflective coating (blue line), solar spectrum (orange line) and thermal radiation at about 380 °C (green line), spectral irradiance without scale (source for transmittance of borosilicate glass: Schott)

Further important receiver components

The temperature changes of the absorber tube require that it is connected in a flexible way with the glass tube. This is guaranteed with the bellows at the receiver ends.
Additionally, the temperature changes of the glass tube and the metallic elements at the receiver ends imply a specific constructive challenge: The thermal expansion coefficients of the glass near the

compensator and the compensator itself have to coincide in order to reduce tension forces. This is necessary especially for the durability of the vacuum in the glass tube.
Furthermore, a getter is integrated into the receiver in order to maintain the vacuum. Especially hydrogen, which emerges in smaller quantities due to cracking processes in the thermo oil, can traverse the absorber tube and diminish the vacuum quality. The getter absorbs the hydrogen and avoids thereby the deterioration of the thermal insulation properties of the receiver.
The receivers have to resist certain pressure. Maximal operating pressures are indicated to be 20 bars for the Archimede receiver and 40 bars for the Schott receiver. This is important for their use in direct steam generating power plants where they limit the steam pressure. Other receivers have to be used (respectively developed) if higher pressures are to be achieved. The Solarlite direct steam generation power plant projects limit the steam pressure to 30 bars.[37] Novatec's Fresnel power plants PE 1 and PE 2, however, are operated with 55 bars.

3.2.2 Receiver efficiency

The following figure illustrates the energy flows at the receiver. There are optical and thermal losses that reduce the useable power in comparison to the radiant flux that is projected onto the receiver.

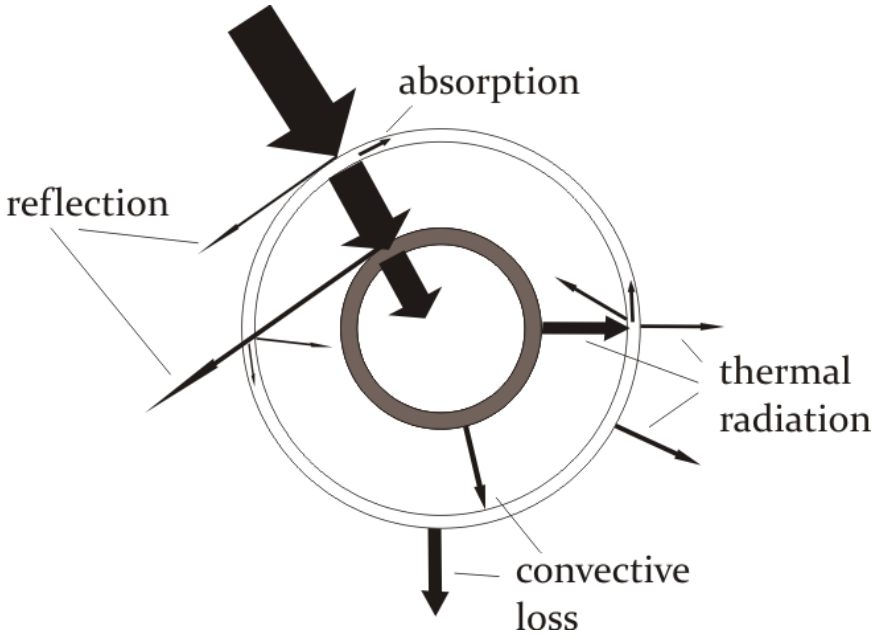

Figure 50: Energy flows at the receiver

Optical losses

Optical losses are produced at the glass tube as well as at the absorber tube. The glass tube has only a limited transmittance so that a part of the radiation is reflected and another part is absorbed. As already mentioned, antireflective coatings and highly transparent glass materials reduce the loss to around 4%. The absorber tube has only a limited absorptance so that another part of the incoming radiation is reflected at the absorber tube. Selective coatings reduce this loss to around 5%. These optical losses amount, hence, to

[37] See www.solarlite.de.

$$\dot{Q}_{loss,opt}/A_{rec,act}G_{rec} = 1 - (1 - 0.04) \cdot (1 - 0.05) = 8.8\% \,,$$

where G_{rec} is the irradiance on the active receiver surface area $A_{rec,act}$.
The foregoing equation relates the losses to the active receiver surface area and not to the total receiver surface area. This is the case because an additional optical loss has to be taken into account: The bellows and metal shields at the ends of the receiver reduce the active receiver area by nearly 4% (Siemens indicates 3.6%). Taking into consideration this additional loss and assuming the mentioned value, the optical losses over the whole receiver amount to

$$1 - \ (1 - 0.036) \cdot (1 - 0.04) \cdot (1 - 0.05) = 12.1\% \,.$$

Thermal losses

Thermal losses are generated by thermal radiation, convection and heat conduction. Heat conduction and convection between the hot absorber tube and the cooler glass tube are reduced considerably by the vacuum. Heat conduction can be neglected and will not be mentioned here.
The thermal losses of a receiver depend strongly on the temperature difference between the absorber tube and the surrounding air. Experiments with the Solel UVAC3 receiver, the forerunner of the actual Siemens UVAC 2010, showed the following losses at an ambient temperature of 23°C (without wind): 130W/m at 300°C, 200W/m at 350°C, 310W/m at 400°C and 450W/m at 450°C.[38] A function that approximates these values is:

$$\dot{Q}_{loss,therm}[\mathrm{W/m}] = 0.26 \cdot \Delta T + 1.05 \cdot 10^{-8} \cdot \Delta T^4, \qquad (17)$$

where ΔT is the difference between heat fluid temperature and ambient temperature.

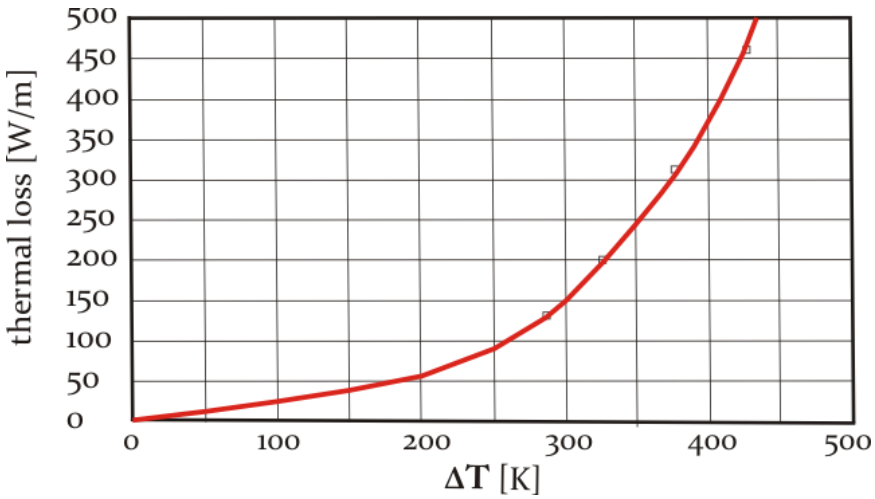

Figure 51: Thermal loss at the Solel UVAC3 receiver, measurement points and approximating function

The combination of a linear dependence on the temperature difference and a dependence on the fourth power of the temperature difference corresponds to the combination of convective heat loss (linear):

$$\dot{Q}_{conv} = h \cdot A \cdot \Delta T \,, \qquad (18)$$

[38] See Burkholder/Kutscher 2008.

where h is the heat transfer coefficient and A the surface area of the tube,
and radiative heat loss (fourth power):

$$\dot{Q}_{rad} = \varepsilon_T \cdot \sigma \cdot A \cdot T^4 \,, \tag{19}$$

where ε_T is the mean emissivity at the temperature T.

Energy balance

Finally, we can establish an energy balance of the complete receiver. One possibility is the following one:

$$\dot{Q}_{use} = A_{rec,act} G_{rec} - \dot{Q}_{refl,glass} - \dot{Q}_{refl,abs} - \dot{Q}_{therm,glass} - \dot{Q}_{conv,glass} \tag{20}$$

$\dot{Q}_{use}$	useable power
$A_{rec,act}$	active receiver surface area
$G_{b,rec}$	irradiance on the receiver
$\dot{Q}_{refl,glass}$	power loss due to reflection on the glass tube
$\dot{Q}_{refl,abs}$	power loss due to reflection on the absorber tube
$\dot{Q}_{rad,glass}$	power loss due to radiant emittance of the glass tube
$\dot{Q}_{conv,glass}$	convective heat loss at the glass tube

In this equation we do not consider the convective and radiative heat loss of the absorber tube, but of the glass tube.
Another possibility, taking into consideration the convective and radiative heat loss of the absorber tube and not of the glass tube, would be:

$$\dot{Q}_{use} = A_{rec,act} G_{rec} - \dot{Q}_{refl,glass} - \dot{Q}_{abs,glass} - \dot{Q}_{refl,abs} - \dot{Q}_{rad,abs} - \dot{Q}_{conv,abs}. \tag{21}$$

$\dot{Q}_{abs,glass}$	power that is absorbed by the glass tube
$\dot{Q}_{rad,abs}$	energy loss due to radiant emittance of the absorber tube
$\dot{Q}_{conv,abs}$	convective heat loss of the absorber tube

The two equations (20) and (21) would render similar values, because the heat losses of the absorber tube and the heat losses of the glass tube are similar. However, they are not identical because of two effects:

- First, a part of the heat that the glass tube loses, especially the radiative loss, is given back to the absorber tube. However, the radiative heat loss of the glass tube, which does not reach high temperatures, is quite low so that the heat flow from the glass tube to the absorber tube is also very low. Additionally, the absorptance of the absorber tube in the infrared spectrum is very low so that the final effect of the infrared reemission of the glass tube on the absorber tube is extremely low.
- Second, a part of the emitted radiation by the hot absorber tube traverses the glass tube and does not appear in the heat losses of the glass tube. The diagram above illustrated the transmittance of borosilicate glass (without antireflective coating), which is about 92% in the visible range, but quite low in the range of 2500nm-9000nm, which is the range of the thermal

radiation of a body with 400°C. However, it is not zero so that a part of the thermal radiation of the absorber tube crosses the glass tube without being absorbed.

An important difference between the heat loss of the absorber tube and the heat loss of the glass tube is the different contribution of the different heat loss processes: At the absorber tube, the radiative heat loss is dominant because of the high tube temperature and because of the vacuum that hardly allows convective or conductive losses (however, as no technically generated vacuum is perfect, there is a rest especially of convective heat loss that is considered in equation (21)). At the glass tube, on the contrary, the convective heat loss is more important than the radiative loss. The temperature difference between the glass tube and the environment is quite small and does not allow high radiative losses, but the surrounding air moves freely around the glass tube so that the convective heat loss is important.

A quantification of the different heat loss processes and their share in the total heat loss is not possible without taking into consideration several boundary conditions as, most importantly, temperature differences, absolute temperatures, wind conditions and air humidity.

3.3 Heat transfer fluid

The heat transfer fluid (HTF) has the task to accumulate the thermal energy in the collectors and to transport it to the power block. There are two fundamental manners how the heat can be transferred to the power block: First, a special HTF is applied, from which the heat is transferred to the Rankine cycle working fluid (water), or, second, the steam for the Rankine cycle is generated directly in the absorber tubes of the parabolic troughs and transported to the turbine. The first version is called *indirect steam generation*, the second one *direct steam generation*. Indirect steam generation power plants contain two fluid cycles, a heat transfer fluid cycle and the Rankine cycle. The thermal connection between them is realized in a steam generator train, which consists of an economizer (feed water preheating), an evaporator and a superheater. Direct steam generation power plants, on the contrary, contain only one fluid cycle, the steam cycle. Preheating, steam generation and (if included) superheating is realized directly within the solar field.
Indirect steam generation systems use a liquid heat transfer fluid. The heat transfer medium in direct steam generation systems is the water/steam of the Rankine cycle itself.

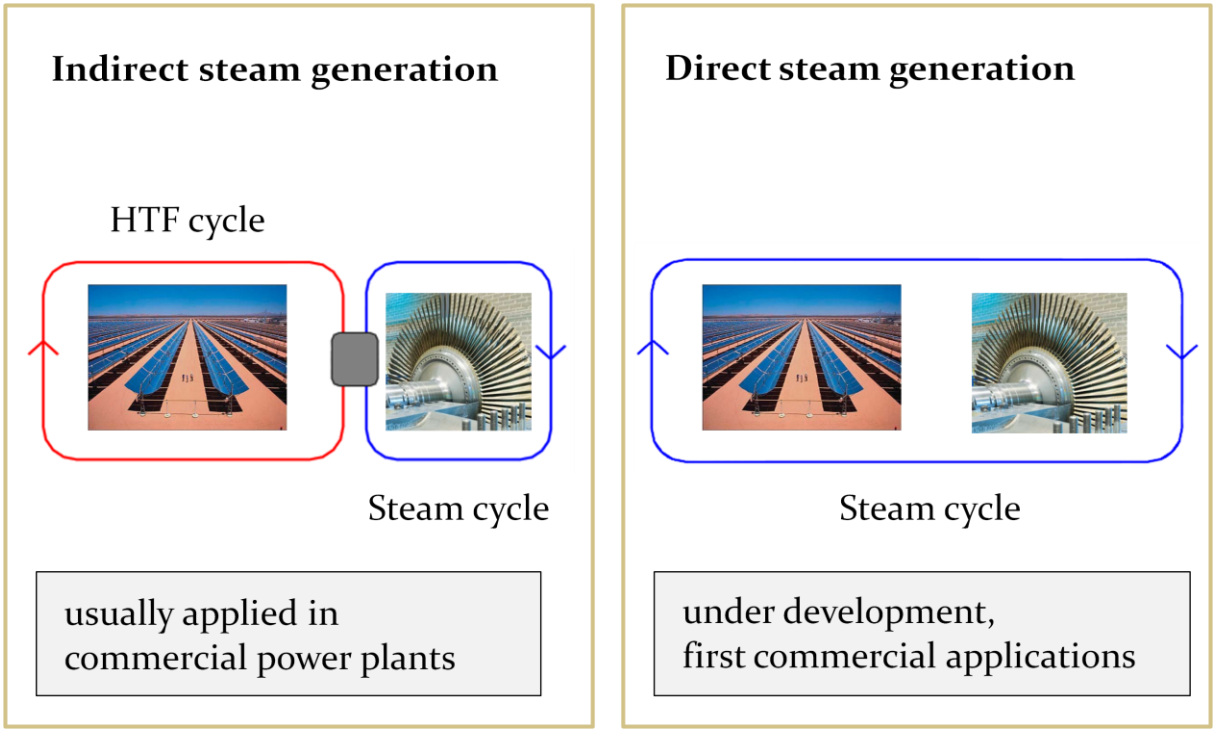

Figure 52: Indirect and direct steam generation

Indirect steam generation is what is usually applied in commercial parabolic trough power plants. Direct steam generation is still in development. However, the first commercial plant is currently being built in Thailand.

3.3.1 Heat transfer fluid in indirect steam generation power plants

A HTF has to fulfil certain requirements:
It must be liquid. That means that it should have a sufficiently high evaporation temperature (under manageable pressures) so that it is not evaporated under the high temperatures that are reached in the

solar field. Additionally, low freezing temperatures are an advantage so that no freezing protection measures are necessary if the temperatures in the solar field get low. It is also important that its thermal stability is sufficient to stand the high operation temperatures (no thermal cracking, for instance). Evaporation temperature and thermal stability determine the maximum operation temperature of a HTF.
In order to store and transport high amounts of thermal energy, a high specific heat capacity is useful. Also high heat conductivity is advantageous for quick heat transfer processes. Low viscosity is important to reduce pumping energy.
Of course, low investment costs and a sufficient availability are also important criteria.
Finally, environmentally friendly materials are preferable as well as materials with low inflammability and low explosivity.

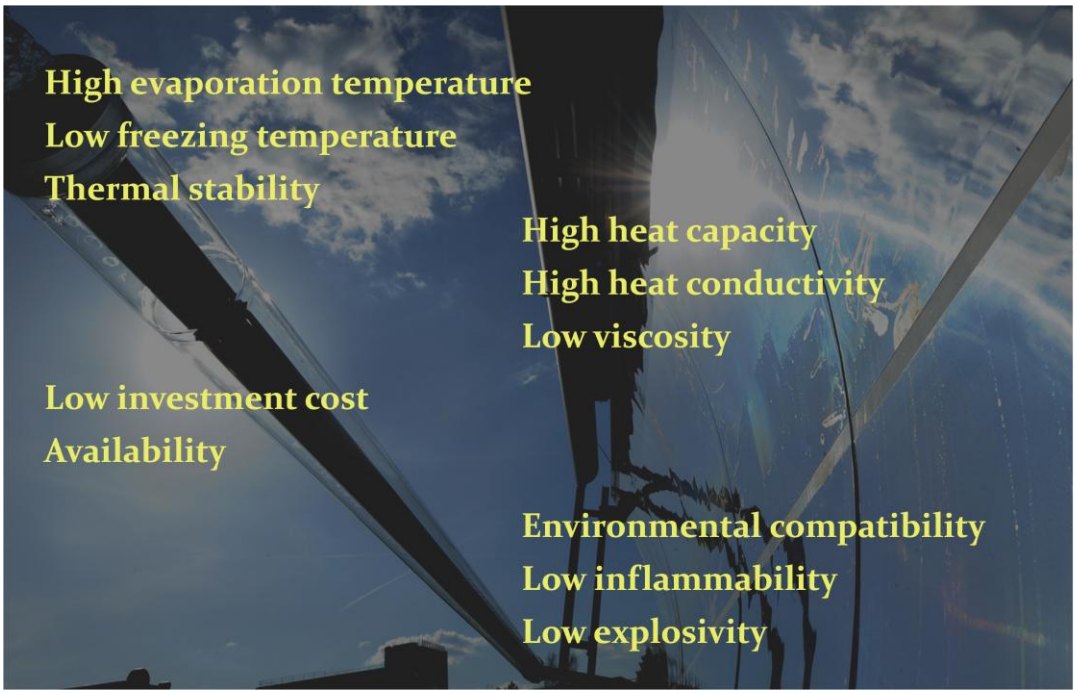

Figure 53: HTF selection criteria

Some criteria are more important than others. Evaporation temperature and thermal stability, for instance, are very important criteria because they determine the maximum steam cycle temperature, which on its part determines the power block efficiency. Low inflammability, on the contrary, is not always considered a decisive selection criterion.
The importance of the different criteria also depends on the system configuration. For instance, if the power plant contains a thermal storage, then it could be an advantage to use the HTF also as storage medium because this means that no additional heat transfer step between HTF and storage medium is required. In this case, when very large quantities of the HTF are needed, economic criteria may be more important than in other cases.
The following table gives an overview over some properties of some materials that are considered as appropriate candidates for a usage as HTF in parabolic trough power plants.

Table 3: Important properties of some possible HTFs (source: Jähnig 2005)

Medium	Max. temperature [°C]	Heat capacity [J/kg/K]	Heat conductivity [W/m/K]	Vol. spez. heat capacity [kWh/m³/K]	Cost
Mineral oil	300	2600	0.12	0.55	+
Synth. oil	400	2300	0.11	0.57	-
Silicon oil	400	2100	0.1	0.525	-
Nitride salt	450	1500	0.5	0.75	O
Nitrate salt	565	1600	0.5	0.8	+
Carbonate salt	850	1800	2.0	1.05	-
Sodium (liquid)	850	1300	71.0	0.3	O

+ low
O moderate
- high

Nearly all parabolic trough power plants use synthetic thermo oil as HTF. Mineral oil was used in an early commercial power plant in the 1980s. Currently efforts are done to use molten salt as HTF. However, synthetic thermo oil is still the standard HTF.

Synthetic thermo oil

Synthetic thermo oil (or simply "thermo oil") is a eutectic mixture[39] of biphenyl/diphenyl oxide. There are more than 25 years of experience with this HTF in parabolic trough power plants. It has been proven that the technology is reliable, which is also an important argument for investors and operators to go on using it.

Synthetic thermo oil satisfies quite well the mentioned requirements. It is liquid until 12°C, which means that freeze protection is quite easy or even unnecessary.[40] It has quite a high specific heat capacity and it can be acquired in large quantities.

However, it has also some disadvantages and limitations:

- The maximum operation temperature is about 400°C. Beyond this temperature, thermal cracking happens, which destroys the thermo oil. It resists higher temperatures than mineral oil. However, live steam temperature is limited to about 370 °C[41], which limits the power block efficiency.
- Thermo oil has to be replaced periodically because of aging processes (i.e. the chemical structure changes over longer time spans).
- Thermo oil is quite expensive. About 5% of the investment costs for the Andasol power plants must be afforded for the HTF.[42]
- The high costs and also high vapour pressures at the operation temperatures impede that thermo oil is used as storage medium.

[39] A eutectic mixture is a mixture in which the proportions of the constituents is selected in such a way that there is a clear melting point at which all constituents melt at the same time. Other mixture proportions have a melting temperature range, within which the different constituents melt one after the other.
[40] Therminol VP-1, see www.solutia.com.
[41] See Hartl et al. 2009.
[42] See IEA 2010.

- Thermo oil is environmentally less friendly than some other possible media. Leakages are not only a problem for the plant operation but also for the environment.

Mineral oil

Mineral oil was used in the first SEGS plant, which started operation in 1985. It had the advantage that a direct storage system could be implemented, i.e. a storage system that uses the HTF directly as storage medium, because mineral oil can be used as thermal storage medium as well. However, the main disadvantage of mineral oil, which motivated its substitution by thermo oil, is its operation temperature limit. At temperatures above 300°C it gets unstable.

Molten salt

Today, the usage of molten salts as HTF is still under investigation. The pioneer in this field is the Italian company Archimede Solar Energy (ASE). The used molten salt mixture is the eutectic mixture of 60% $NaNO_3$ and 40% KNO_3.
The most important advantage of these molten salts as HTFs is that the output temperature of the solar field can be increased to 450-550°C, which allows a higher Rankine cycle efficiency than in thermo oil systems.
The usage of molten salt as HTF allows also the integration of a direct storage into the power plant Molten salt is already used in parabolic trough power plants (with thermo oil as HTF) as storage medium. Additionally, and independently on the storage medium, the higher operation temperatures of systems with molten salts as HTF allow the reduction of the storage size for a given capacity because of the higher temperature level of the charged storage.
Molten salts are cheaper than thermo oil. They are used in agriculture as fertilizer and are available in large quantities. Additionally, they are environmentally friendlier. They are non-toxic and also non-inflammable.
An important disadvantage of molten salts is the high freezing point, which is between 120 and 220°C for binary[43] and ternary[44] molten salts. That means that strategies have to be developed to avoid the freezing of the molten salts. Different solutions are conceivable: The piping system could be heated or the HTF could be stored in a sufficiently insulated tank during the night.
The higher temperature and the more aggressive characteristics of salt may also imply that superior and more expensive materials have to be used.
Since July 2010 a demonstration plant with molten salt as HTF is in operation in Sicily/Italy.

3.3.2 Direct steam generation

Direct steam generation (DSG) means that the steam is generated directly in the solar field and not indirectly through heat transfer from a distinct HTF. The heat transfer medium that flows through the receivers of the solar field is the working fluid of the Rankine cycle itself. Of course, this working fluid is normally water. Water is, indeed, quite an ideal HTF if we consider the suitability criteria for HTFs mentioned above. Only the criterion of the high evaporation temperature does not apply, but this criterion is of no importance in the case of direct steam generation, because evaporation is just intended. For small systems and temperature levels below 400°C, however, organic working media may be an alternative; they allow acceptable plant efficiencies also at low operation temperatures.

[43] A binary mixture is a two-part mixture of some substance
[44] A ternary mixture is a three-part mixture of some substance

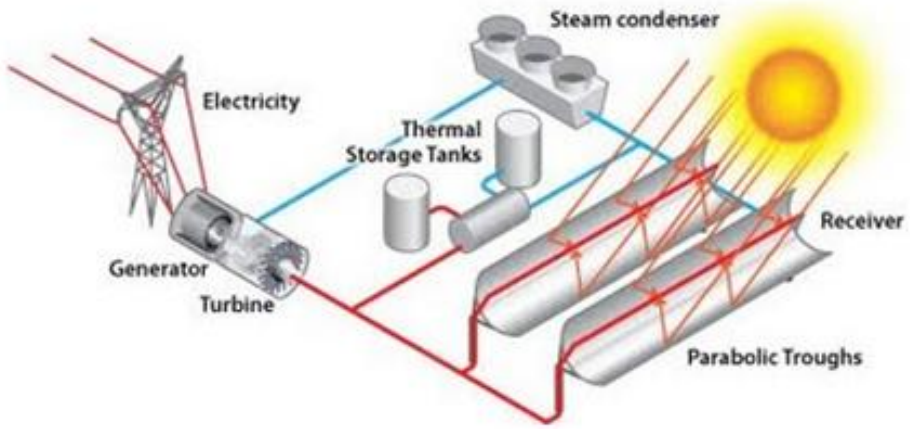

Figure 54: Direct steam generation system (source: www.4.bp.blogspot.com)

DSG is the standard solution in Fresnel power plants, while parabolic trough power plants until now were constructed as indirect steam generation systems. However, there are continuous efforts to develop also DSG for parabolic trough power plants. Currently, the first commercial parabolic power plant with DSG is under construction in Kanchanaburi, Thailand.

Advantages and challenges of DSG

Advantages:

- Steam as heat transfer fluid allows higher temperatures because there is no danger of thermo oil cracking. This allows higher steam cycle efficiencies. The aspired steam parameters go up to 550°C and 120 bars[45] (thermo oil systems: 400°C and 100 bars). In 2011, a DSG test loop was integrated by DLR in a conventional Endesa power plant in Carboneras (Spain). In this test loop, temperatures of up to 550 °C are reached.
- The number of construction components can be reduced because no heat exchange has to be realized between a solar field heat transfer fluid and Rankine cycle working fluid.
- The thermo oil itself is an expensive component of CSP plants so that the lack of thermo oil is a direct economic advantage.[46]
- As there is no heat transfer between two heat transfer fluids, there is one thermal loss factor less.
- The usage of steam as a heat transfer fluid may reduce the mean heat transfer fluid temperature in the absorber tube (even at higher final temperatures) and reduce, hence, thermal losses. This reduction is possible because in a large part of the receivers the boiling process is realized, which takes place at a reduced temperature. Only in the small part, where the superheating of the steam is realized (if there is superheating), high temperatures are reached.
- Water has further advantages in comparison to other HTFs: It is environmentally friendlier than thermo oil so that leakages in a directly steam generating plant do not imply environmental dangers. It is less corrosive than salt. Its freezing temperature is much lower than the freezing temperature of salt and even slightly lower than of thermo oil. The effort required to ensure adequate anti-freeze protection is reduced significantly.

[45] See Eikhoff/Zarza 2007.
[46] The heat transfer fluid for the Andasol power plants account for 5 % of the total investment costs (IEA 2010, 27).

According to studies, the levelized electricity costs with a directly steam generating system can (under certain boundary conditions) be lower by more than 10% in relation to the conventional indirect steam generation technology.[47]

Challenges:

- An important challenge of the DSG technology is the high pressure of the water/steam in the absorber tubes. As there is no separation between solar field HTF fluid cycle and power block steam cycle, the water/steam in the solar field has the pressure of the live steam. This was the main problem why DSG was not applied in parabolic trough power plants for a long time. Especially the fact that the receivers must be moveable and need flexible connections was an obstacle for the application of DSG in parabolic trough power plants. This problem does not exist in Fresnel solar fields, where the receivers are fixed; therefore DSG is the standard solution in Fresnel power plants. For parabolic trough power plants, on the contrary, indirect steam generation was chosen as the standard technology.
- There are still no commercially available large storage systems for DSG systems. Until now, only short time steam storages for DSG systems with saturated steam generation are commercially applied. A large storage system for DSG should be a modular storage with sensible heat storage modules for preheating and superheating and a latent heat storage module for evaporation. DLR is currently testing an appropriate storage system in the mentioned demonstration DSG loop in the Endesa power plant in Carboneras.[48]
- The solar field control is more difficult than in indirect steam generation systems. This holds especially for superheated steam generating systems.
  In the test loop at the PSA (see below "Experiences"), three different loop operation concepts for the generation of superheated steam - continuous flow concept, injection concept and recirculation concept - were compared and evaluated.

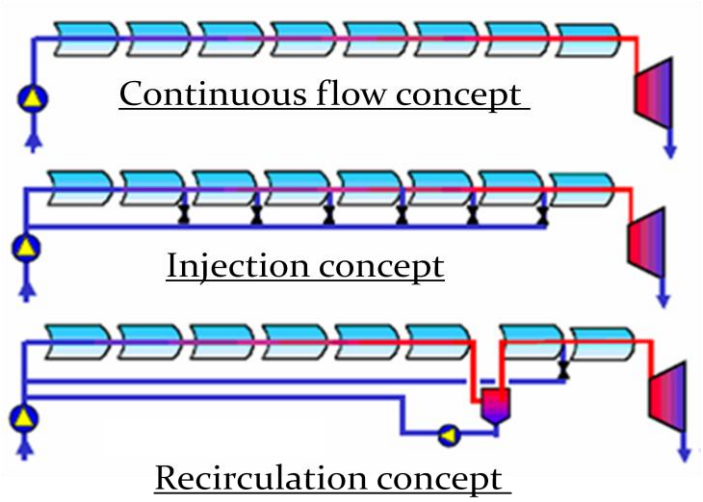

Figure 55: DISS operation concepts (source: Eikhoff/Zarza 2007)

The recirculation mode was demonstrated to be the most appropriate for direct steam generation.[49] A steam separator in the collector field separates the evaporation zone from the superheating section. This implies the advantage that the shifting of the evaporation and overheating zones in the collector is avoided. Stable evaporation and superheating sections

[47] See Feldhoff et al. 2009.
[48] See Laing et al. 2011.
[49] See Eck et al. 2003.

reduce the thermal stress in the receivers and allow a safer collector operation. The water that is not evaporated is pumped back to the beginning of the loop (recirculation). The recirculation concept can be applied also to generate saturated steam. In this case there is no superheating section; the steam separator is located directly between the solar field and the power block.

An important result of the tests at the PSA was that the two phase flow (liquid and vapour) within horizontal tubes can be handled and that it does not cause too high temperature gradients in the absorber tubes.[50]

Experiences

- An important step in the development of the DSG technology was the installation of a 700m long experimental DSG loop in 1999 at the Plataforma Solar de Almería. During more than 10,000 operation hours the feasibility of the direct steam generation in parabolic trough collectors was demonstrated. Steam conditions of 100 bars and 400 °C were reached. New absorber tubes and flexible receiver connections had to be developed in order to withstand the high pressures. Important results were, for instance, the experiences with the loop control, which were mentioned in the preceding section.

Figure 56: DISS test facility at Plataforma Solar de Almería (source: Eck 2008)

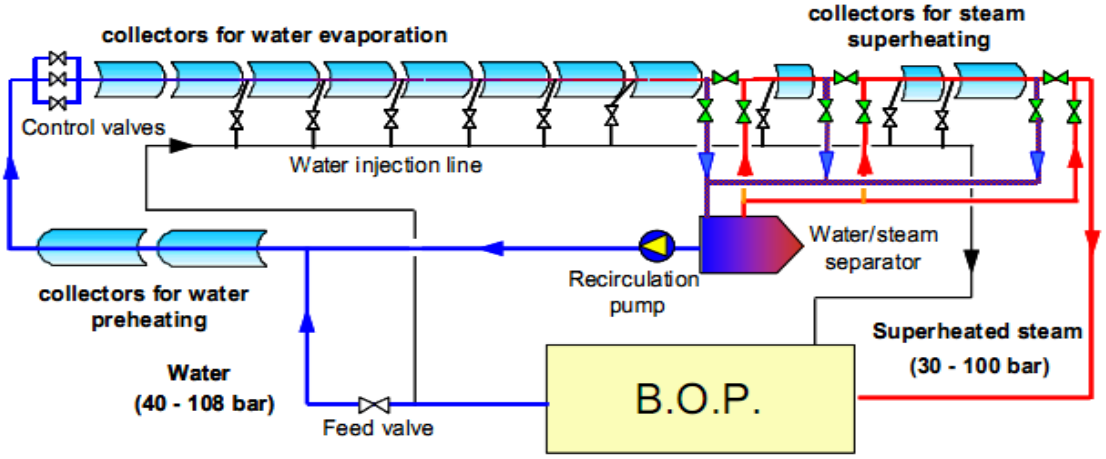

Figure 57: Schema of DISS test facility (source: Eikhoff/Zarza 2007)

[50] See Eikhoff/Zarza 2007.

- The first commercial parabolic power plant with direct steam generation is under construction in Kanchanaburi, Thailand.[51] The German company Solarlite constructs a 5 MW_e plant, which will be extended in a second step to a 9 MW_e plant. The generated electricity is delivered to the public grid. The solar field produces superheated steam. It contains 12 evaporator loops and 7 superheater loops.
  A combination of recirculation and injection concept is applied for the generation of the superheated steam. It is claimed that the advantage of combining these two concepts is a better controllability of the process parameters even during fluctuating DNI conditions. The recirculation mode ensures that the receivers in the evaporator solar field are well cooled and the system pressure is maintained. The injection concept enables better temperature stability of the superheated steam.
  Wet cooling is applied.
  The operating parameters are 330°C and 30 bars. At these conditions the power block reaches an efficiency of 26 %. The receivers have a slightly stronger wall thickness than the receivers in indirect steam generation systems in order to withstand the higher pressures.

Figure 58: Kanchanaburi Solar Thermal Power Plant (source: Solarlite)

Saturated vs. superheated stem generation

Direct steam generation provides both the possibility to generate saturated steam and to generate superheated steam. Superheated steam requires a superheating section behind the steam separator, while saturated steam is provided to the power block at the evaporation temperature at the respective pressure (e.g. 285 °C at 70 bars).

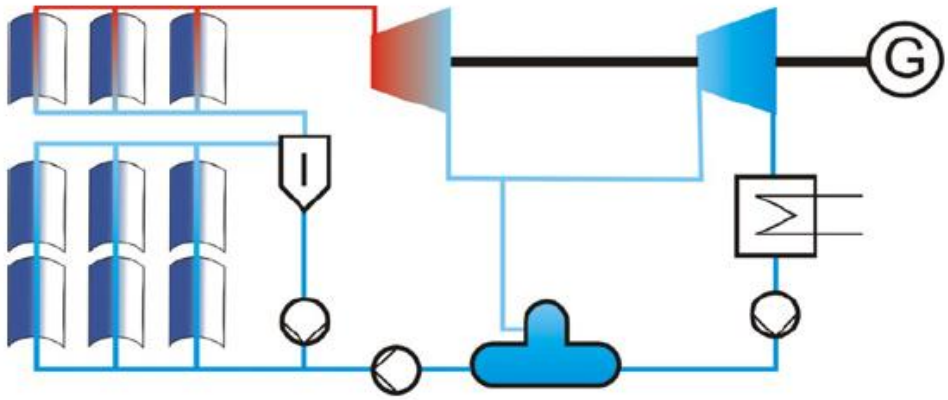

Figure 59: Superheated steam generation (source Eck/Zarza 2006)

[51] For more information about the Kanchanaburi plant, see Krüger et al. 2010.

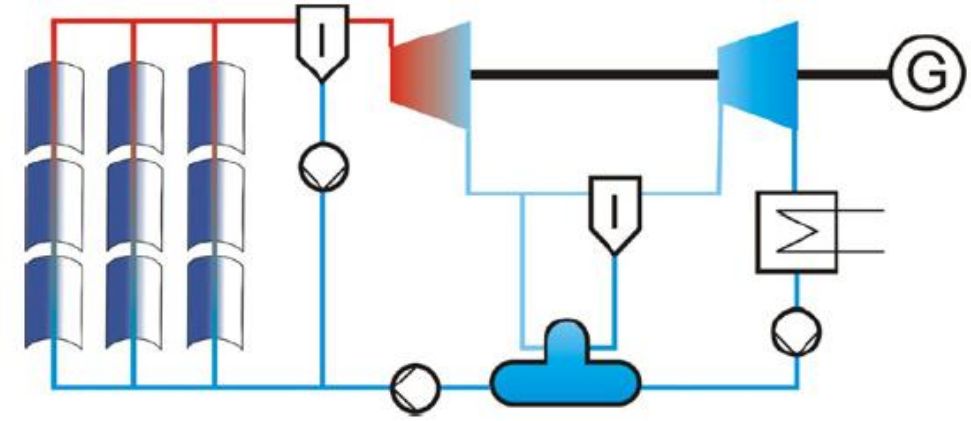

Figure 60: Saturated steam generation (Eck/Zarza 2006)

The aim of superheating the steam is to raise the upper temperature of the Rankine power cycle in order to increase the cycle efficiency. On the other hand, thermal losses in the solar field become higher. The overall efficiency of the plant, however, was calculated to be slightly higher if certain boundary conditions are given.[52]

For near term applications the saturated steam mode might be an interesting alternative for power generation in the small capacity range due to the simpler set up of the collector field and the existing experiences with the collector field operation.

The main advantage of the saturated steam option was found to be the possibility to overcome short cloud transients when operating at sliding pressure. The water/steam separator at the interface between the solar field and the steam turbine can act as a short time thermal storage.

The PSA investigations concluded that for a 5 MW DISS power plant the annual net electricity generation was 4% higher for the saturated steam option. But, the investment costs were calculated to be higher by 5%, mainly because of the power block.

[52] See Eck/Zarza 2006.

3.4 Solar field

The solar field is the totality of the collectors of a power plant and their arrangement on the power plant ground. In this section we will describe the orientation, the structure and the size of the solar field of parabolic trough power plants.
We leave the excursus to direct steam generation systems and come back to the standard indirect steam generation systems.

3.4.1 Solar field orientation

Theoretically, the parabolic troughs in the solar field of a CSP plant can have any orientation. It is always possible to track the Sun. However, there is a preferred orientation, which is the north-south alignment with the respective east-west tracking. East-west alignment with the respective north-south tracking was applied for experimental purposes only.
Depending on the latitude where the power plant is installed, different orientations have different effects on the energy yield of the power plant. For Sun Belt locations, i.e. at latitudes below 40° and, generally, not too close to the equator (not below 15°), the following holds:

- **East-west alignment** has the following advantages and disadvantages:
    - The collector performance over the day is quite uneven. Due to large incidence angles, the collector performance is reduced considerably in the hours after sunrise and the hours before sunset. At noon, the full aperture always faces the Sun, i.e. the incidence angle is zero. This means that the highest possible thermal peak power of the solar field at a given direct irradiance is always reached if it has east-west alignment (but not necessarily if it has a north-south alignment).
    - Energy yield differences between summer and winter are smaller than for north-south alignment. Contrary to north-south alignment, incidence angles on the collector are not larger in winter than in summer.
    - Quite small tracking movements are required during the day.
    - The annual energy yield is lower than for north-south alignment.
- **North-south alignment** has the corresponding advantages and disadvantages:
    - The collector performance over the day is quite even. Generally, the cosine loss is higher at noon than in the morning and evening and tends to compensate, hence, the different DNI conditions.
    - Due to incidence angle differences between summer and winter, the seasonal energy yield differences are larger than for east-west alignment.
    - The annual energy yield is higher than for east-west alignment.

All these differences are based on different incident angles and the corresponding cosine effect. The following figure compares the cosine effect at north-south and east-west oriented collectors. It shows the irradiance on the aperture over the day at summer solstice, equinox, and winter solstice. A location at 30° latitude was chosen. It is to be seen:

- Collector irradiance over the day is more equilibrate for north-south orientation
- Seasonal collector irradiance variance is lower for east-west orientation
- Peak irradiance (at solar noon) is higher for east-west orientation (at a location outside the tropics this is the case during the whole year)

What is more difficult to see in the diagram is that the total energy yield over the year is higher for north-south orientation. However, if we consider the sum of the areas below the curves (taking the equinox curve twice for spring and autumn), which represents a good comparative representation of

the annual collector irradiation [kWh/m^2/y] for both orientations, then a higher annual collector irradiation for the north-south orientation can be discerned.

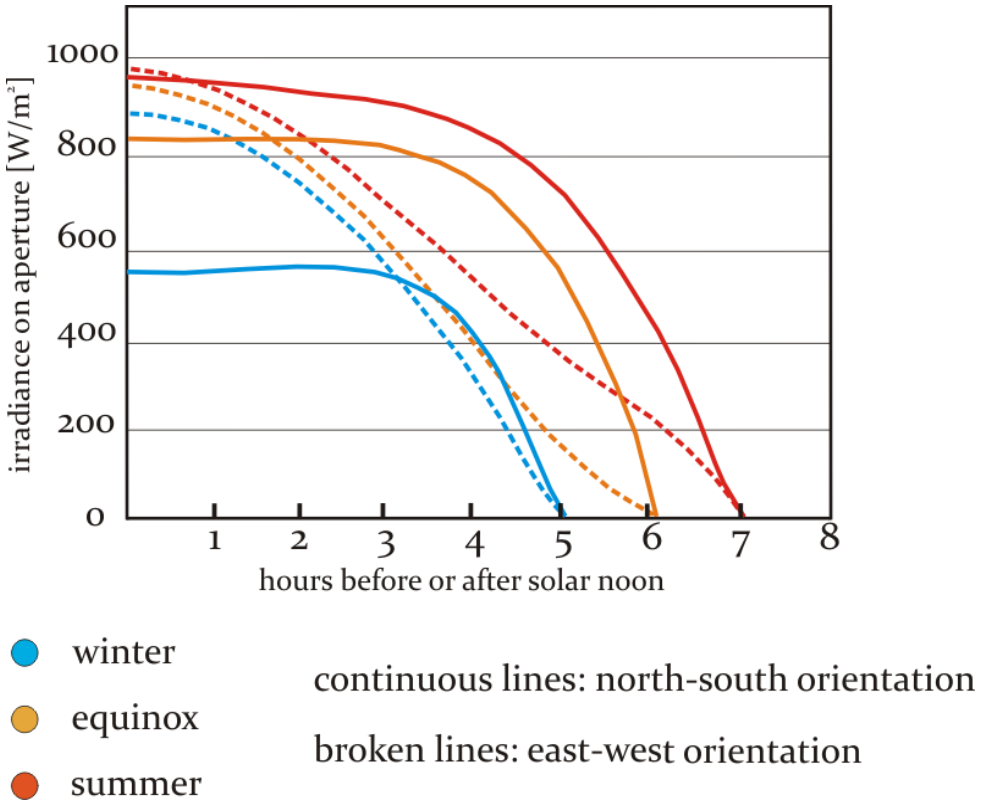

Figure 61: Irradiance on the aperture over the day in different seasons at north-south and east-west oriented parabolic troughs (source: Garg 1987)

3.4.2 Solar field structure

In this section the typical solar field structure of current parabolic trough power plants with a capacity between 30 and 80 MW and indirect steam generation with thermo oil as HTF is described. The structure of the solar field may differ if the power plant capacity changes, if another heat transfer medium is used or if direct steam generation is realized.[53] Moreover, future plants with new collector designs may have different solar field structures.

The solar field of current parabolic trough power plants has a rectangular structure, nearly a square. In many cases, the power block is located in the centre or near the centre of the solar field. This, together with the square structure, allows that the pipes are as short as possible in order to reduce thermal losses; the way of the hot heat transfer medium to the power block becomes shorter.

One pipe that leads the "cold" heat transfer fluid to the solar field and one pipe that leads the hot heat transfer fluid from the solar field to the central power block represent the connection of the power block with the solar field. In many cases, two pairs of these pipes, which are also called cold and hot headers, exist.

[53] For example, the molten salt solar power plant Archimede in Italy, with a rated power of 5 MW_{el}, consists of 9 loops, i.e. 18 rows, each of which consists of only three solar collector assemblies. See http://www.nrel.gov/csp/solarpaces/project_detail.cfm/projectID=19.

The following figure shows the principal layout. The power block in the centre and the two pairs of cold and hot headers are indicated. All collector loops are connected to these cold and hot headers. A loop is indicated at the bottom right corner.

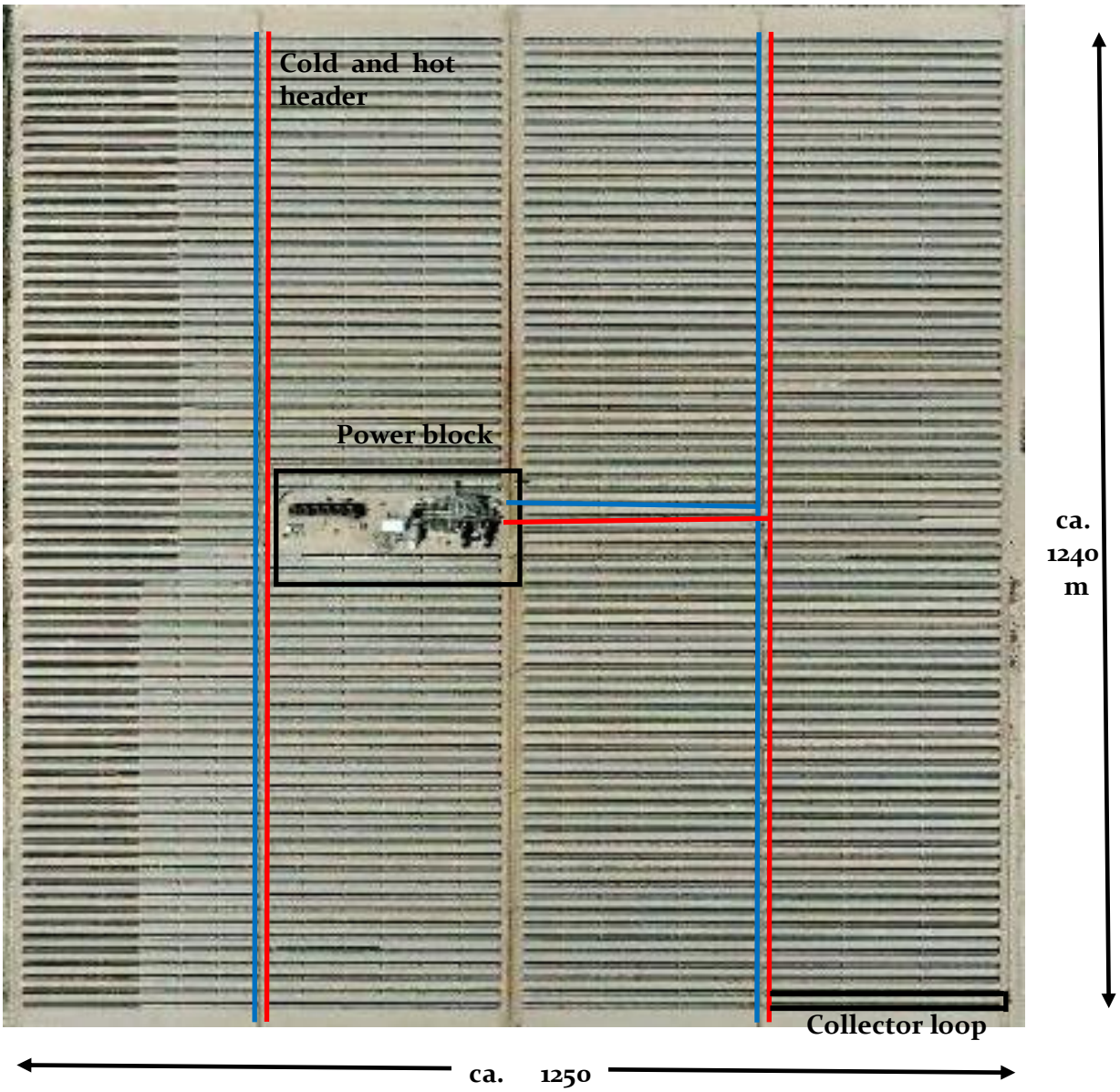

Figure 62: Solar field layout of SEGS VIII and SEGS IX (source: Google)

Many large parabolic trough power plants have four columns of collector loops. In many power plants 30 to 40 loops (or 60 to 80 collector rows) are connected in parallel to the headers.[54]
A collector loop contains always two parallel collector rows that are connected in series. One end of the loop is connected to the cold header and the other to the hot header. The loops have generally a length of about two times 300m, i.e. 600m. That means that the heat transfer fluid is heated while it flows through a distance of about 600m. The following figures illustrate the collector loops.

[54] Mohr et al., 1999; Herrmann et al. 2002.

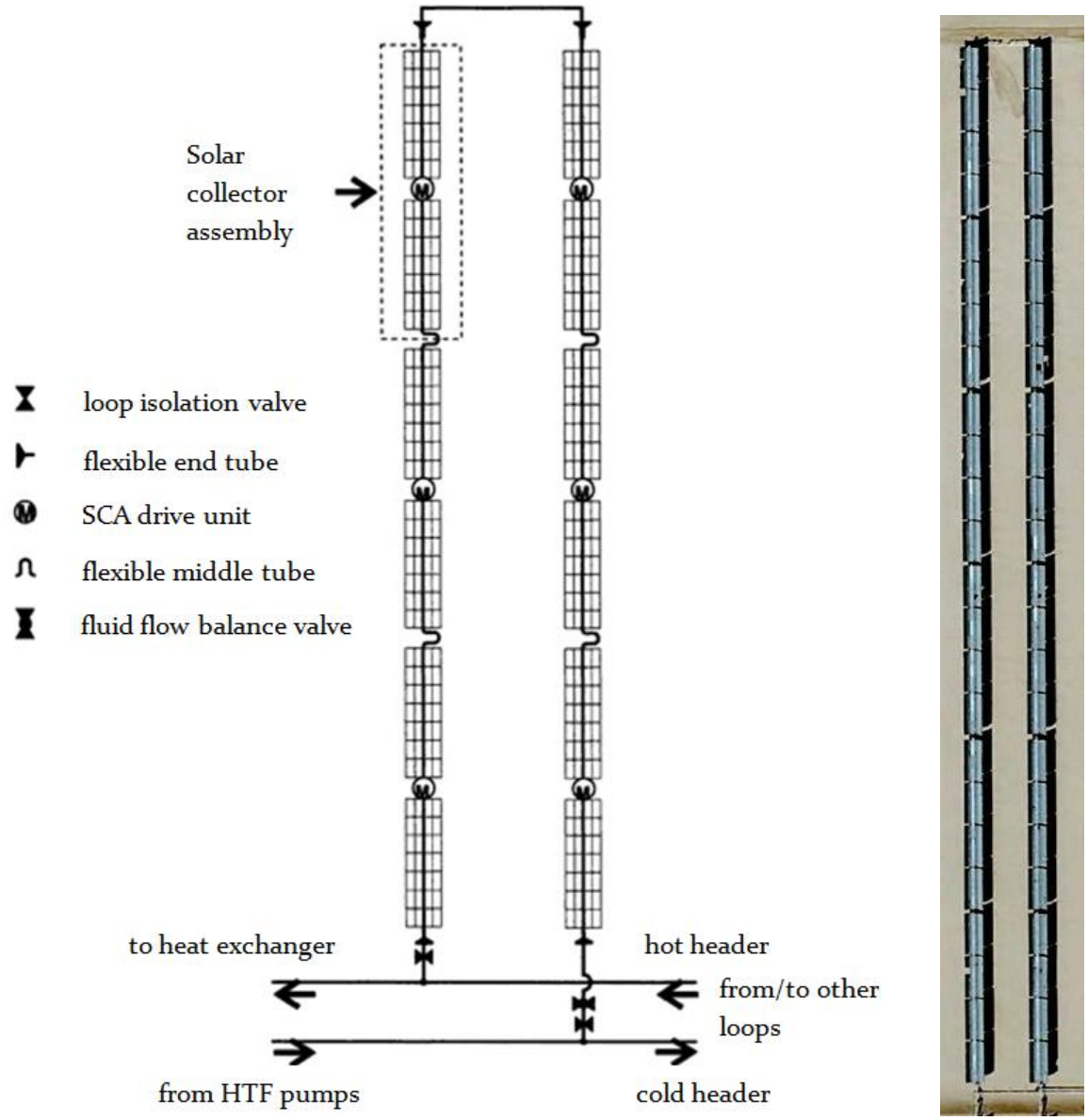

Figure 63: Collector loop (source: Mohr et al. 1999, Google)

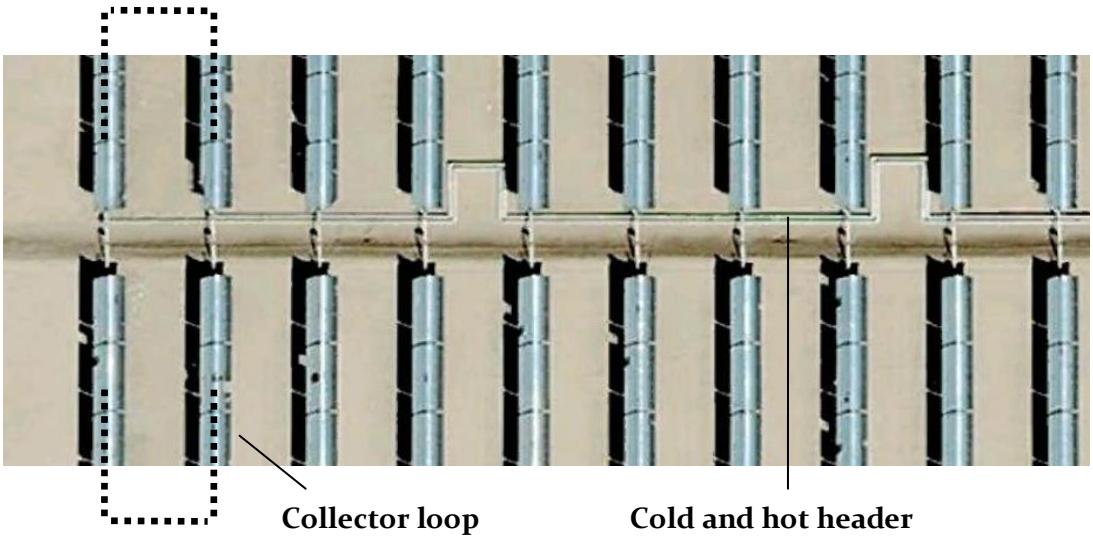

Figure 64: Collector loops connected to the cold and hot header in SEGS VIII (source: Google)

Figure 65: Connection of two collector rows to one loop (source: Simon Csambor)

The collector rows are composed of solar collector assemblies. A solar collector assembly is a combination of several collector modules that are tracked by one common driving unit. Collector assemblies have a length between 100 m and 191 m (Heliotrough). That means that they contain between 8 and 12 modules.

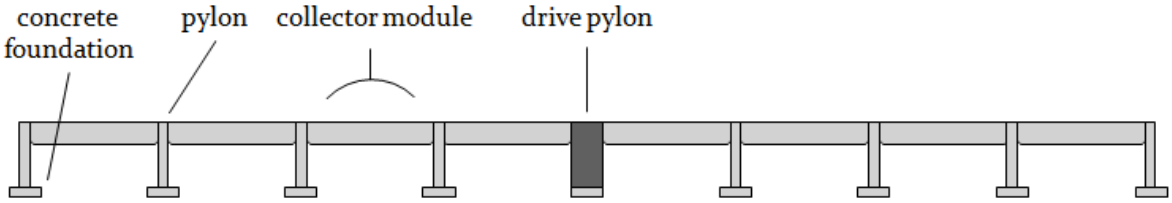

Figure 66: Solar collector assembly (SCA), consisting of 8 collector modules (e.g. LS-3)

Concerning the distance between the collector rows, it should neither be too small nor too big. If it is too small, then the shading between the rows increases too much. If the distance is too large, then the pipes become long and the thermal losses as well as the investment costs increase. A good distance between the rows (between pylon row and pylon row) is about three times the aperture width.[55]

3.4.3 Solar field size

The size of the solar field can be characterized as the total aperture area as well as the total solar field ground area. The ground area depends on the aperture area and the distance between the collector rows. The aperture area depends on many parameters and the determination of the ideal aperture area for a given electric power plant capacity is a complex optimization task.[56] In this section, we want to understand which parameters determine the plant size. And we want to present a rough approximation of the aperture area. With this result we also can approximate the solar field ground area (and, hence, the power plant ground area, which is nearly the same).

[55] Mohr et al. (1999, p. 48) indicate a row distance of 12.5m for the LS-2 collector (aperture width 5.00m) and 16.2m for the LS-3 collector (aperture width 5.76m).
[56] See Quaschning et al. 2002.

Roughly, the aperture area depends on the rated power plant capacity, the available direct solar radiation, the total solar-to-electric efficiency, the solar multiple, and economic optimization considerations.

- The rated power plant capacity is unproblematic and can be considered as a given value.
- The available direct solar radiation is determined by the considered power plant location. A reference irradiance value has to be determined as the design point. This reference value is below the peak irradiance and can be more or less closed to it. The solar field is dimensioned according to this design point, the determination of which depends on economic optimization considerations, as we will explain below.
- The solar-to-electric efficiency of the power plant has to be considered at the design point, where it reaches its highest value. Peak solar-to-electric efficiencies (related to the aperture area) in new parabolic trough power plants are at about 25% or a bit higher (Andasol 28%); annual average solar-to-electric efficiencies are at 12% to 16%. The overall plant efficiency depends on a vast number of parameters, which can be grouped together as the optical efficiency of the collector (how much of the incident direct radiation is absorbed by the absorber tubes), the thermal losses in the solar field and in the steam generators, the thermal-to-mechanical efficiency of the power block (considering thermal and pressure losses in the steam generating and pipe system, turbine efficiency), generator efficiency, and parasitic energy consumption.
- The solar multiple is the factor by which the solar field is amplified in relation to a power plant without thermal storage, i.e. a power plant with SM=2 has the double solar field size of a power plant with SM=1 (without storage) and the same rated electric power.
- Economic optimization considerations refer especially to the question which radiation conditions are considered as the design point. If a very high direct irradiance is taken, which is reached only few times in summer, than the power block is nearly always operated under part-load conditions, which reduces the power block efficiency. If, on the contrary, the design point is chosen to be at quite weak radiation conditions, than the solar field gets very large (which raises the investment costs) and it will happen more frequently that thermal energy from the solar field cannot be used in the power block and has to be dumped. Simulations concerning a specific 50MW plant in southern Spain rendered the result that the optimal design direct collector irradiance corresponds to the value that has a frequency distribution of 55-60%[57], which for the considered location was at 650-700W/m^2. This value, however, can be different at other locations; it depends on many boundary conditions.

The following equation approximates roughly the aperture area for a given power plant project (solar only):

$$A_{ap} = \frac{P_{el} \cdot SM}{\eta \cdot G_{b,ap}},$$

where P_{el} is the rated electric power, SM the solar multiple, η the solar-to-electric efficiency (related to the irradiance on the aperture) and $G_{b,ap}$ the direct irradiance (at the design point) on the collector aperture.

The following diagram shows the aperture areas of parabolic power plants with different rated powers and solar multiples. A solar-to-electric efficiency of about 25% and a direct irradiance on the collector

[57] That means that at 55-60% of the periods, when direct radiation is available, the direct radiation on the collector aperture reaches this value or is higher.

aperture at the design point of about 800 W/m^2 are assumed. Four existing power plants, three in the USA and one in Spain, are introduced, which confirm the approximation.

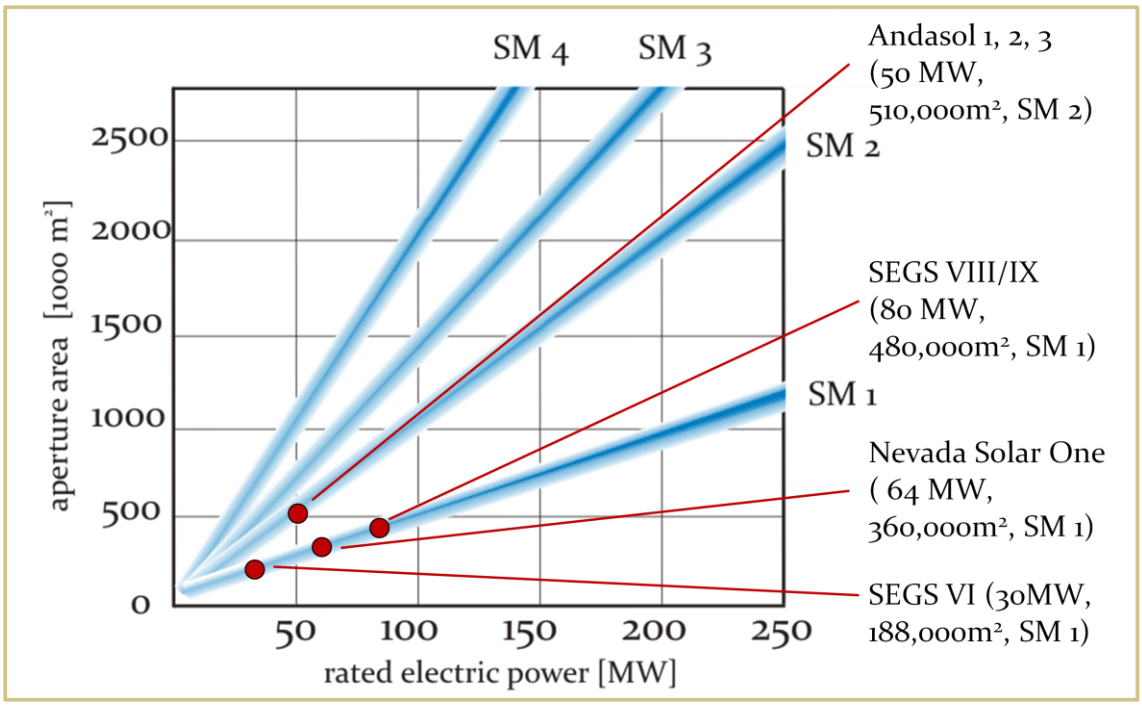

Figure 67: Aperture area of parabolic trough power plants

The total solar field ground area, and, consequently, the power plant ground area, depends basically on the aperture area. As mentioned above, the distance between the collector rows is about three times the aperture width. That means that the solar field ground area is at least three times the aperture area. Including the area for the pipes and transport ways, the total solar field area is about 3.5 times the aperture area. Including the power block and an optional storage, the power plant ground area is about 3.5 to 4 times the aperture area. In the case of the Andasol plants, the aperture area is 0.51 km^2 and the power plant ground area is 2km^2.

4 Power plant integration

There are many plant design and configuration parameters that have to be chosen if a parabolic trough power plant is to be built at a given site and for a given electricity supply task. An important question is, for instance, whether the plant should be able to produce base load electricity, intermediate electricity or peak load electricity. Therefore, the solar field size in relation to the power block capacity and the integration of a thermal storage system has to be decided. Another question (not necessarily separated from the former) is, whether a parabolic trough power plant should have some kind of fuel-based supplementary energy source (hybridisation). This section deals with these questions.

4.1 Solar field size, storage, solar multiple

If a parabolic trough power plant is to be built, then the rated power of the plant may be fixed. Plant function, technical considerations, financial conditions or political decisions (like in Spain, where the applied promotion scheme for CSP projects allows only plants up to 50 MW rated electric power) may define the plant power. The rated power alone, however, does not define the solar field size and other parameters. Economic and further considerations determine these parameters.

Concerning the solar field size, it was already mentioned that it depends also on the design point that is chosen. Considering a plant without thermal storage system, the following holds: A small solar field, which is less costly, implies that the rated power is reached only in few occasions, when the direct irradiance is near the maximum. A larger solar field implies that the rated power is reached more frequently and that the energy output of the plant increases. But, a larger solar field is more expensive and thermal power has to be dumped at excellent radiation conditions. The optimum solar field size can be defined as the economic optimum between a very large and a very small solar field.

There is a further parameter in the decision about the solar field size in relation to a given rated power of the power plant: thermal storage systems. The solar field can be enlarged so that its thermal power exceeds by far the thermal power that can be converted into electric energy in the power block. The thermal energy that is generated at good radiation conditions and that cannot be processed immediately in the power block is stored in a thermal storage and can be used for additional power generation during times with no or low solar radiation availability. The ratio of solar field size and rated power of the power block is specified as the “solar multiple” of the power plant. More exactly, the solar multiple (SM) is the ratio of the thermal power of the solar field at design point to the required thermal power for the full-load operated power block.

There is a direct relation between the SM and the storage size: Larger solar fields (in relation to the rated power of the power block) require larger storages.

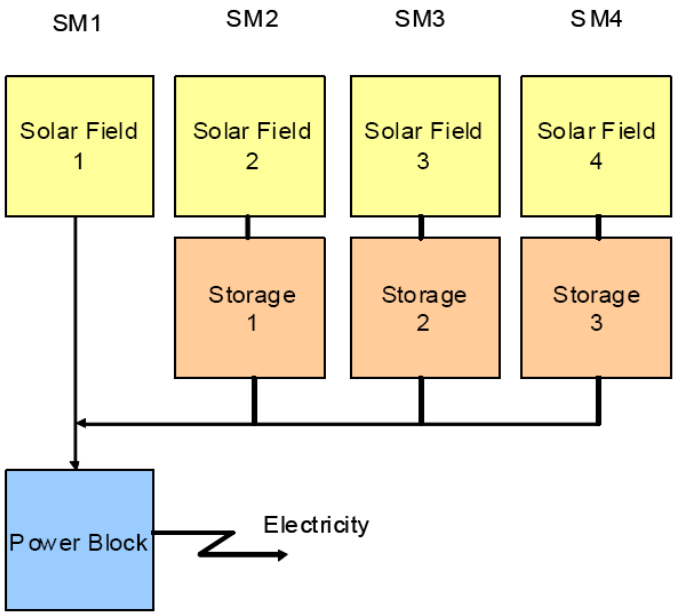

Figure 68: Solar multiple and storage size (source: DLR)

The most important advantage of a solar multiple higher than 1 is that the power block utilization (full load hours) rises. The same power block can generate more electric energy over the year.

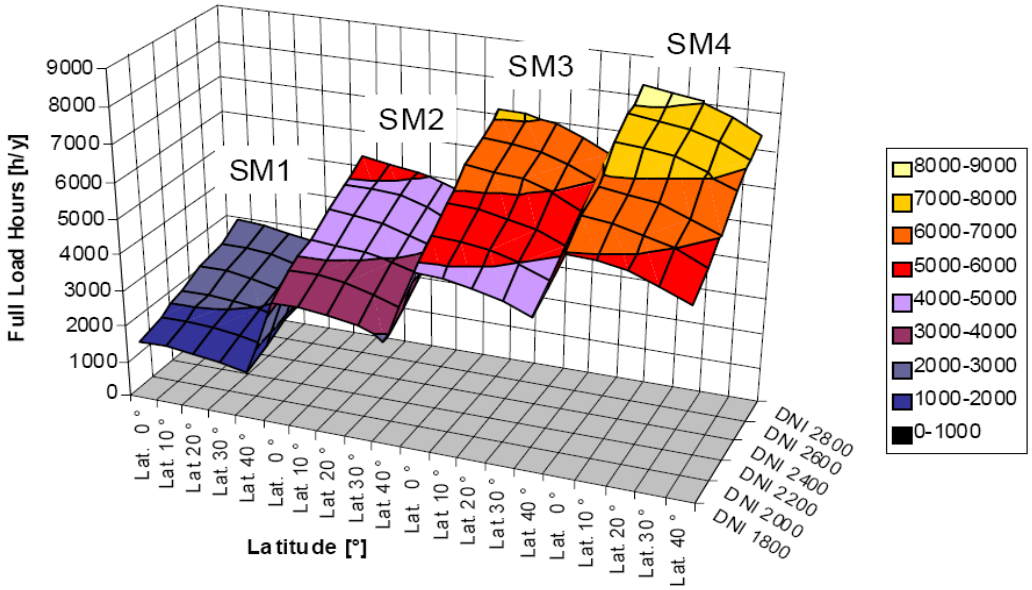

Figure 69: Solar multiple and power block utilization (source: DLR)

A storage system can also help to bridge transient cloudiness and to compensate other weak radiation conditions in the sense that the power block is operated more frequently under full load conditions and less under part load conditions, which helps to reach higher power plant efficiencies.
Additionally, the integration of a thermal storage allows that the power plant can generate electricity on demand. This may be interesting for the power plant operator because the electricity can be generated specifically at peak demand, which allows higher revenues if peak pricing is applied in the respective grid. For the grid operation itself, it may be interesting too because the capacity to generate power on demand can be useful to stabilize the grid. This holds even more if more electricity is generated from fluctuating energy sources, solar radiation and wind, with technologies that cannot

balance the fluctuations. Parabolic trough power plants with thermal storage systems have the interesting characteristics that they can balance the electricity generation and that they can generate power on demand although they depend on unstable solar radiation conditions.

4.2 Base load, intermediate load and peak load plant configuration

The possibility of the integration of a thermal storage allows the provision of electricity at different demand situations: base, intermediate and peak demand. According to the selected supply task, steam turbine capacity, solar field size and storage size have to be matched in an appropriate way. In the following, we consider a fixed solar field size, which implies that the generated electricity can be taken to be constant at the considered configurations.

- A parabolic trough plant as **base load plant** needs a very large storage, which makes possible the generation of electricity also over long longer periods without solar radiation.[58] The turbine is quite small because the electricity is generated continuously, i.e. the generation is distributed over many operation hours.

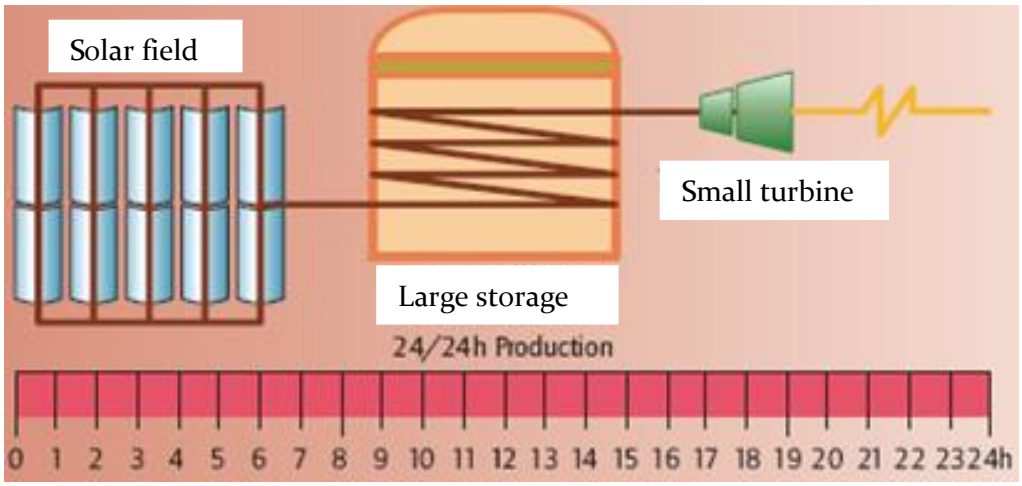

Figure 70: Base load configuration (source: Octobre/Guihard 2009)

- An **intermediate load** power plant with operational hours over the day needs only a small storage because less energy has to be stored for a shorter operation time. The turbine must be larger than in the base load configuration, because the electric energy is generated in less time than in the base load power plant. The investment cost for intermediate load trough plants are lower than for base load plants because of the small storage and the medium size turbine. Among parabolic trough power plants, plants with these characteristics generally have the lowest levelized costs of electricity.[59]

[58] See Geyer 2007.
[59] See Octobre/Guihard 2009.

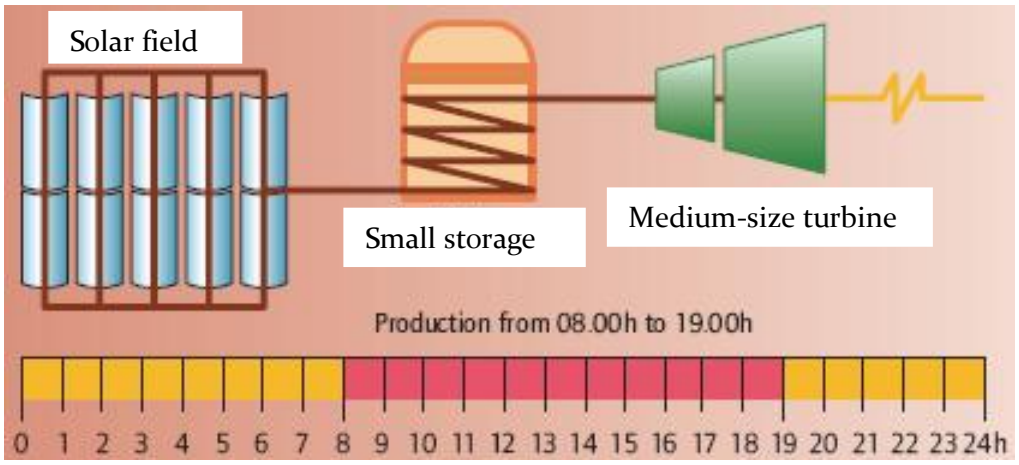

Figure 71: Intermediate load configuration (source: Octobre/Guihard 2009)

- Trough plants with **delayed intermediate load** configuration store a larger part of the collected solar energy although they distribute the electricity generation over the same time span. The turbine has the same intermediate size like in the foregoing configuration, but the storage must be larger in order to allow the electricity generation during hours with less solar input.

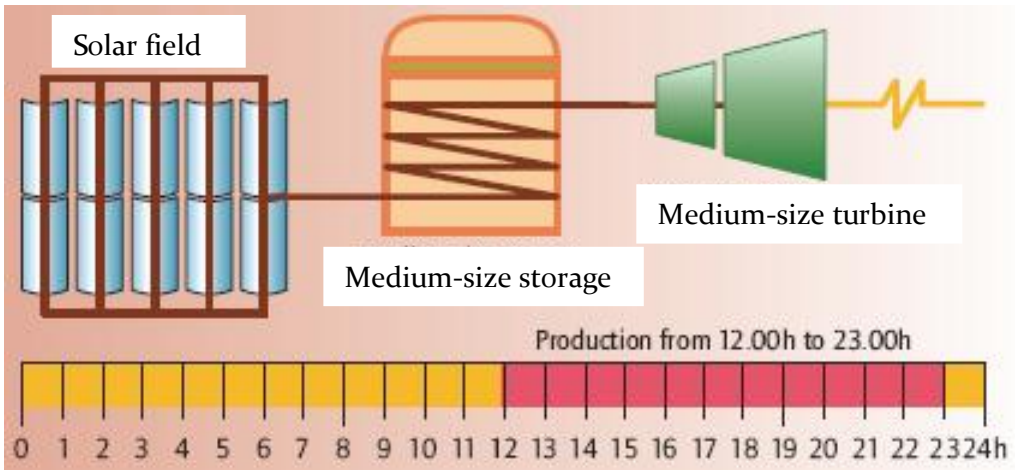

Figure 72: Delayed intermediate load configuration (source: Octobre/Guihard 2009)

- A **peak load** plant is operated only during few hours. Therefore it needs a large turbine. The electricity generation is concentrated in a small time span. Additionally, the storage has to be large because much solar energy input has to be stored in order to be converted in a short time into electricity. The peak load configuration implies the highest levelized electricity costs among the considered configurations.

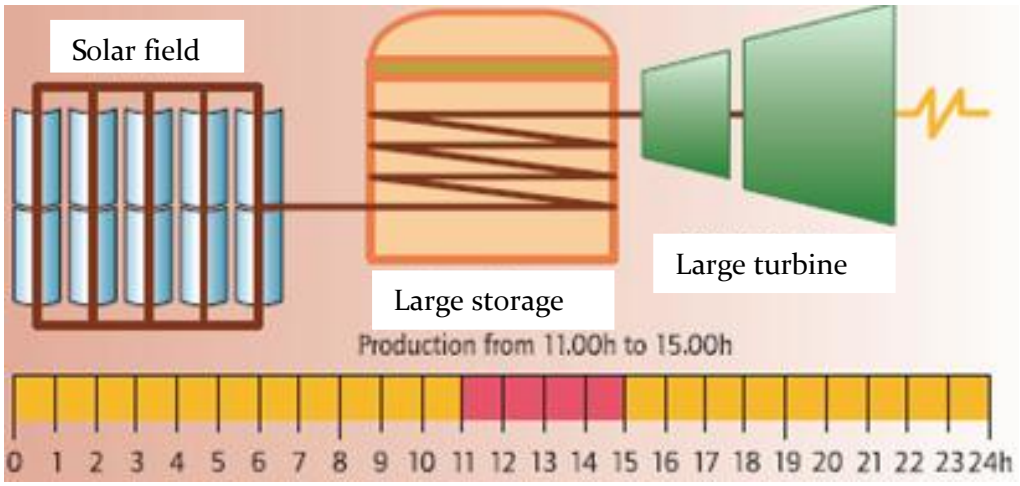

Figure 73: Peak load configuration (Octobre, Guihard 2009)

For practical contexts, computer-based simulation tools were developed that can be used to evaluate plant dimensioning and configuration concerning performance and cost parameters. Such tools are SAM (NREL), Greenius (DLR), Ebsilon Professional (Evonik/DLR), IPSEpro and Thermoflex.

4.3 Hybridisation

"Hybridisation" in general means the combination of different energy conversion technologies in one system. In the case of parabolic trough power plants, hybridisation is the combination of the thermal energy that is provided by the parabolic trough collectors with thermal energy from other sources. These other sources are fuels, and the thermal energy is provided by combustion. We can distinguish three different kinds of how a hybridisation can be reached:

a) A parabolic trough power plant is equipped with fuel-fired backup heaters.
b) A parabolic trough power plant is equipped with a fuel-fired burner for additional steam superheating.
c) A parabolic trough solar field is integrated into a combustion-based power plant adding a solar share to the fuel-based heat.

a) Fuel-fired backup heater

If "solar only"[60] parabolic trough power plants are not equipped with a thermal storage, then they produce electricity just when direct solar radiation is available. This means that the plant capacity factor is quite low. At sites with favourable radiation conditions, a parabolic trough plant reaches only about 2000 full load hours per year. As discussed in the preceding section, one possibility to increase the capacity factor is the integration of a thermal storage into the plant. Another possibility to reach a higher power block utilization is the integration of fuel-fired backup boilers and heaters that can substitute a part or the total of the solar heating. Additionally to the better power block usage, hybridization can contribute to stable grid conditions because they reduce power gradients or make them controllable. They can bridge intermittent cloudiness, equilibrate day/night-rhythms and they allow the generation of power on demand. Moreover, backup heaters can improve the power block efficiency if they are used to run the power plant more frequently at its rated power.

[60] "Solar only" is a common denomination of non-hybridized systems.

Besides the mentioned advantages, the hybridisation has the advantage of a faster introduction of solar power technologies in oil and gas-producing Sun Belt countries. This holds especially for ISCCS (see below).

Different fuel types can be used in backup firing systems: gas, coal, biofuels, waste. However, liquid and gaseous fuels are more suitable than solid fuels. Burners or heaters that are operated with liquid or gaseous fuels allow a faster control than systems that use solid fuels and are, therefore, more appropriate for quick reactions to quick changes in the radiation conditions (cloudiness).

There are different options how to integrate a backup system into a parabolic trough plant. One option is that the backup heater heats directly the water/steam of the steam cycle. Another option is the integration of the backup heater into the solar field cycle where it heats the solar field heat transfer medium. In the first option, the backup is quite independent from the solar field. The second option has the advantage that the backup heater can be used additionally to protect the heat transfer medium against freezing. The following figure shows both integration options.

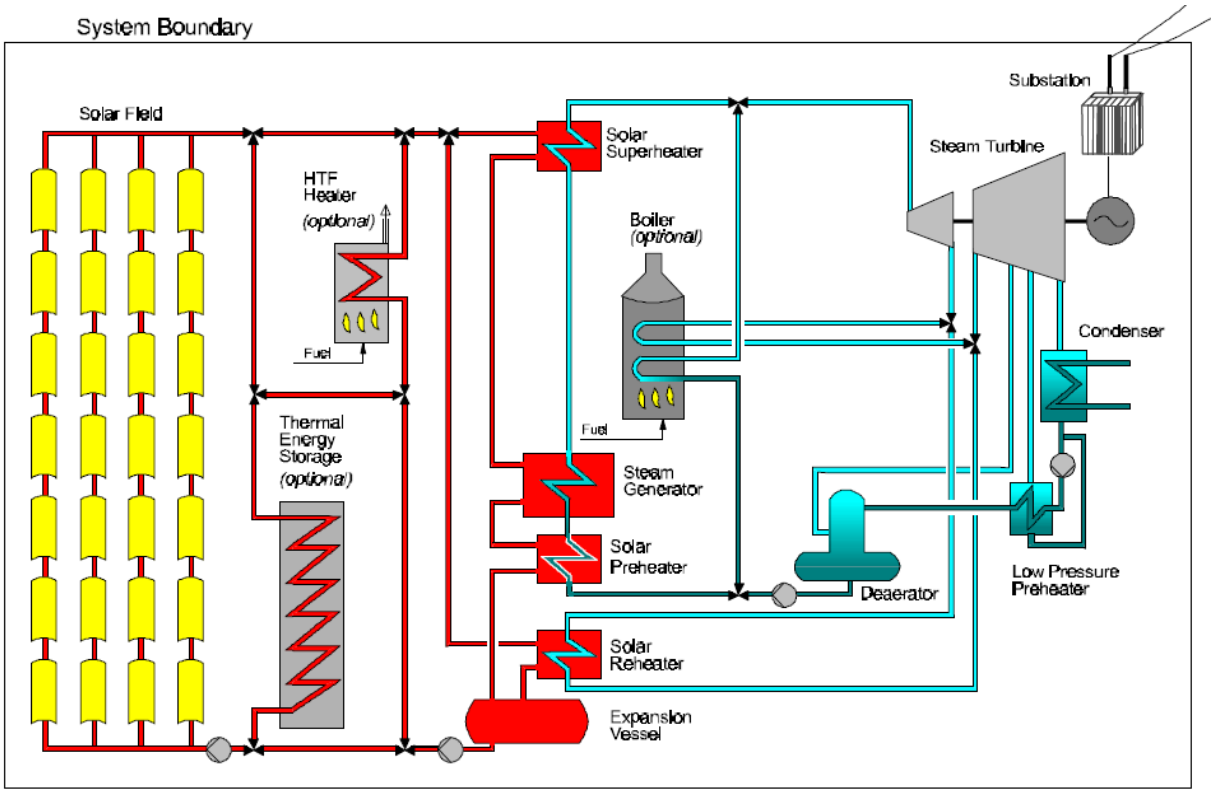

Figure 74: Parabolic trough power plant with integrated fossil fired backup technology

The SEGS plants in California are equipped with gas-fired backup systems. The use of gas is limited to 25% of the thermal energy generation in order not maintain the status as solar energy systems. The real fossil share is quite below this threshold. The operators use the backup system in order to produce electricity in the late afternoon and after sunset, when mid-peak pricing applies. During winter, the gas is used to achieve the rated power by supplementing low solar irradiance.[61]

The motivation to integrate combustion-based backup heaters into a parabolic trough power plant is similar to the motivation to integrate a thermal storage system. In both cases the power block utilization can be increased and power can be generated on demand. A combination of both, thermal storage and backup heater, is perfectly possible. A possible power management of a corresponding base-load power plant is shown in the following figure.

[61] See IEA 2010, p. 16.

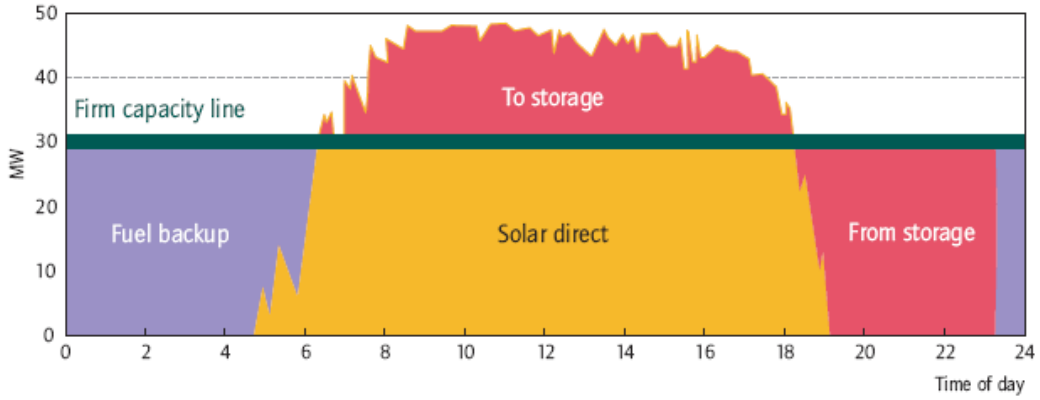

Figure 75: Combination of storage and hybridisation in a solar plant (source: Geyer 2007)

b) Fuel-fired superheating

As explained above, parabolic trough power plants with thermo oil as heat transfer fluid reach live steam temperatures of only about 380°C, which constrains the power block efficiency. A possibility to enhance the power block efficiency is the integration of an additional fuel-fired superheater. This is planned in the power plant Shams 1 (100MW) in the United Arab Emirates. Contrary to a fuel-fired backup, the additional superheater will be operated continuously during sunshine hours to raise the steam temperature up to 540°C. (Additionally to this fossil superheater, Sham 1 will also have a fossil backup heater.)[62]

c) Integrated Solar Combined Cycle Systems (ISCCS)

While the configurations explained in the preceding lines are CSP plants with fuel-based supplementary heating, the contrary is also possible: a combustion-based thermal power plant with additional solar heating. The most important plant configuration is the integration of solar heat in combined cycle gas power plants. Such plants are called Integrated Solar Combined-Cycle Systems (ISCC or ISCCS). Currently, there are several ISCCS projects in countries like Algeria, Australia, Egypt, Iran, Italy and the USA.
In current systems, the solar heat is fed exclusively into the steam cycle. There are two possibilities to do that. One possibility is the use of the solar heat for evaporation and the subsequent superheating in the heat recovery steam generator as shown in the following figure.

[62] See IEA 2010, p. 16.

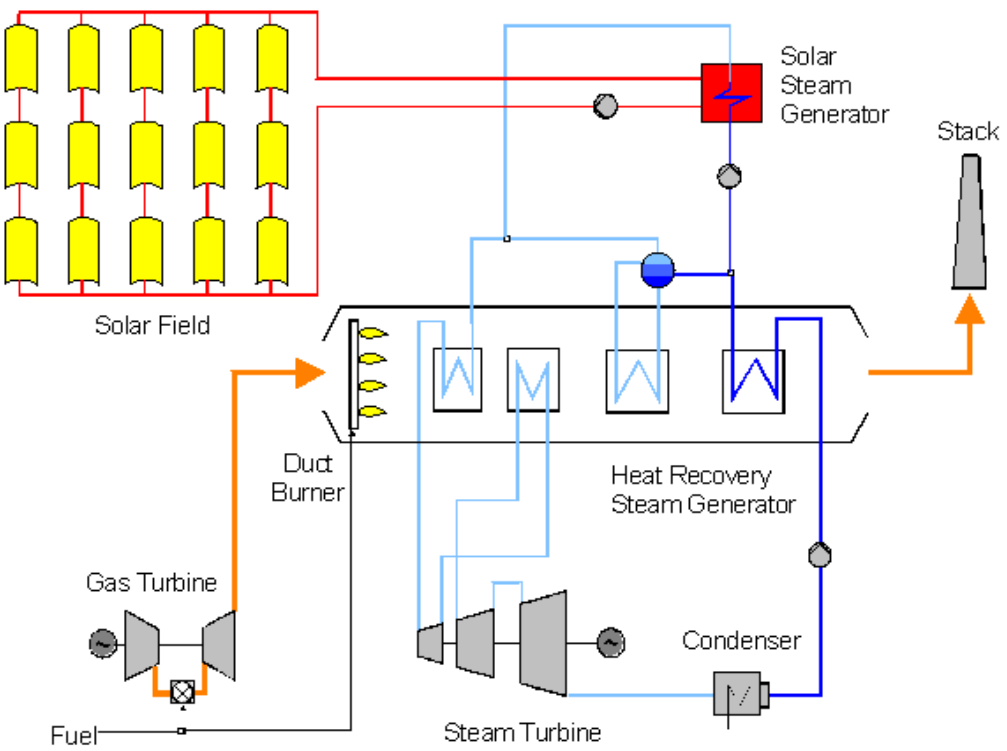

Figure 76: ISCCS with solar steam generation and additional superheating in the heat recovery steam generator (source: Dersch)

Another possibility is the parallel operation of the solar steam generator independently from the heat recovery steam generator and the combination of the steam from both steam generators to one steam flow that is supplied to the turbine. The parallel operation of the solar steam generator has the disadvantage that the "solar steam" cannot reach the same high temperatures like the steam that is generated in the heat recovery system. Therefore, the steam cycle efficiency may decrease at higher solar shares and the conversion efficiency of the fossil fuel may be reduced. Furthermore, the steam turbine runs in part load during times without solar input causing also a reduction in efficiency compared to an optimised CC plant. The latter holds for all ISCCS without compensation measures for missing solar input.

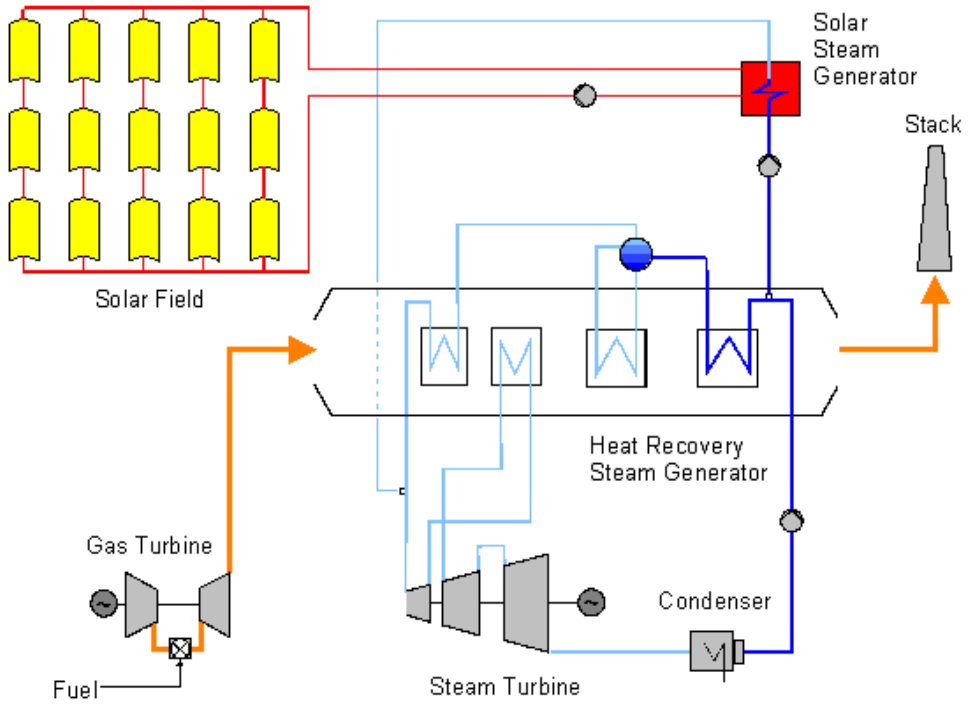

Figure 77: ISCCS with parallel solar steam generation without integration into the HRSG steam generation (source: Dersch)

5 Efficiency of parabolic trough power plants

5.1 Solar-to-electric efficiency

The overall efficiency of a parabolic trough power plant at a given moment can be defined as the ratio of the electric power to the direct irradiance on the collector aperture multiplied with the total aperture area of the solar field:

$$\eta = \frac{P_{use}}{P_{in}} = \frac{P_{el}}{A_{ap} \cdot G_{b,ap}} .$$

The overall efficiency of a parabolic trough power plant is also called the solar-to-electric efficiency. It can be subdivided into the solar field efficiency η_{SF} and the power block efficiency η_{PB}:

$$\eta = \eta_{SF} \cdot \eta_{PB}$$

If a power plant disposes of a storage system, then an additional storage efficiency can be taken into account. The solar field efficiency is the solar-to-thermal efficiency, which is the ratio of the heat flow difference between inlet and outlet of the solar field to the direct irradiance on the total aperture area of the solar field. The power block efficiency is the ratio of the generated electric power to the heat flow difference between inlet and outlet of the solar field.

The solar field efficiency can be subdivided additionally into the optical solar field efficiency (taking into consideration the optical losses that occur until the radiation is converted into heat in the absorber tube) and the thermal solar field efficiency (taking into consideration the heat losses that occur from the radiation conversion into heat in the absorber tubes to the heat transfer to the power block).

Contrary to fossil fuel power plants, which can have quite stable power flows and other constant working conditions and, therefore, quite stable efficiencies, parabolic trough power plants are operated under changing operation conditions, with fluctuating power flows and fluctuating efficiencies: the varying Sun position implies different optical efficiencies, and different heat flows in the receivers generate different thermal losses and power block efficiencies. The efficiency of a parabolic trough power plant varies between zero and a certain peak efficiency, which is reached at favourable radiation and other (e.g. ambient temperature) conditions. That's why it is necessary to distinguish between peak efficiencies and average efficiencies.

Peak overall efficiencies of new parabolic trough power plants are indicated to be 23 % for Nevada Solar One (2007) and 28 % for Andasol I (2009). The older Californian SEGS power plants have considerably lower peak efficiencies.[63] Average solar-to-electric efficiencies are nearly 12 % for Nevada Solar One and 16 % for Andasol I.

Subdividing into solar field efficiency and power block efficiency, for Nevada Solar One 66% peak solar field efficiency and 35% peak power block efficiency are indicated, for Andasol I 70% peak solar field efficiency and 50% average solar field efficiency and 40% peak power block efficiency and 30% average power block efficiency.[64]

[63] SEGS VI has a peak efficiency of about 18%; older SEGS plants have even lower efficiencies. See Cable 2001.

[64] For the Andasol numbers see Solar Millennium 2008. For the Nevada Solar One numbers see http://www.dotyenergy.com/Markets/CSP.htm.

5.2 Solar field efficiency

In the solar field, the following losses occur:

- Optical losses
  - Losses due to geometrical inaccuracies
  - Losses due to limited reflectivity, absorptance and transmittance
  - Losses related to beam incidence angle variance
  - Shadowing losses
- Thermal losses

Optical losses

Optical losses are caused, first, by **geometrical inaccuracies**.

Such inaccuracies are, for instance, macroscopic and microscopic mirror errors. Macroscopic mirror errors are basically slope and form errors. Microscopic mirror errors are local roughness areas in the mirror surface that cause a larger spread of the reflected beam radiation. Another group of geometrical errors are positioning errors, which can refer to the mirror position as well as to the receiver position. Tracking errors are another type of geometrical inaccuracies as well as collector orientation errors due to collector torsion. All these errors cause the reduction of the *intercept factor*. The intercept factor is defined as the ratio of the reflected radiation that hits the absorber to the total reflected radiation. It is a measure of the reflected radiation that gets lost because it does not hit the target, i.e. the absorber. Intercept factors of current commercially available parabolic troughs are between 0.96 and 0.97.[65]
The reached intercept factor is a result of an economic optimization, which has to trade off higher investment costs for higher geometrical accuracy against optical efficiency gains. Additionally, it depends on the absorber diameter, which is determined in another optimization, which has to trade off a higher intercept factor at larger absorber diameters against higher thermal losses (because of larger absorber surface areas).

Optical losses are caused, second, by the limited **reflectivity**, **absorptance** or **transmittance** of the optical components.
The mirrors have a limited reflectivity. The silver (or aluminium) layer has a limited reflectivity and the mirror glass (if there is any) has a limited transmittance. Flabeg indicates the reflectivity of their glass mirrors to be $\rho = 0.94$.[66] The transmittance of the glass envelope of the receiver is indicated by Schott to be about $\tau = 0.96$.[67] The reflectivity of the mirrors and transmission of the glass envelope tube depend on the soiling conditions. The indicated values hold only for absolutely clean mirrors and receivers. They are, therefore, rather theoretical values because mirrors and receivers are never absolutely clean under real operation conditions. Frequent cleaning is very important in order to reduce additional losses.
The absorber tube has also a limited absorptance. Selective coatings maintain the reflectance very low in the solar spectrum so that high absorptance values of $\alpha = 0.95$ are reached.[68]

[65] See Ulmer et al. 2007.
[66] See Flabeg 2011.
[67] See Schott 2011.
[68] See Schott 2011.

Optical losses are caused, third, by the **variance of the angle of the direct radiation incidence on the collector**.
Parabolic troughs are tracked only around one axis. Contrary to two-axis tracked solar dishes, where the direct radiation always hits the aperture with the incidence angle zero, the incidence angle at a parabolic trough changes continuously. For the common north-south trough alignment, the incident angle θ depends in the following way on the solar zenith angle θ_z, the declination δ and the hour angle ω:

$$\cos\theta = \sqrt{\cos^2\theta_z + \cos^2\delta \cdot \sin^2\omega}\,.$$

Variable incidence angles influence the geometrical and optical performance in several ways:

- Influence on optical parameters

The reflectivity of the mirrors, the transmittance of the receiver glass tube and the absorptance of the absorber tube are reduced with a growing incidence angle. An optical parameter variance factor ξ_{OP} can be defined that describes the reduction of the optical efficiency due to changing reflectivities, transmittances and absorptances at incidence angles larger than zero.

- Influence on the intercept factor

The higher the incidence angle the longer is the way of the sunbeams from the mirrors to the receiver. The longer way causes a stronger widening of the sunbeams, which reduces the intercept factor. An intercept variance factor ξ_{IC} can be defined that describes the reduction of the optical efficiency due to lower intercept factors at incidence angles larger than zero.

- Row end losses

Incidence angles larger than zero imply losses at the end of the collector rows. At one end, the radiation that is reflected on the last mirrors misses the absorber tube and at the other end a part of the absorber tube is not illuminated by the reflected radiation. The receiver length l that is not illuminated depends on the focal length f and the incidence angle θ:

$$l = f \cdot |\tan\theta|\,.$$

The following collector length use factor can be defined:

$$\xi_{CL} = \frac{L-l}{L}\,,$$

where L is the collector row length.

The mentioned additional loss effects that depend on the incidence angles can be combined in an incidence angle modifier (IAM), which is the ratio of the optical solar field efficiency at a given incidence angle to the optical solar field efficiency at $\theta = 0$:

$$IAM = \xi_{OP} \cdot \xi_{IC} \cdot \xi_{CL} = \frac{\eta_{SF,opt}(\theta)}{\eta_{SF,opt}(\theta=0)} .$$

Optical losses are caused, fourth, by **mutual shading of the collector rows**.

At small solar altitude angles, the collector rows can shade each other. It is an important solar field optimization task to define the distance between the rows: Small distances imply high shadowing losses; large distances imply large solar field areas and longer pipes with higher material costs and higher thermal losses. The optimum row distance is considered to be at about three times the aperture width.[69]

The following figure shows the approximate losses due to the varying incident angle and the shadowing losses for a parabolic trough power plant at spring or autumn equinox at a latitude of 30°.[70]

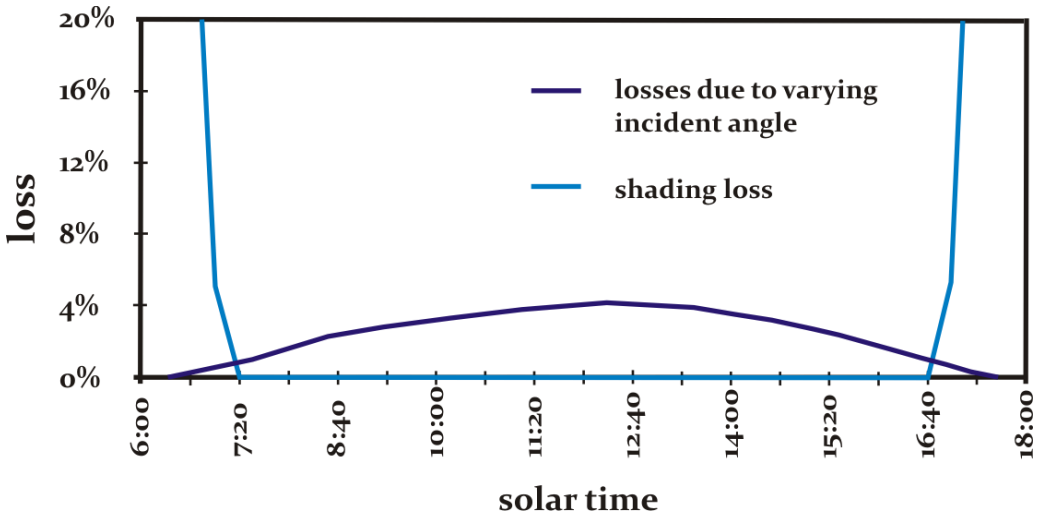

Figure 78: Losses due to varying incident angles and shading in a parabolic trough solar power plant at spring or autumn equinox and at a latitude of 30°

Thermal losses

Thermal losses occur in the absorber tubes and in the HTF pipes. In a given system, the losses depend on the temperature differences between the heat transfer medium and the surrounding air. The following figure shows the thermal loss per meter at different receiver models. What is to be seen is that the heat losses grow more than proportionally with the temperature difference.

[69] Sometimes cosine losses are also considered as an optical loss mechanism. This is the case when direct *normal* irradiance on the aperture area is taken as the initial value of the power flow. In this case, the cosine loss takes into consideration that the radiation does not always hit the aperture with an incidence angle of zero and that this means that the direct irradiance on the aperture is not the direct normal irradiance but the direct normal irradiance times $\cos\theta$. However, as we take the real, i.e. not necessarily *normal* direct irradiance on the aperture area as the power input (and not the direct normal irradiance), there is no cosine loss to be taken into consideration.

[70] See Trieb et al. 2004, 8.

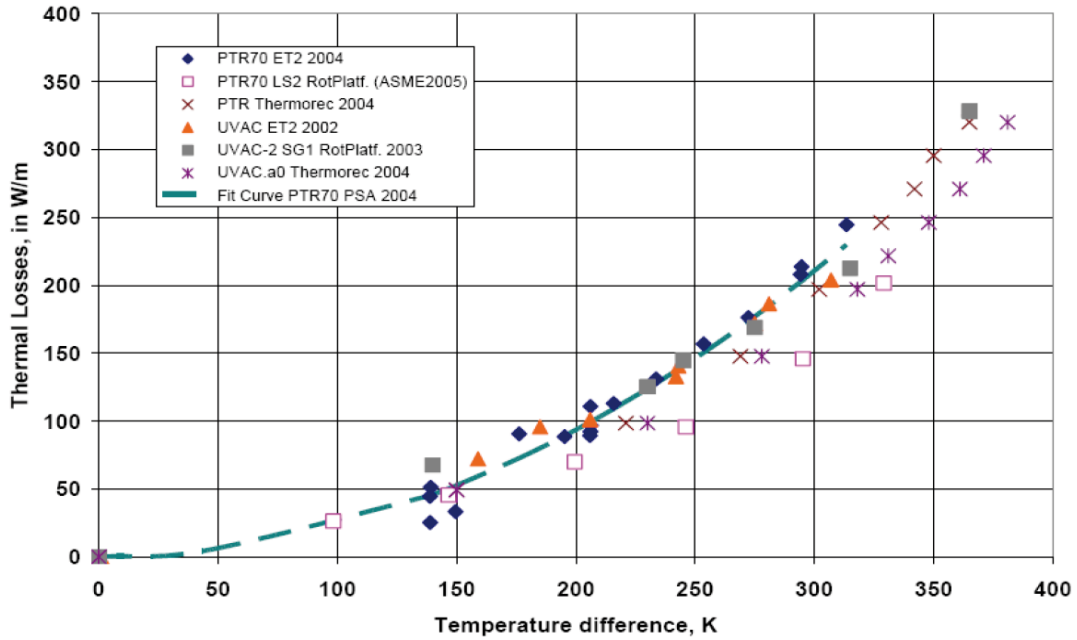

Figure 79: Thermal losses of different receiver models (source: Lüpfert/Schiricke 2009)

This can be understood if we take into consideration the heat transfer mechanisms that are responsible for the heat losses. Generally, heat losses from a warmer surface to the ambient air occur because of convection and thermal radiation.
Convection grows proportionally with ΔT:

$$\dot{Q}_{conv} = h \cdot A \cdot \Delta T.$$

h is the heat transfer coefficient and A the heat transfer surface area. The heat transfer coefficient, which describes the heat transfer from the receivers and pipes to the surrounding air, is not a constant, but depends on the wind conditions and on air humidity.
The radiative heat loss grows more than proportionally with ΔT. The radiation balance, taking into consideration the absorption of the thermal radiation at ambient temperature and the radiant emittance at the surface temperature of the considered heat transfer element, can be approximated as follows:

$$\dot{Q}_{rad} = \alpha_{T_{amb}} \cdot \sigma \cdot A \cdot T_{amb}^4 - \varepsilon_{T_{HTE}} \cdot \sigma \cdot A \cdot T_{HTE}^4 \,,$$

where σ is the Stefan-Boltzmann constant, T_{amb} the ambient air temperature and T_{HTE} the surface temperature of the considered heat transfer element (receiver or pipe). α_T and ε_T are weighted average radiant absorptance and emissivity for the thermal radiation spectrum at the temperature T. The difference between $\alpha_{T_{amb}}$ and $\varepsilon_{T_{HTE}}$, taking T_{amb} to be around 290K and T_{HTE} to be 653K for a common parabolic trough power plant with thermo oil as heat transfer medium, is quite small; often they are treated as being equal and the equation is simplified to

$$\dot{Q}_{rad} = \varepsilon \cdot \sigma \cdot A \cdot \left(T_{amb}^4 - T_{HTE}^4\right).$$

Anyway, the effect of the absorption of the thermal radiation of the system surroundings, which is indicated in the left part of the equation, is very small.

The radiant heat loss from the absorber tube to the ambient air is reduced by means of a selective coating that reduces considerably the radiant emittance at common absorber operation temperatures. The selective effect is reached by a high absorptance for the solar spectrum (thermal radiation at 5777K) and a low emissivity for the thermal radiation at absorber operation temperature (up to 653K).
The convective heat loss is reduced by an evacuated glass tube that covers the absorber tube. The mean heat loss mechanism at the absorber tube is thermal radiation. The mean heat loss mechanism at the glass tube, however, is convection because the glass temperature is much lower than the absorber temperature.[71] In steady state operation, the heat loss from the absorber tube and the heat loss from the glass tube are roughly the same.

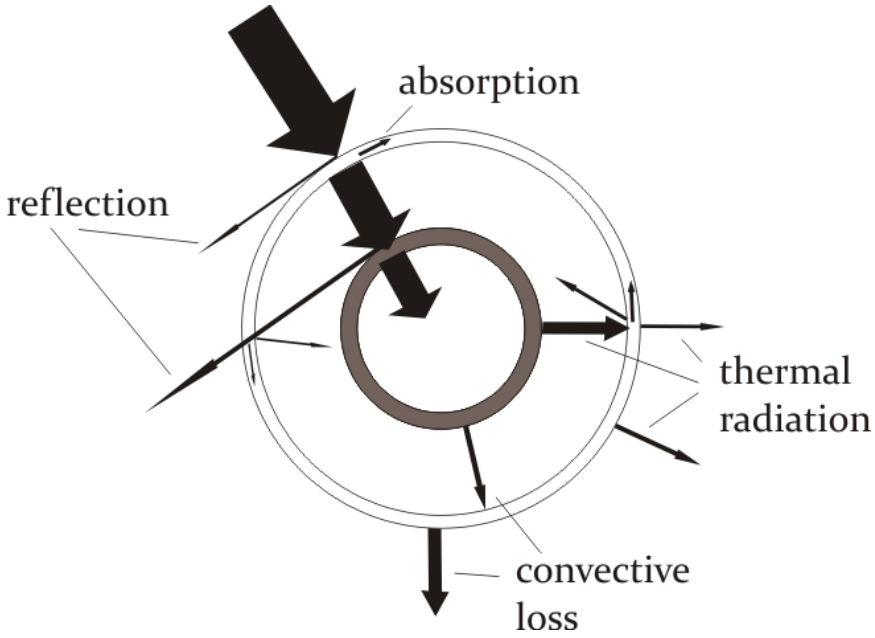

Figure 80: Energy flows at a parabolic trough receiver

In the HTF transport pipes, a thermal insulation reduces the temperature of the outer surface. In this case, the heat flow is by conduction from the HTF to the outer surface and from there to the ambient air by convection. Radiation plays a minor role because the temperature difference between the pipe surface and the ambient air is rather low.
Analogue to the convective heat transfer, the conductive heat transfer grows proportionally with ΔT:

$$\dot{Q}_{cond} = \frac{\lambda}{b} \cdot A \cdot \Delta T$$

λ is the thermal conductivity of the insulation material and b is the insulation thickness. ΔT is in this case the temperature difference between the inner and the outer pipe surface. The inner pipe surface temperature is approximately the HTF temperature.
As both dominating heat loss mechanisms in the HTF transport through the pipes depend proportionally on the temperature differences, the whole temperature loss process in the pipes grows roughly proportionally with the difference between HTF temperature and air temperature.

[71] Generally, radiative heat loss dominates at high temperatures and convective heat loss dominates at low temperatures.

It is important to maintain the pipes as short as possible in order to maintain thermal losses low. This is an important motivation to locate the power block inside the solar field and not outside.

Collector performance parameters

There are different parameters that allow the quantification of the collector performance. One of them is the collector efficiency and another is the mentioned incident angle modifier (IAM). The collector efficiency indicates the thermal output of the collector in dependence on the direct irradiance and on the difference between heat transfer fluid temperature and ambient temperature. The following figure indicates the collector efficiency of the Eurotrough 150 collector equipped with a Solel/Siemens receiver. As clearly to be seen, higher HTF temperatures imply higher thermal losses and hence lower collector efficiencies. Lower direct irradiance (at a given HTF temperature) implies also lower collector efficiency because the ratio of the thermal losses to the energy supply is higher. If the difference between HTF temperature and ambient temperature is zero, then the collector efficiency does not depend on the irradiance, because the optical losses, which are the only losses that exist if receiver and ambiance are at thermal equilibrium, are the same for any irradiance.

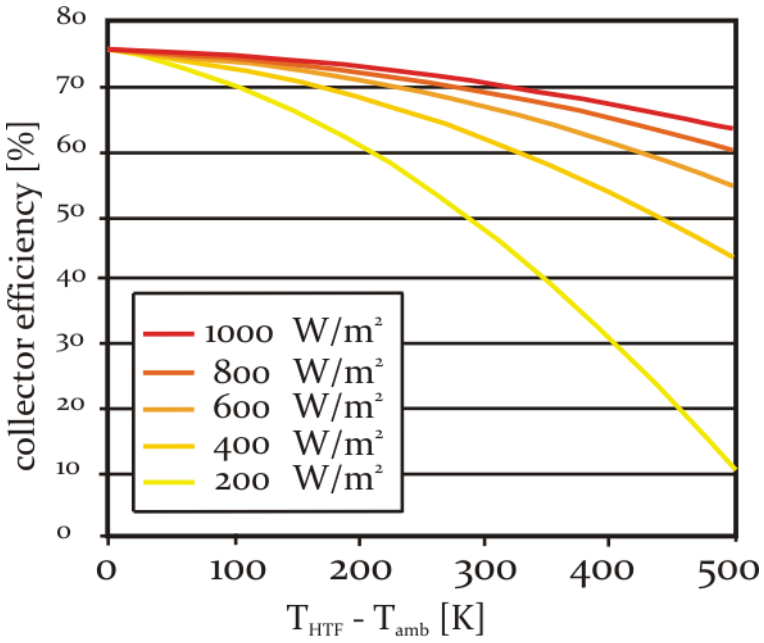

Figure 81: Collector efficiency of the Eurotrough 150 with Solel (now Siemens) receiver in dependence on direct irradiance and heat transfer fluid temperature (source: Geyer et al. 2002)

As the collector efficiency is indicated without reference to the incidence angle, the incidence angle modifier can be used additionally to specify the behaviour of the collector at incidence angles larger than zero. As explained above, varying incidence angles implicate varying reflectivity and transmittance as well as varying intercept factors and collector row end losses.
With these two parameters, collector efficiency and incidence angle modifier, the collector quality can be described.

5.3 Power block losses

Power block losses include:

- additional thermal losses in the power block (heat transfer from the solar field HTF to the water/steam)
- thermal-to-mechanic conversion loss (second law of thermodynamics)
- pressure losses
- mechanical losses (friction)
- mechanic-to-electric loss (generator loss)

The most important energy loss in the energy conversion chain of a parabolic trough power plant (like in any thermal power plant) occurs at the conversion of thermal energy to mechanical energy. The second law of thermodynamics says that the maximum thermal-to-mechanical conversion efficiency (for *any* conversion of thermal energy into mechanical energy) depends in the following way on the involved temperature levels:

$$\eta_{tm,max} = 1 - \frac{T_L}{T_H},$$

where T_L is the low temperature level of the process and T_H is the high temperature level (measured in K). According to this, parabolic trough power plants could reach a maximum thermal-to-mechanical efficiency of about 50.5%, taking 380°C as T_H (considering the maximum operation temperature of thermo oil) and 50°C as T_L. However, the Rankine cycle cannot even theoretically reach this value. In the case of the Rankine cycle, the heat supply is not isothermal. In this case the *mean* temperature at which the heat supply takes place must be taken instead of the *maximum* temperature T_H: $\eta_{RC,max} = 1 - \frac{T_L}{\bar{T}_H}$. Assuming that the steam pressure is 100 bars and that the mean heat supply temperature is near the evaporation temperature, i.e. at 311°C, the maximum thermal-to-mechanical efficiency would be about 45%.

Due to the fact that real processes are always non-isentropic, i.e. that there are losses in the compression and especially in the expansion step, this efficiency cannot be reached in real parabolic trough power plants. Larger turbines have an isentropic efficiency of about 85%.[72]

Additional thermal losses in the power block occur in the steam generator; and pressure losses occur in the steam flow.

Generator losses are quite low. Smaller generators (20 MW) reach an efficiency of about 97%, larger ones (50MW and more) reach 98%.[73]

Mechanical losses in larger power blocks do not exceed 1%.

[72] http://tu-dresden.de/die_tu_dresden/fakultaeten/fakultaet_maschinenwesen/iet/kwt/lehre/Vorlesungen/Vorlesung3.pdf, slide 46

[73] http://tu-dresden.de/die_tu_dresden/fakultaeten/fakultaet_maschinenwesen/iet/kwt/lehre/Vorlesungen/Vorlesung3.pdf, slide 47

5.4 Parasitic energy uses

The power plant itself needs electric power to be operated. Most of this power is needed for the HTF pumps and for the collector tracking. Due to the considerable length of the collector rows and due to the high number of collectors, the parasitic energy consumption in parabolic trough power plants is higher than in most other power plants. It amounts to around 10% of the generated power or about 2% of the input power.[74]

The following figure illustrates the energy flow in a parabolic trough power plant. The input power is the direct irradiance on the aperture. Solar field losses (optical and thermal losses) reduce the power by around 40%. More than the same power share gets lost in the power block, especially because of the heat rejection in the condenser. About 18% of the power input is transformed into electric power and about 16% is the useable electric output. This value indicates approximately the average overall efficiency of Andasol I. Peak efficiencies are higher, as explained at the beginning of this section.

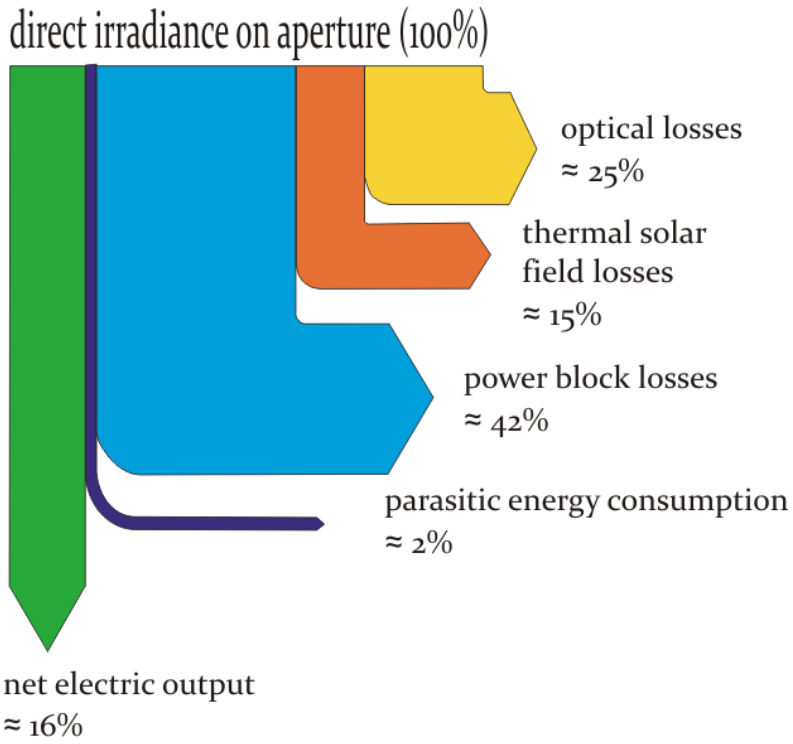

Figure 82: Approximate energy flow in a parabolic trough power plant (average values)

[74] See Jones 2001.

Reference List

Archimede Solar Energy (2011): HEMS08 Archimede Solar Receiver Tube for Thermodynamic Power Plant Technical Data. http://www.archimedesolarenergy.com/download.htm [June 2011]

Blanco-Muriel, M., Allarcon-Padilla, D. C., Lopez-Moratalla, T., & Lara-Coira, M. (2001). Computing the solar vector. *Solar Energy* (70), pp. 431-441.

Burkholder, F./Kutscher, C. (2008): "Heat-Loss Testing of Solel's UVAC3 Parabolic Trough Receiver". Technical Report NREL/TP-550-42394. http://www.nrel.gov/docs/fy08osti/42394.pdf [June 2011]

Cable, R. (2001): "Solar Trough Generation – The California Experience". http://www.nrel.gov/csp/troughnet/pdfs/cable_frier_calexpr.pdf [June 2011]

Castañeda, N., Vázquez J., Domingo M., Fernández, A., León, J. (2006): "Sener Parabolic Trough Collector Design and Testing", Solar Paces 2006 ftp://ftp.crs4.it/pub/References/SolarPaces2006/A2/A2-S3-CASTANEDA.pdf [June 2011]

Çengel, Y.A., Turner, R.H. (2005): Fundamentals of Thermal-Fluid Sciences, second edition, Published by Mc Graw-Hill 2005

Eck, M., Hennecke, K. (2007): „Die solare Direktverdampfung – Vergleich mit anderen technologischen Optionen" DLR http://www.dlr.de/sf/Portaldata/73/Resources/dokumente/Soko/Soko2007/Vortraege/Direktverdampfung_Vgl___Hennecke.pdf [June 2011]

Eck, M., Zarza, E. (2006): "Saturated steam process with direct steam generating parabolic troughs". *Solar Energy* 80 (2006), 1424-1433

Eickhoff, /Zarza, E. (2007): „Solare Direktverdampfung in der Praxis" DLR http://www.dlr.de/sf/Portaldata/73/Resources/dokumente/Soko/Soko2007/Vortraege/Direktverdampfung_Praxis___Eickhoff.pdf [June 2011]

Elliot, T.C., Chen K., Swanekamp, R.C. (1997):*Standard Handbook of Powerplant Engineering*, Second Edition

Esposito, S. et al. (2009): "Fabrication and optimisation of highly efficient cermet-based spectrally selective coatings for high operating temperature". Thin Solid Films 517, 6000-6006

Feldhoff, J.F., Benitez, D., Eck, M., Riffelmann, K.-J. (2009): "Economic Potential of Solar Thermal Power Plants with Direct Steam Generation Compared to HTF Plants". Proceedings of the ASME 2009 3rd International Conference of Energy Sustainability, San Francisco 2009

Flabeg (2010): "Reflecting the Future – Solar Mirrors for all CSP Applications". http://www.flabeg.com/files/solar/downloads/PDFs/FLABEG_SolarBroschuere.pdf [June 2011]

Flabeg (2011): "Mirrors for parabolic trough". http://flabeg.de/index.php?id=142&L=1 [June 2011]

Flagsol (2010): "Advanced High Temperature Trough Collector Development, CSP Program Review", 2010, www1.eere.energy.gov/solar/pdfs/csp_prm2010_solar_millennium.pdf [June 2011]

Garg, H.P. (1987): *Advances in solar energy technology*, Dordrecht: Reidel

Geyer, M., Lerchenmüller, H., Wittwer, V., Häberle, A., Lüpfert, E., Hennecke, K., Schiel, W., Brakmann, G. (2002): *Parabolrinnensysteme*, FVS Themen, 2002

Geyer, M. (ed.) (2007): *SolarPACES Annual Report* 2007

Hampel, M./Lahmeyer International (2010): Lecture Notes "CSP" University of Kassel 2010

Hartl et al. (2009): Konzentrierte Solarenergie: Konzepte, Kostenreduzierung und Versorgungssicherheit, www.eeg.tuwien.ac.at [June 2011]

Hering, G., Schug, A. (2010): „Sonne, Hitze, Strom". *Photon*, September 2010

Hermann, U., Geyer, M., Kistner R. (2002): "The Andasol Project", Flabeg, Solar Millenium, http://www.nrel.gov/csp/troughnet/pdfs/uh_anda_sol_ws030320.pdf [June 2011]

Hoffschmidt,B. (2008): Lecture notes, Aachen University of Applied Sciences, 10.11.2008 http://www.fh-aachen.de/uploads/media/RE_4_ThermischeSpeicher_ho.pdf [June 2011]

IEA (2010): *Technology Rodamap. Concentrating Solar Power*. International Energy Agency. http://www.iea.org/papers/2010/csp_roadmap.pdf [July 2011]

Jähnig, D. (2005): Entwicklung und Optimierung eines Parabolrinnenkollektor-systems zur Erzeugung von Prozesswärme für industrielle Produktionsprozesse, Fabrik der Zukunft – eine Initiative des Bundesministeriums für Verkehr, Innovation und Technologie, Gleisdorf, 2005
www.aee-intec.at/0uploads/dateien26.pdf [June 2011]

Jones, S.A. et al. (2001): "TRNSYS Modeling of the SEGS VI Parabolic Trough Solar Electric Generating System". Proceedings of Solar Forum 2001: Solar Energy: The Power to Choose

Kearney, D. (2007): *Parabolic Trough Collector Overview*, NREL, Golden CO http://www.nrel.gov/csp/troughnet/pdfs/2007/kearney_collector_technology.pdf [June 2011]

Kearney, D. et al. (2002): "Assessment of a molten salt heat transfer fluid in a parabolic trough solar field" *Journal of Solar Energy Engineering*, http://pointfocus.com/images/pdfs/saltw-troughs.pdf

Kennedy, C., Terwilliger, K., Lundquist, C. (2005): "Provide status of test results of candidate solar mirror samples and identify promising candidates" CSP FY 2005 Milestone Report. http://www.abetterfocus.com/files/Reflector_Milestone_Report_9-05.pdf

Kennedy, C. (2008): "CSP: Advanced Systems: Optical Materials". http://www1.eere.energy.gov/solar/review_meeting/pdfs/prm2008_kennedy_nrel.pdf

Krüger, D., Krüger, J., Pandian, Y. Feldhoff, J.F., Eck, M., Eickhof, M., Hennecke, K. (2010): "Kachanaburi Solar Thermal Power Plant with Direct Steam Generation – Layout". Solar Paces 2010. http://www.pressebox.de/attachments/details/id/332940

Kuckelkorn, T., Graf, W. (2004): "Absorber mit einer strahlungsselektiven Absorberbeschichtung und Verfahren zu seiner Herstellung". http://www.patent-de.com/20050630/DE102004010689B3.html

Laing, D. et al. (2011): "Thermal energy storage for direct steam generation". *Solar Energy* 85, 627-633

Lüpfert, E., Schiricke, B. (2009): QUARZ Zentrum –Übersicht der entwickelten Prüfmethoden im DLR-Test- und Qualifizierungszentrum für konzentrierende Solartechnik, DLR. http://www.dlr.de/sf/Portaldata/73/Resources/dokumente/Soko/soko2009/Praesentationen/6_Luepfert_Soko090609c.pdf

Mohr, M., Svoboda, P., Unger, H. (1999): *Praxis solarthermischer Kraftwerke*. Berlin/Heidelberg: Springer

Morgan, M.J., Shapiro, H.N. (2008): *Fundamentals of Engineering Thermodynamics*, 6th edition, John Wiley & Sons Inc.

Nava, P.; Aringhoff, R.; Svoboda, P.; Kearney, D. (1996): *Status Report on solar trough Power Plants*, Cologne, Germany, 1996, http://www.solarpaces.org/Library/docs/PiStaRep.pdf (retrieved Mai 2011)

NREL: Concentrating Solar Power Commercial Application Study: Reducing Water Consumption of Concentrating Solar Power Electricity Generation
Report to Congress, U.S. Department of Energy
http://www.nrel.gov/csp/troughnet/pubs_power_plant.html

Octobre J., Guihard, F. (2009): Systèmes Solaires

Price, H., Lüpfert, E., Kearney, D., Zarza, E., Cohen, G., Gee, G., Mahoney, R. (2002): *Advances in Parabolic Trough Solar Power Technology*, ASME Journal of Solar Energy Engineering Vol 124, 2002

Quaschning, V, Kistner, R., Ortmanns, W. (2002): Influence of Direct Normal Irradiance Variation on the Optimal Parabolic Trough Field Size: A Problem Solved with Technical and Economical Simulations. Journal of Solar Energy EngineeringVo. 124, 160-164

Ragheb, M. (2011): *Historical Perspective*, University of Illinois at Urbana-Champaign, https://netfiles.uiuc.edu/mragheb/www/NPRE%20498ES%20Energy%20Storage%20Systems/Historical%20Perspective.pdf (retrieved May 2011)

Sargent & Lundy (2003): *Assessment of Parabolic Trough and Power Tower Solar Technology Cost and Performance Forecasts*. Sargent & Lundy LLC Consulting Group, Chicago. http://www.nrel.gov/docs/fy04osti/34440.pdf

Schiel, W. (2007): "World's biggest solar power plant under construction in Spain", Schlaich, Bergermann und Partner, Stuttgart

Schott (2011): "Schott PTR 70 Receiver. The Next Generation".
http://www.schottsolar.com/de/produkte/solarstromkraftwerke/schott-ptr-70-receiver/

Siemens (2011): "The unrivaled benchmark in solar receiver efficiency. The Siemens UVAC 2010 is designed for outstanding thermal output."
http://www.energy.siemens.com/co/en/power-generation/renewables/solar-power/concentrated-solar-power/receiver.htm

Skyfuel a: "ReflechTech Mirror Film", Product Information
http://www.skyfuel.com/downloads/brochure/Brochure_ReflecTech.pdf
(retrieved May 2011)

Skyfuel b: "Skytrough", Product Information
http://www.skyfuel.com/downloads/brochure/SkyTroughBrochure.pdf
(retrieved May 2011)

Solar Millennium (2008): "The parabolic trough power plants Andasol 1 to 3".
http://www.solarmillennium.de/upload/Download/Technologie/eng/Andasol1-3engl.pdf

Tamme et al. (2005): Speicherung für Hochtemperaturwärme, FVS Themen 2005 http://www.fvee.de/fileadmin/publikationen/Themenhefte/th2005/th2005_06.pdf

Trieb, F. et al. (2004): SOKRATES-Projekt. Solarthermische Kraftwerkstechnologie für den Schutz des Erdklimas. http://www.dlr.de/tt/Portaldata/41/Resources/dokumente/institut/system/projects/AP_2_1_Modellbildung.pdf

Ulmer, S., Pottler, K., Lüpfert, E., Röger, M. (2007): *Measurement techniques for the optical quality assessment of parabolic trough collector fields in commercial solar power plants.* Forschungsbericht, DLR, PSA

Weiss (2005): Solarwärme für industrielle Prozesse, Erneuerbare Energie: Zeitschrift für eine nachhaltige Energiezukunft, 2005

Winter, C.J., Sizmann, R.L., Vant-Hull, L.L (1991): *Solar Power Plants – Fundamentals, Technology, Systems, Economics*, Springer-Verlag Berlin, Heidelberg

Annex

1 Proof that a parabola has a focal point

In the following, we will demonstrate that a parabola focuses incoming axially parallel radiation on one point. The figure below illustrates the geometric relations. It shows a cross section through a parabolic mirror in a coordinate system. Locating the parabola in a coordinate system, as indicated in the figure, it can be represented mathematically as the graph of the function $y = px^2$. The red lines represent the light that enters the mirror in rays parallel to the parabola's axis and crosses the axis, after reflection, at the focal point F.

In order to show that such a parabola really has a focal point (for axially parallel radiation) we take one arbitrary light ray that is parallel to the y-axis and we determine where the reflected ray crosses the axis. We show that this point does not depend on the point were the ray hits the mirror and we thereby demonstrate that all rays parallel to the parabola´s axis pass through this point, the focal point F, after reflection.

We take the ray that hits the mirror, or the tangent $\overleftrightarrow{EB}$, at the point E under the incident angle α and that leaves E under the same angle. $\angle BED$ is the vertical angle of the incident angle and therefore it also equals to α.

Now we determine the point B on the x-axis. B is the point of intersection of $\overleftrightarrow{EB}$ with the x-axis. As E is on the graph of the function $y = px^2$, the coordenates of E, $(x_E; y_E)$, can be determined as $(x_E; px_E^2)$. The gradient of $\overleftrightarrow{EB}$ is the gradient of the function $y = px^2$ at the point E, i.e. $\frac{dy}{dx}(x_E) = 2px_E$. According to this, $\overleftrightarrow{EB}$ has the analytical form $y = 2px_E x + b$. Filling $(x_E; px_E^2)$ in this equation, we get $b = -px_E^2$ and, consequently, $y = 2px_E x - px_E^2$. For B, the intersection of this line with the x-axis, that means for $(x_B; 0)$ we get $x_B = x_E/2$. So, B devides $\overline{AD}$ in two equal parts. We can draw the line through F and B and get the point C such that ΔABF and ΔBCD are congruent. Furthermore, these triangles are similar to ΔBDE. Now, because of this similarity it is $\overline{AF}/\overline{AB} = \overline{BD}/\overline{DE}$ and with $\overline{AB} = \overline{BD} = x_E/2$ and $\overline{DE} = px_E^2$ we get

$$\overline{AF} = f = 1/(4p)\,. \qquad (1)$$

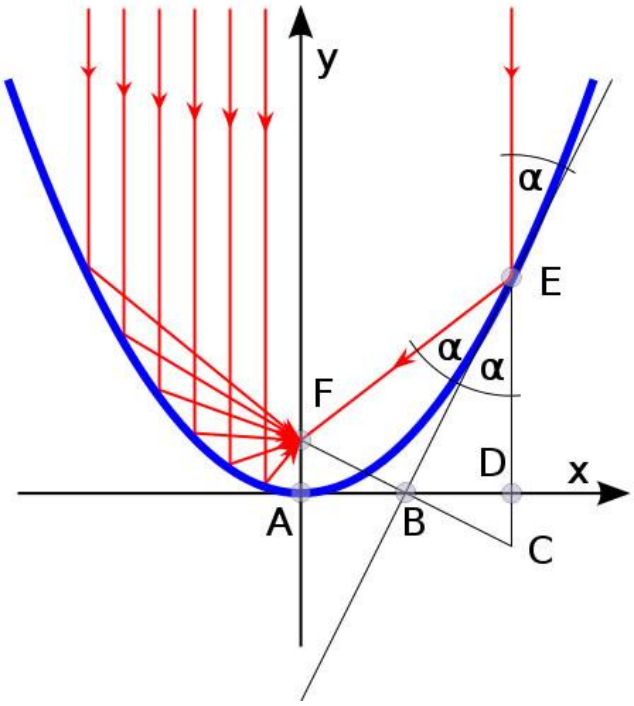

Figure 83: Path of parallel rays at a parabolic mirror

We see that the point of intersection of the reflected ray with the x-axis is independent from the incident point E. That means that there *is* a focal point where all incident rays, that enter the mirror parallel to its axis, meet. The focal length of a parabola, i.e. the distance of the focal point from the vertex, is, according to equation (1), $f = 1/(4p)$.
Therefore, the parabola's analytic representation can be expressed as

$$y = \frac{1}{4f}x^2 \ . \qquad (2)$$

2 Proof that parabolas with the same rim angle are geometrically similar

In the following we want to show that the cross-sections of parabolic troughs with the same rim angle are geometrically similar. More specifically, we will show that the slope of parabolas with the same rim angle is identical at points that correspond to each other. In other words, we will show that the slope characteristics of a parabola depend exclusively on its rim angle. We consider a parabola $y = \frac{x^2}{4f}$:

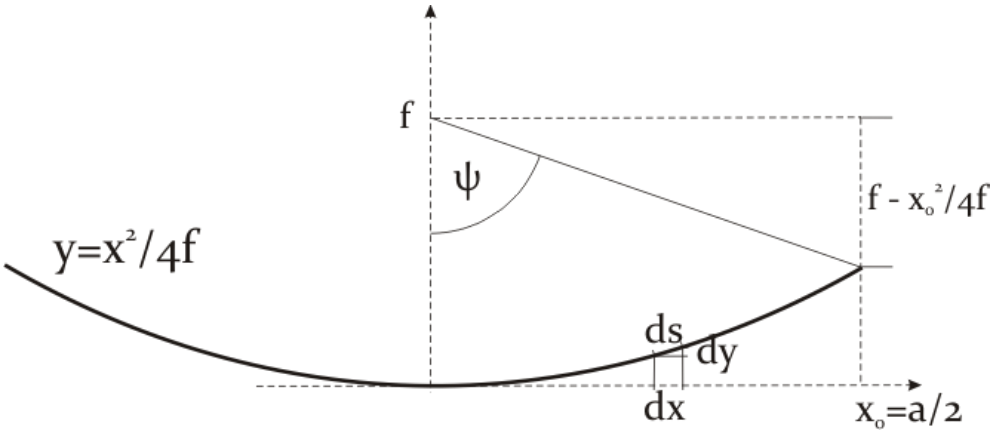

In a first step we want to show that the slope angle at the rim is exclusively a function of the rim angle ψ. As to be seen in the foregoing figure, we can formulate the following relation:

$$\tan\psi = \frac{x_0}{f - \frac{x_0^2}{4f}}. \tag{1}$$

From (1) we get:

$$x_{0_{1,2}} = 2f\left(-\frac{1}{\tan\psi} \pm \sqrt{\frac{1}{\tan^2\psi} + 1}\right) \tag{2}$$

We consider only the positive value of x_0 and reduce (2) to:

$$x_0 = 2f\left(-\frac{1}{\tan\psi} + \sqrt{\frac{1}{\tan^2\psi} + 1}\right) \tag{3}$$

The slope of the parabola is described by the derivation of $y = \frac{x^2}{4f}$ with respect to x:

$$y' = \frac{1}{2f}x \tag{4}$$

The slope at x_0 is then:

$$y'(x_0) = \left(-\frac{1}{\tan\psi} + \sqrt{\frac{1}{\tan^2\psi} + 1}\right), \tag{5}$$

which depends only on the rim angle and which is, consequently, independent from f.
In a second step we can show that parabolas with different f have also the same slope at all the points between $x = 0$ and $x = x_0$, i.e. at the points $x = cx_0$, with $0 \leq c \leq 1$. The parabola between the two points takes the form $y = \frac{(cx_0)^2}{4f}$ and the derivation with respect to cx_0 takes the form $y' = \frac{1}{2f} cx_0$. Taking into consideration (3), the slope is, then:

$$y'(cx_0) = c\left(-\frac{1}{\tan\psi} + \sqrt{\frac{1}{\tan^2\psi} + 1}\right) \qquad (6)$$

which, once more, depends only on the rim angle and on the factor c, but not on f.

3 Derivation of the relation between rim angle, focal length and aperture width

Taking into consideration that $2x_0 = a$, where a is the aperture width of the collector, we can transform equation (1) of the foregoing proof into:

$$\tan\psi = \frac{\frac{a}{f}}{2-\frac{1}{8}\left(\frac{a}{f}\right)^2}. \tag{7}$$

and we get already the mathematical relation between focal length, aperture width and rim angle.
Equation (3) permits to express the ratio of the aperture width to the focal length as a function of the rim angle:

$$\frac{a}{f} = -\frac{4}{\tan\psi} + \sqrt{\frac{16}{\tan^2\psi} + 16} \tag{8}$$

4 Derivation of the parabolic trough surface area

The surface area is

$$A = S \cdot l\,, \tag{12}$$

where S is the length of the parabola that is the cross-section of the trough.
S can be calculated according to the formula:

$$S = \int_{-\frac{a}{2}}^{\frac{a}{2}} \sqrt{1 + \left(f'(x)\right)^2}\, dx\,, \tag{13}$$

A parabola with the focal length of f is represented analytically by the funcion $f(x) = \frac{1}{4f}x^2$. The derivation of this function is $f'(x) = \frac{1}{2f}x$. The length of the parabola is, hence

$$S = \int_{x_1}^{x_2} \sqrt{1 + \left(\frac{x}{2f}\right)^2}\, dx\,. \tag{14}$$

The following indeterminate integral holds:

$$\int \sqrt{1 + \left(\frac{x}{2f}\right)^2}\, dx = \frac{1}{2}\left[x\sqrt{1 + \frac{x^2}{4f^2}} + 2f \cdot ln\left(\frac{x}{4f} + \sqrt{1 + \frac{x^2}{4f^2}}\right)\right]. \tag{15}$$

With $\frac{a}{2}$ as the half aperture width, S can be determined:

$$S = \int_{-\frac{a}{2}}^{\frac{a}{2}} \sqrt{1 + \left(\frac{x}{2f}\right)^2}\, dx = \frac{a}{2}\sqrt{1 + \frac{a^2}{16f^2}} + 2f \cdot \ln\left(\frac{a}{4f} + \sqrt{1 + \frac{a^2}{16f^2}}\right) \tag{16}$$

and the surface area of the parabolic trough is calculated according to

$$A = \left(\frac{a}{2} \sqrt{1 + \frac{a^2}{16f^2}} + 2f \cdot \ln \left(\frac{a}{4f} + \sqrt{1 + \frac{a^2}{16f^2}} \right) \right) \cdot l \, . \qquad (17)$$

Questions

1) Complete the following sentences about the geometrical properties of a parabolic trough:

   a) If the rim angle is enlarged (at a fixed aperture width), then the focal length … .
   b) If the aperture width is enlarged (at a fixed rim angle), then the focal length … .
   c) If the rim angle is enlarged (at a fixed focal length), then the aperture width … .

2) Taking the concentration ratio as the ratio of the collector aperture area to the Sun image size, which assertion is false?
   a) At constant focal length, the concentration ratio depends on the rim angle.
   b) At constant rim angle, the concentration ratio depends on the aperture width.
   c) At constant aperture width, the concentration ratio depends on the focal length.

3) "At larger the rim angles, the concentration ratio should be larger because more solar radiation is concentrated per meter collector length." Why is this assertion false if we take the ratio of the collector aperture area to the Sun image area as the concentration ratio?

4)
   a) In an innovative research project you plan a parabolic trough power plant for a small local grid first in an arid area in northern China (latitude 45°) and, second, in southern Egypt (latitude 22°). The plant is the principal electricity source in the respective local grid. Besides the large thermal storage of the plant (SM 3), which can bridge nights and also some cloudy days, the system considers many distributed energy storages the individual consumers dispose of (battery banks). Only few special larger consumers, like the local medical station, have a diesel generator for emergency situations. In general, the individual storages together with the large thermal storage of the plant should be sufficient to supply the needed energy. Energy consumption is quite stable over the year.
      Do the different latitudes have a consequence on your considerations about the solar field orientation?
   b) Now you plan a parabolic trough power plant for both locations with connection to the national transmission grid. That means, the consumers do not depend on the particular CSP plant, because they are connected to the grid. Does the connection to the grid change your considerations?

5) You design a new large collector type with a focal length of 2.50 m and a rim angle of 85°.
   a) What is the aperture width?
   b) What should be the absorber tube diameter if you take a dispersion angle of 0.4° and if you consider a reference incidence angle of 30°?

6) Thermal losses in a receiver grow with higher heat transfer fluid temperatures. Especially radiative losses grow strongly. That means that the collector efficiency becomes lower at higher heat transfer fluid temperatures. The HTF temperatures in thermo oil systems are below 400°C; in molten salt and direct steam generating systems they do not exceed 550°C.
   Which problem concerning the selective coating of the absorber would cause much lower collector efficiencies if the HTF temperature got much higher, for instance up to 800°C?

7) There are 1.5 km^2 available for the construction of a parabolic trough power plant.
   a) If the power block size is determined to be 50MW, which solar multiple can be reached?
   b) Taking a system without storage, which could be the rated electric power of the plant?

Answers

1) a) is reduced
   b) grows
   c) grows

2) Assertion (b) is false. The rim angle determines the concentration ratio completely.

3) Considering perfect mirrors, the assertion is false because not only the harvested energy per receiver meter grows, but also the Sun image. The Sun image grows because of the beam spread of the direct solar radiation and the growing distance between mirror and receiver at larger rim angles. In real mirrors the additional beam spread because of microscopic geometrical mirror errors has to be added.

4)
   a) In an isolated local grid with the parabolic trough power plant as the dominating power plant, it is important to achieve a stable electric power generation over the year. In the case of China seasonal radiation differences are quite big. In particular, it is important to harvest as much energy as possible during the winter. In summer, there will be some electricity surplus. In this case, it may be preferable to choose an east-west oriented solar field.
   In the case of the plant in Egypt, the seasonal variance is very small. Therefore, the common north-south orientation with a higher annual energy yield should be preferred.
   b) In both cases the north-south orientation should be preferred, which allows higher annual energy yields.

5)
   a) $a = f\left(-\frac{4}{\tan\psi} + \sqrt{\frac{16}{\tan^2\psi} + 16}\right) = 2.5\left(-\frac{4}{\tan 85°} + \sqrt{\frac{16}{\tan^2 85°} + 16}\right)\text{m} = 9.16\text{m}$

   b) incidence angle zero: $d_0 = \frac{a \cdot \sin\frac{\alpha_D + \delta}{2}}{\sin\,\psi} = \frac{9.16 \cdot \sin\frac{0.53° + 0.4°}{2}}{\sin 85°} = 74.6\text{mm}$
   incidence angle 30°: $d = \frac{d_0}{\cos 30°} = 86.2\text{mm}$
   It would be possible to use, for instance, Schott's PTR 90 receiver.

6) The black body spectrum at 800°C overlaps already quite much with the solar spectrum. That's why the selective effect of any coating would be limited. This would mean that or the solar weighted absorptance becomes lower or the emittance (operation-temperature weighted) becomes higher or both, which implies a lower collector efficiency. The more the spectra overlap the lower is the selective effect.

7) $A = 4 \cdot A_{ap} = 4 \cdot \frac{P_{el} \cdot SM}{\eta \cdot G_{b,coll}}$
   a) $1.5\text{km}^2 = 4 \cdot \frac{50\text{MW} \cdot SM}{0.25 \cdot 800\frac{\text{W}}{\text{m}^2}}$
   $SM = 1.5$
   b) $1.5\text{km}^2 = 4 \cdot \frac{P_e \cdot 1}{0.25 \cdot 800\frac{\text{W}}{\text{m}^2}}$
   $P_e = 75\text{MW}$

Exercises

The rated gross electric output of a parabolic trough power plant is 50MW. The plant has a reheat turbine. The inlet steam parameters are 370°C and 100 bars. The steam parameters at the outlet of the high pressure turbine are 200°C and 18 bars. An isobaric reheating gets the steam once more to 370°C. The steam parameters at the outlet of the low pressure turbine are 42°C, 0.08 bars and a steam content of 0.91. The power plant is equipped with a wet cooling tower. The cooling water demand is about 4 m³/MWh.

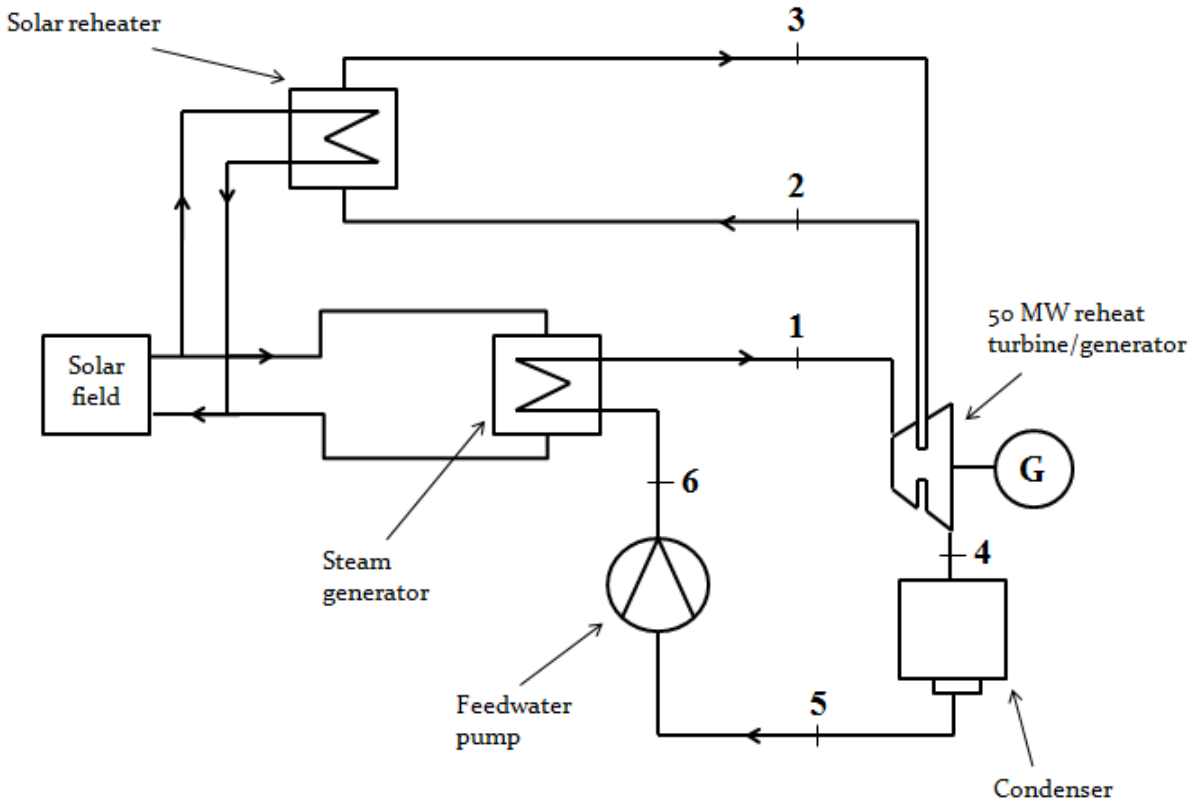

a) What is the annual gross energy output of the power plant assuming a capacity factor of 24%?

b) What is the annual cooling water demand?

c) What are the specific enthalpies of the steam at the points 1 to 4? Use the entropy-enthalpy diagram!

d) Which steam mass flow is necessary to reach the 50MW? Disregard mechanical and generator losses.

e) Calculate the heat flow of the waste heat that is rejected in the condenser. The enthalpy of liquid water at 42°C (h_5) is 176 kJ/kg.

f) What is the thermal energy flow from the solar field that is needed to reach the 50 MW (overall losses of steam generator and solar reheater: 5%).

g) What is the power block efficiency?

h) Calculate the aperture area of the solar field when we assume a design point at a solar irradiance of 800 W/m² and overall solar field losses of 35 %.

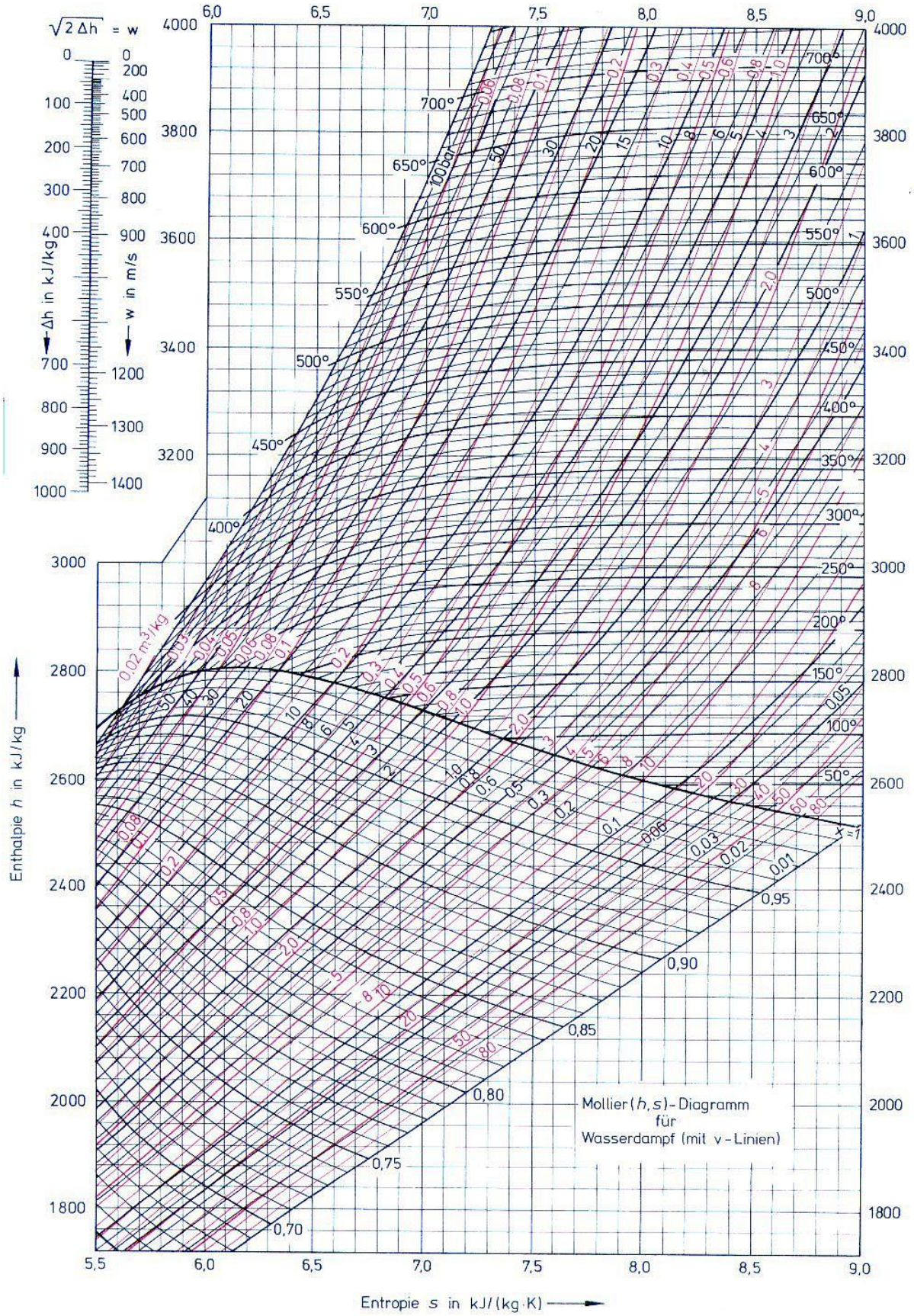
√2 Δh = w
Δh in kJ/kg
w in m/s
Enthalpie h in kJ/kg
Entropie s in kJ/(kg·K)
Mollier (h, s)-Diagramm
für
Wasserdampf (mit v-Linien)

Solutions

a)

$$E = 8760\,\frac{\mathrm{h}}{\mathrm{y}} \cdot 0.24 \cdot 50\mathrm{MW} = 105\,\frac{\mathrm{GWh}}{\mathrm{y}}$$

b)

$$V_W = 105000\,\frac{\mathrm{MWh}}{\mathrm{y}} \cdot 4\,\frac{\mathrm{m}^3}{\mathrm{MWh}} = 420000\,\frac{\mathrm{m}^3}{\mathrm{y}}$$

c)

$h_1 = 3020$ kJ/kg
$h_2 = 2800$ kJ/kg
$h_3 = 3180$ kJ/kg
$h_4 = 2360$ kJ/kg

d)

$$P_e = \dot{m} \cdot \Delta h = 50\mathrm{MW}$$

$$\Delta h = (h_1 - h_2) + (h_3 - h_4) = 1040\,\frac{\mathrm{kJ}}{\mathrm{kg}}$$

$$\dot{m} = \frac{50\mathrm{MW}}{1040\,\frac{\mathrm{kJ}}{\mathrm{kg}}} = 48.1\,\frac{\mathrm{kg}}{\mathrm{s}}$$

e)

$$\dot{Q}_C = \dot{m} \cdot (h_4 - h_5) = 48.1\,\frac{\mathrm{kg}}{\mathrm{s}} \cdot (2360 - 176)\,\frac{\mathrm{kJ}}{\mathrm{kg}} = 105\mathrm{MW}$$

f)

$$\dot{Q}_{SF} = \left(P_e + \dot{Q}_C\right) \cdot 1.05 = 162.7\mathrm{MW}$$

g)

$$\eta_{PB} = \frac{50\mathrm{MW}}{162.7\mathrm{MW}} = 0.31$$

h)

$$A_{ap} = \frac{162.7\mathrm{MW}}{800\,\frac{\mathrm{W}}{\mathrm{m}^2}} \cdot 1.35 = 275000\mathrm{m}^2$$